UNIVERSITY OF SOUTHAMPTON

FACULTY OF ENGINEERING, SCIENCE & MATHEMATICS
SCHOOL OF CIVIL ENGINEERING AND ENVIRONMENT

Analysis of reduced modulus action in U-section steel sheet piles

by

Richard William Mawer

Thesis for the degree of Doctor of philosophy

SEPTEMBER 2005

UNIVERSITY OF SOUTHAMPTON

ABSTRACT

FACULTY OF ENGINEERING, SCIENCE & MATHEMATICS
SCHOOL OF CIVIL ENGINEERING AND ENVIRONMENT

Doctor of Philosophy

ANALYSIS OF REDUCED MODULUS ACTION IN U-SECTION STEEL SHEET PILES

by Richard William Mawer

U-section steel sheet piles are used in the construction of retaining walls *inter alia*. They are connected together by sliding joints or interlocks that are located along the centre line of the wall. Inter-pile movement along these joints can potentially reduce the stiffness and bending strength typically by 70% and 55% respectively. This interlock slippage is known as Reduced Modulus Action.

U-section piling has been used for many years without consideration of Reduced Modulus Action (RMA). This potential for substantial losses of performance has been demonstrated in all laboratory based tests to date. However, having concluded that RMA is a significant problem it is rarely witnessed in practice. This inconsistency between practical and theoretical observation is addressed herein. The first research into this phenomenon dated back to 1934 and more recent concern surrounding the potential of RMA has provided an inclusion of strength and stiffness reduction factors in the forthcoming Eurocode 3 Part 5. These reduction factors may often lead to uneconomical designs.

The aims of this research are to increase the understanding of RMA. It aims to accurately model realistic loading conditions present in practical pile walls, accurately predict the amount of friction developed in the interlock of a steel sheet pile and develop a series of reduction factors dependant on the situation in which the retaining structure is used.

This thesis presents tests carried out using miniature piles loaded for the first time in a manner that closely replicates that of a steel sheet pile (SSP) wall. Tests show that friction between piles can in certain circumstances largely prevent the development of RMA. Investigations prior to this research have found that interlock friction causes only mild increase in strength. The present investigations provided a more realistic simulation of ground conditions, adopting span to depth ratios similar to those found in real life pile walls.

A numerical model simulating the behaviour of realistic pile wall conditions has been developed and validated using the results from scale piles. Use of the numerical model has demonstrated that restrained SSP walls with capping beams are unlikely to exhibit RMA. However, cofferdams propped at their tops and bottoms are likely to exhibit the full effects of RMA and should be strengthened as a result to ensure safe design. This numerical model has produced a series of curves that can be used to estimate the effects of RMA on strength and stiffness of U-section piles.

Table of contents

List of figures

List of tables

Acknowledgements

Firstly, I would like to say to everyone that I had contact with over the duration of my research that always offered a solution to the problem, 'Thank you'. However, I would also like to say to all those that didn't, a bigger 'Thank you!'

As with all research projects there are always people whom without their help and understanding the research would never be completed. These people have provided opinions, advice, materials and products all of which aided the research. At Cranfield University, the Engineering Systems Department's staff and technicians whom provided an excellent service from technical advice to the workshop's ability to produce quality products whatever the design. Acknowledgement must also be made to the sponsors of the research, the Engineering and Physical Science Research Council and the Corus Group, without their support and need for technological advance this research would not have taken place. I must also mention British Aluminium for supplying all my test specimens.

Half way through the research I had to transfer Universities. At first I thought this would present difficulties for both me and the progress of the work. I was wrong! Cranfield and Southampton University made the transfer simple and straight forward with both helping in everyway possible to accommodate me, I am very grateful for this.

Having transferred university the staff and technicians at Southampton provided a great service in both the laboratory and the office. They made me feel like I had been there for the whole of my research. I initially had my doubts that my research would take 2nd place to those already there, this never happened and I was accommodated to the full. I am most grateful to Southampton University for taking on my research. I feel I must also mention my friends at Southampton; Chris White, Howard Clarke and Ken Lewis, all of which made me feel welcome in both the office and of course the pub, where some of our best philosophies were founded!

A special thank you has to go to Chris Couldrick and Mike Dalzell as my life as a PhD student may well have been bland, uninteresting and hassle free had it not been for them. If it wasn't for their incessant interruptions and frolicking about I may

well have only half enjoyed the life of a researcher. Cheers lads and thanks for the beers and space hoppers!

To my girlfriend Clair, the one that has put up with time apart and my incomprehensible rambles about a subject in which she has little interest. Somehow, Clair always made me feel that she was following my work. Thank you for providing conversation other than academic nonsense and engineering drivel, for your company and for your opinions of me when I am 'not in the best of moods'... Thank you.

Thanks are also due in the direction of my family, my parents and my siblings. I would like to thank my parents for putting up with me back at home when I needed food and shelter so I could complete my writing. To my brother and sister, for wishing me good luck every time I saw them. I am sure without luck this may not have been possible to complete.

Finally, I feel I should mention my supervisor, Dr. Mike Byfield, without which this project would not exist. I would like to thank him for his constant support encouragement and mentoring by which I mean badgering, harassing and generally kicking me into shape to enable the research to progress at a good pace. Undoubtedly I owe this project to Mike, his enthusiasm and his over active red pen. I am sure that pen will be bored without me! Thank you once again.

Richard Mawer

Notation

The following notation has use throughout this thesis:

i. Latin upper case letters

A	cross sectional area
E	Young's Modulus
F	Force
I	second moment of area
L	length
$N.A.$	neutral axis
M	moment
P	applied load
R	Normal force
T	axial force
W	section modulus
Z	Elastic section modulus

ii. Latin lower case letters

a	variable distance
b	section width
d	section depth
e	eccentric distance
f	yield stress
h	section group depth
x	distance to pile pan
y	distance to pile interlock

iii. Greek letters

β	design reduction factor
γ	Partial safety factor
δ	deflection
σ	direct stress
μ	coefficient of friction

iv. Subscripts

ad	adhesion
b	reference to bending strength
composite, comp	fully composite action
C. Rd	resistance of the cross section
d	reference to stiffness
eff	effective
el	elastic
i	interlock
max	maximum value
m	section classification
p	pan
pair	non-composite pair
pl	plastic
R	frictional force
s	skin friction
section	single section
single	single section
y	relating to y-axis

Calibration of Equipment

All equipment used within this thesis was calibrated by the manufacturer or supplier of the apparatus, unless otherwise noted. Each item carried a certificate indicating the date of calibration and renewal date. Only equipment within these dates was used for measurements taken in the experimental work.

Any equipment that did not require calibration by the manufacturer or supplier was calibrated 'in house' using the relevant recommended procedures some of which are outlined within the body of the thesis.

1 Introduction

Steel sheet pile (*SSP*) walls are used extensively around the world. The two main sections used in the industry are the Larssen or 'U-section' and Frodingham or 'Z-section' piles (Fig. 1.1). Both types are connected together by interlocks running the length of the pile, which allow the sections to be slotted together to form continuous walls.

Fig. 1.1 U-section (left) and Z-section (right) profiles

Z-sections are marketed under the Frodingham brand name in the UK and U-sections are marketed under the Larssen brand. In general, both Z and U sections have the same range of applications. Typical uses include permanent works such as quay walls and bridge abutments, in addition to temporary works such as cofferdams in both marine and land based constructions. The use of *SSPs* is a relatively high cost solution. They are therefore usually uneconomical in situations where alternative concrete technologies are practical, such as diaphragm walls or secant pile walls. An advantage of *SSPs* in temporary works is that they can be extracted after use, allowing for recycling or direct use in new constructions.

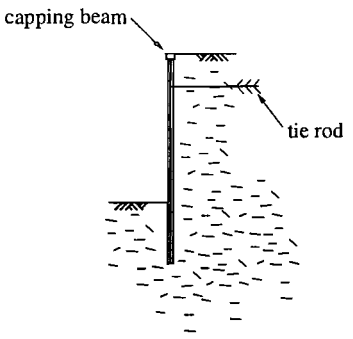

Fig. 1.2 Sheet piling

Although both Z and U profiles have a similar range of applications, Z-section piles have to be driven in pairs, because the low product second moment of area (I_{xy}) of a single Z-pile will cause the piles to buckle if driven singly. Importantly, U-sections can be driven as singles as well as pairs. The ability to be driven singly makes them well suited to hard driving conditions. This feature is particularly important in the UK, where over-consolidation boulder clays are a regular geological feature.

U-section piles have been in widespread use throughout most of the 20th Century. Relatively recently, concern has been raised about the bending strength of this pile section, because U-piles are connected together by interlocking joints located along the pile wall centreline (Fig. 1.3). As piles resist bending moments, inter-pile movement can significantly increase bending stresses. When this occurs the wall is said to have exhibited *reduced modulus action* (RMA), reducing bending strength and stiffness below the fully composite values normally assumed during design. In view of this concern, the recently introduced Eurocode 3 Part 5 has introduced reduction factors to account for the effects of RMA.

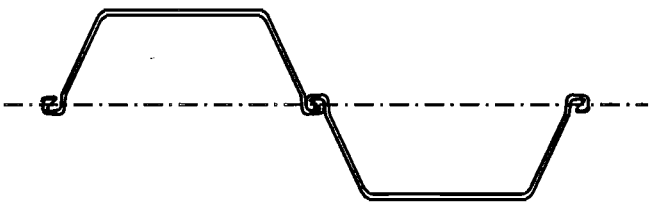

Fig. 1.3 U-section steel sheet pile pair

1.1 Reduced Modulus Action (RMA)

RMA is the effect of incomplete shear transfer between adjacent sections allowing relative movement between pile sections. This inter-pile movement can reduce the elastic bending strength by 50% of the strength of the composite pair (Eurocode 3). It has been noted (Lohmeyer, 1934) that shear transfer in U-section piles can vary between two boundary cases of zero shear transfer (Fig. 1.4a) and full shear transfer (Fig. 1.4b). In reality interlock friction will result in partial shear transfer (Fig. 1.4c), producing a stress distribution lying within the region bounded by the full and zero shear transfer conditions.

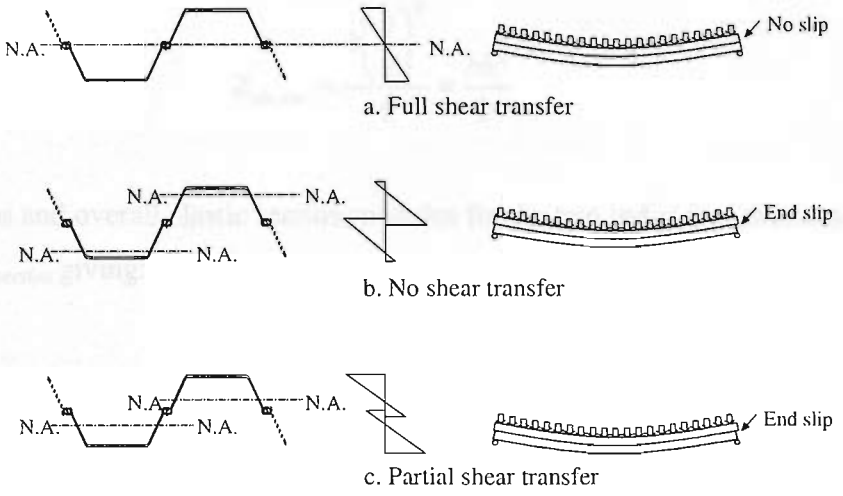

Fig. 1.4 Cases of shear transfer in pile section

1.1.1 Section Modulus Reduction

RMA is the result of partial shear transfer between two sections. This can be illustrated using two rectangular shaped sections and subjecting them to simple bending. First consider the two sections as a single element (Fig. 1.5) and the elastic section modulus, Z, is given as:

$$Z_{composite} = \frac{bh^2}{6} \qquad ...(1.1)$$

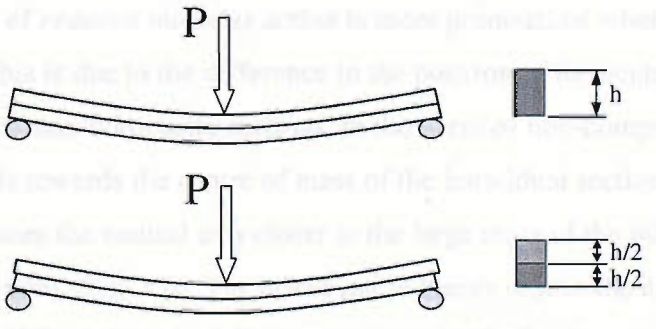

Fig. 1.5 Composite and non-composite sections subject to bending

In the case of non-composite behaviour consider the two sections to act individually, where no shear force is transferred from one section to the other (Fig. 1.5). Therefore the elastic section modulus is given as:

$$Z_{section} = \frac{b\left(\frac{h}{2}\right)^2}{6} = \frac{bh^2}{24} \quad \text{...(1.2)}$$

This gives and overall elastic section modulus for the two individual sections as double $Z_{section}$ giving:

$$2Z_{section} = Z_{pair} = \frac{bh^2}{12} \quad \text{...(1.3)}$$

From this simple analogy it can be seen that the elastic section modulus of a composite section is twice that of a pair of sections acting individually. i.e. non-composite action halves the elastic bending strength in this case. Properties of various U-piles are given in Table 1.1 for both single and combined sections.

Table 1.1 Properties of Corus made LX series steel sheet piles (British Steel, 1997)

		Combined sections		Individual sections	
LX series Steel sheet piles	**Depth mm**	**S_x cm^3/m**	**I_x cm^4/m**	**S_x cm^3**	**I_x cm^4**
LX 12	310	1208	18723	272	3236
LX 16	380	1641	31175	403	5615
LX 20	430	2022	43478	531	8148
LX 25	450	2525	56824	577	9607
LX 32	450	3201	72028	632	10938

The effect of *reduced modulus action* is more pronounced when applied to U-sections piles. This is due to the difference in the position of the neutral axis between the composite and non-composite sections. In the event of non-composite action the neutral axis shifts towards the centre of mass of the individual sections. This repositioning places the neutral axis closer to the large mass of the pile pan than in composite conditions (Fig. 1.6). The effect can in theory reduce the elastic bending strength to only 45% of that of a fully composite pair of piles for a mid-size pile such as the LX 20 pile produced by Corus.

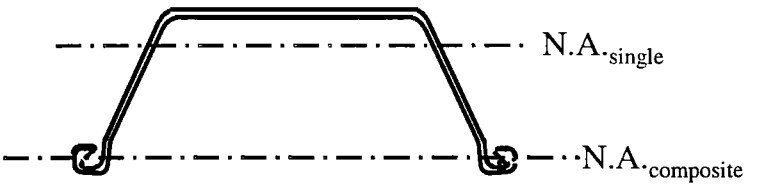

Fig. 1.6 Positions of neutral axis for composite and single pile sections

1.1.2 Second Moment of Area

The effect of partial shear transfer also effects the second moment of area and can have serious effects on the stiffness of a pile pair. This can again be illustrated using two rectangular shaped sections and subjecting them to simple bending. First, consider the two sections as a single entity and the second moment of area, I, is given as:

$$I_{composite} = \frac{bh^3}{12} \qquad ...(1.4)$$

In the case of non-composite behaviour where the two sections act individually the second moment of area for a single section is:

$$I_{section} = \frac{b\left(\frac{h}{2}\right)^3}{12} = \frac{bh^3}{96} \qquad ...(1.5)$$

Giving an overall second moment of area for the two individual sections a double $I_{section}$:

$$2I_{section} = I_{pair} = \frac{bh^3}{48} \qquad ...(1.6)$$

It can be seen that having two independent sections produces a reduction of 75% in comparison with the fully composite second moment of area. Once again, the effect is more pronounced on a U-section pile because of the position of the neutral axis. For example, *I* falls by 66% for the LX25 pile, in comparison with the fully composite equivalent section.

1.2 Eurocode

The recently introduced Eurocode 3 Part 5 (CEN, 1996) suggests that U-section *SSPs* do not act as combined sections and therefore do not develop the full section modulus when in bending. For this they have produced a set of advisory reduction factors (β–values) to be applied to the bending strength and stiffness of the sections. Specific values for the reduction factors are tabulated in *National Application Documents* (NADs) for each given country, allowing individual nations their own discretion in the selection of the final values.

1.2.1 Serviceability Limit States

In sheet pile wall design, excessive movement of the structure can have serious implications on adjacent structures and services. Eurocode 3 has highlighted that single U-piles are prone to large deflections. When calculating the deflections of U-pile walls the use of an effective flexural stiffness, I_{eff} is recommended. This is determined by taking into account the effect of incomplete shear transfer in the interlocks:

$$I_{eff} = \beta_d I_{comp} \qquad ...(1.7)$$

The recommendations made by the Eurocode for the reduction of stiffness (β_d) are shown in Table 1.2. These reduction factors suggest that crimping piles in pairs (doubles) or threes (triples) helps reduce the effect of reduced modulus action. Crimping involves welding of the interlocks to provide a full shear connection between adjacent sections.

Table 1.2 Eurocode recommended stiffness reduction factors for U-section SSPs

Section	β_d
Single	0.35 – 0.8
Double	0.7 – 1.0
Triple	1.0

1.2.2 Ultimate Limit States

To allow for reductions in the ultimate bending strength of U-piles due to the increase in stress caused by RMA, a second reduction factor has been incorporated

into the design code. This factor should be applied as follows (for class 1 and 2 cross-sections), where:

$M_{c.Rd}$ = Moment resistance of X-section

W = Section Modulus (el – elastic; pl – plastic)

f_y = yield stress

γ= partial safety factor

$$M_{c.Rd} = \frac{\beta_b W_{pl} f_y}{\gamma_{mo}} \quad ...(1.8)$$

For class 3 cross-section reduced bending strength is given by:

$$M_{c.Rd} = \frac{\beta_b W_{el} f_y}{\gamma_{mo}} \quad ...(1.9)$$

The reduction in bending strengths suggested by the Eurocode can be seen in Table 1.3. Eurocode 3 also suggests that paired sections (crimped) do not achieve full modulus due to phenomenon called oblique (biaxial) bending. This effect has subsequently been proven to be negligible (Crawford & Byfield, 2001). The concept of crimping piles involves the welding or pressing together of common interlocks to form a panel of two or three sections. According to Eurocode 3 this prevents any inter-pile movement, but it can present driving problems in hard soil conditions.

Table 1.3 Eurocode 3 recommended bending strength reduction factors for U-section SSPs

Section	β_b
Single	0.55 – 1.0
Double	0.8 – 1.0
Triple	1.0

1.3 Anecdotal Evidence

As stated previously, RMA is a rare structural phenomenon and to the author's best knowledge; there are no published accounts of RMA occurring in practice (British Steel, 97). Thus, anecdotal evidence gained from conversations with piling experts is presented. In many applications of U-section SSP walls, the effects of RMA have rarely been witnessed. RMA has been shown to occur in the laboratory, yet practical walls exhibiting RMA are rare, especially in the UK. Furthermore, it is

common practice in the UK, and other countries such as France and Japan, to ignore the effects of RMA during design. Interlock slippages, however, have been observed in certain types of constructions. Cantilever walls (Fig. 1.7) present one of the most notorious situations for interlocks to slide (Thompson, 2003).

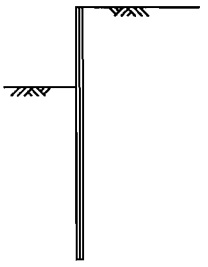

Fig. 1.7 Cantilever wall

Cantilever walls typically have two thirds of the piles embedded in the soil and one third exposed. They are generally used when ground anchors cannot be utilised to support the head of the pile. Therefore this system of support relies on the passive pressure to ensure stability. Soft soil conditions can hinder the development of full modulus action and an allowance for RMA is advisable. However, it has not yet been accurately quantified as to how soft a soil has to be before allowing for the reductions in section modulus, this decision is left to engineering judgement. This is eloquently suggested by Tomlinson (1977):

'Piling is both an art and a science'

Temporary cofferdams (Fig. 1.8) subjected to hydrostatic loads have been identified as another situation conducive to RMA. In cases of cofferdams in riverbeds the depth of embedment can be difficult to achieve as the soft alluvium often lies upon hard rock. If the thin layer of soft material lies upon impenetrable rock so that piles cannot achieve their required depth of embedment then the resistance to inter-pile movement can be significantly reduced.

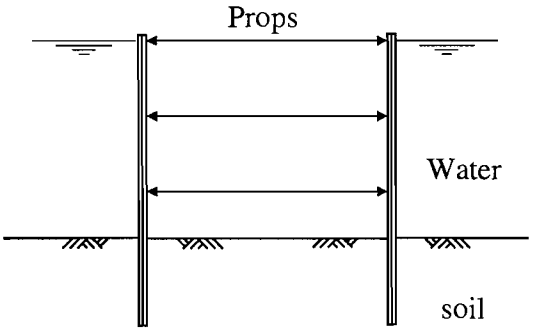

Fig. 1.8 Temporary cofferdam subjected to hydrostatic load

The presence of walings may have little effect in preventing RMA as they are typically only connected to the out pans of the pile wall. This still allows every other pile to act individually and effectively only increases lateral stiffness and has little effect on the overall bending strength. To increase the walls ability to act as a single entity would require walings welded to every pile section giving a solid physical connection across the interlocks. Creating this connection at the head of the piles is simply done by providing a capping beam, not usually used with cofferdams and cantilever walls, however this does not provide any restraint lower down the section. However, the primary reason why cofferdams resisting hydrostatic loads suffer from RMA is believed to be because they receive their full design loading immediately, which may not be the case with soil loads; and because there is no soil in the interlocks throughout the majority of the length of the piles.

In both cantilever walls and cofferdams with hydrostatic loads, piles can also be used in crimped or welded pairs, or in extreme cases triples. This helps the piles to generate their full section modulus while in conditions conducive to interlock slippage.

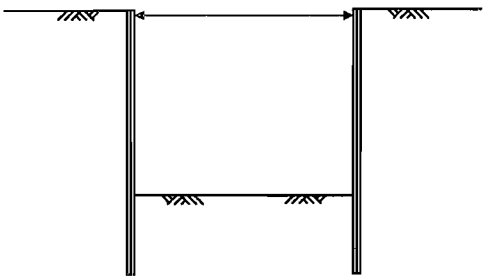

Fig. 1.9 Temporary cofferdam subjected to soil load

Not all situations involving cofferdams prove to be a problem. Temporary cofferdams with soil load (Fig. 1.9) have not generally presented problems with RMA. The reason why this occurs is yet to be quantified or fully understood and provides one of the aims of the research reported herein. The presence of soil in the interlocks may have the effect of increasing friction and therefore allowing greater shear force to be transferred.

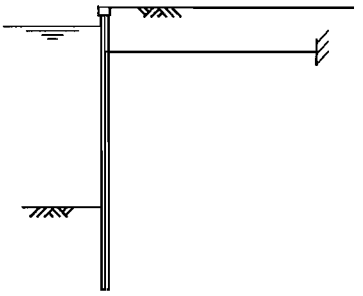

Fig. 1.10 Quay wall

Quay walls constructions (Fig. 1.10) are the least likely forms of sheet piling to be susceptible to RMA. Although subjected to hydrostatic loads on one side this presents no problem to the shear force transfer across the pile interlocks. Quay walls have two features that could be the major factors in preventing RMA from occurring. Firstly, the process of driving the piles introduces soil into the interlocks. The second factor is that inter-pile movement is further prevented with the presence of a capping beam usually formed from concrete and effectively prevents any movement at the pile head.

1.4 Aim of Research

The research presented in this thesis is based on experimental data from the testing of $1/8^{th}$ scale piles extruded from aluminium. Scaled sections have been used due to the difficulties in testing full-scale piles in a laboratory. Using these tests it is the authors aim to provide an increased understanding of the structural behaviour and interaction of U-section sheet piles installed as single sections. This will provide new knowledge detailing the influence of how realistic loading arrangements affect the interaction of adjacent sections. The research will also investigate factors such as interlock friction caused by soil-structure interaction. These laboratory based tests will be used to validate a mathematical model that will predict behaviour of sections

connected along the neutral axis of the combined sections. Thus attempting to provide answers for the following:

- What influences RMA?
- Quantify the effect of RMA under realistic loading arrangements.
- Effect of soil-structure interaction and friction within the interlocks.

As a result of the limited research in this particular area there are no prescribed testing procedures or apparatus dedicated to this field of investigation. To enable the research to be carried out test apparatus have had to be designed and fabricated. Previous tests in the area consisted of simply supported beams tested under 3 or 4-point loading systems. These conditions do not accurately model the ground conditions that sheet piling would experience in practice. The development of the new testing apparatus has made possible the application of more intricate loading systems that closely simulate realistic ground pressures.

2 Literature review

Piling has been used for many centuries and as technology has advanced throughout the years different materials have been used to fabricate piles. This chapter presents a brief history of how piling has developed and reviews the classical design methods and early research. The chapter also looks briefly into modern design methods, codes of practice and research carried out to investigate RMA. Consideration is also given to the impending European standards and the research supporting the document that has led to the widespread concern over *reduced modulus action.*

2.1 Historical Background

The objective of the bearing pile is to allow softer weaker soils to be bypassed by transferring load though to stronger layers. In contrast *SSP*s retain soil to form walled structures such as quay walls. From the first millennium to modern day constructions, piling has been an effective method for building load bearing foundations and retaining walls.

The very first use of piling has not been credited to a particular civilisation but it is generally accepted that the earliest developments in timber piles where during the Chinese Han Dynasty (200 BC to 400 AD). In Britain there are numerous examples of piling used to construct riverside structures, such as bridge piers and abutments that date back to the Roman Empire (Tomlinson, 1977). The Pagoda of Longhua, built in 977 during the Sung Dynasty is regarded as one of the first examples of bearing piles used to support large-scale structures (Kerisel, 1987). The next major advance in piling technology was the birth of the cast iron pile in the 19th century. First used in the UK in the 1820's to build Bridlington Harbour's North Pier, these sections where brittle and fractured easily when they encountered hard driving conditions. The USA continued to favour timber piling until improved sections were developed. Wrought iron took over from cast iron in the early 1900's but was still a difficult material to manipulate and complex rolled sections were impossible with the available technology (Mackley, 1977).

In 1897 Larssen invented his U-section pile. Larssen's pile was constructed using a rolled trough with riveted Z-sections to form the interlocks. The main advantages of the section remain unchanged and include:

- Low cost
- Minimum need for bracing
- Stiffness to enable driving without deforming the section
- Water tightness
- Economical and practical manufacturing process.

The first hot rolled *SSP*s were manufactured in 1901 in Chicago and were known as the Jackson Pile (Mackley, 1977), although they were developed through various establishments, including the Appleby Frodingham Steel Co. Ltd, the British Steel Corporation (presently Corus) and Larssen (which merged with Hoesch in 1966).

2.2 Geotechnical background

In comparison with other areas of structural engineering, there have been relatively few investigations carried out to understand the behaviour of *SSP*s. The majority of the research that is available has been concerned with the geotechnical aspects of the retaining structures, rather than the structural aspects of behaviour. In this topic of research the focus has been directed towards the modelling of soils in order to calculate soil pressures acting on the structure.

The method developed by Coulomb in 1776 for the design of retaining walls, albeit with modifications is still employed today. Coulomb observed that the majority of failures tended to be planer and proposed that the ultimate loading could be calculated by considering the point at which the structure begins to fail i.e., the Limit State (Craig, 1997). The following presents a review of the development of Coulombs first design method.

2.2.1 Classical design methods

Early methods of design have followed the geotechnical research of the time. It is a valuable exercise to examine the early methods before considering the basis of modern codes of practice and design. This first documented method of design was the conventional method established by Coulomb in 1776 and further developed by

Rankine in 1857 (Smith & Smith, 1988). The method developed from Coulomb's early work for the design of retaining walls is known today as the *Free Earth Support* method. It is called this because the bending moment is calculated assuming the pile is simply supported between the prop and the lower third point of the passive resistance and there is no consideration of fixity below the level of excavation.

2.2.1.1 Free earth support

The free-earth support design approach assumes that the base of the wall can move forward and is free to rotate. Free earth conditions cannot be applied to cantilever walls because if the toe of the wall is able to rotate then the wall will fail. It is assumed that the active and passive pressures acting to the back and front of the wall are fully mobilised. However, this method produced heavier and uneconomic solutions compared to previous timber wall designs using older empirical methods. This prompted Christiana in 1902 and Ehlers in 1910 to analysis existing timber sheet piling (Williams, 1989). Using the free earth support theory the walls were found to be overstressed by up to four times that of the design stresses normally used in design. Evidently these walls had stood the test of time and showed no signs of degradation and the study concluded that the design methods were over conservative. Engineers accounted for this variation by assuming a redistribution of the active earth pressure on the back of the structure as a result of soil arching causing a reduction in the overall bending moment experienced by the piling. As a result of these findings Christiani & Neilson carried out the design of a reinforced concrete anchored sheet pile wall at Aalborg (Crawford, 2003). Assuming only three times the allowable stress in the design, the wall was more economic than previous corresponding timber structures and is still standing today. Unfortunately this design did not provide any precise method that future designs could follow despite the obvious success of the structure.

The relative failure of this method to produce approach to design led to further development by the Danish Society of Civil Engineers and was known as the *Danish Rules Method for the design of sheet pile walls* (Williams, 1989). First published in 1923 the method was a modification of the free earth support method, with allowances for the redistribution of soil pressure behind the pile wall, known as soil arching. The investigations were made on existing timber walls with the difference

between the inferred bending moments and those calculated by conventional methods being accounting for by soil arching. Leading on from these findings research into the effect of arching on the back of flexible walls was carried out (Stroyer, 1935). These tests were carried out on small scale, approximately 1m long, sections in a sand box. The box was filled with sand whilst the wall was prevented from flexing by applying moments to the wall. This produced an active pressure distribution behind the wall, also determining the maximum bending moment acting on the wall. The wall was then flexed outwards by reducing the applied moments by known increments. By comparing the moments applied to the wall and the measured deflection Stroyer was able to determine if there had been any pressure redistribution and by how much it had reduced the maximum bending moment. He concluded that there had been a redistribution of pressure on the back of the flexible walls. This reduction was to some extent supported by the *Danish Rules Method.* However the reduction measured was considerable smaller than that assumed in the Danish Rules, thus there is a suggestion that there must be some other form of moment reduction with anchored sheet pile walls.

2.2.1.2 Fixed earth support

Whereas the Danish engineers were considering an empirical view of the problem, two German engineers approached the situation from a theoretical stance. There assumed that if the wall is sufficiently embedded lateral movement would be prevented and that the toe of the pile would be restrained against rotation. From this they presented what is now known as the *fixed earth support* method of design. The embedment depth is calculated by treating the wall as an elastic beam that is simply supported at the point of anchorage and fixed at its base. The resulting design is known as the 'elastic line' method. Unfortunately this method was considered laborious (Padfield & Mair, 1975) due to the iterative process required to determine the depth of embedment and therefore a further simplification of this method was often used. The simplified method was proposed by Blum around 1930 (Blum, 1931) and was known as the 'equivalent beam' method. This method assumed that the point of contraflexure is located near the toe of the wall. The earth pressures developed below the point of contraflexure can be modelled by the application of a single point load. To ease calculation the remaining earth pressure is idealised from

the true distribution and given a triangular distribution. This method transforms the statically indeterminate structure into one that is determinate, simplifying the calculation of the bending moments and the depth of embedment significantly. However, this lower point of contraflexure is dependant on the internal angle of friction of the soil and is determined using the *elastic line* method.

2.2.2 Research into sheet pile walls

During 1940's Tschebotarioff carried out a series of tests on anchored sheet pile wall models, continuing Stroyer's work. One of the main intentions was to investigate the considerable reduction in bending moment, from conventional values, often to be thought of the result of soil arching (Tschebotarioff, 1949). Tschebotarioff found that the soil below the excavated level could not be ignored and developed a test apparatus that was capable of modelling an anchored sheet pile wall allowing the soil above and below the excavated level to be monitored.

Two methods were performed to analyse the model sheet pile wall. Firstly, a straight forward drive and excavate test which involved attaching a tie-rod to a pile placed in a sand box. It was then filled both sides of the wall. Datum readings were then taken and then one side of the wall was excavated to the required depth and measurements were recorded. The second method was to simulate a 'back filled' wall. This is where soil is placed evenly on both sides of the wall to a depth equal to the required embedment. The tie-rod was then attached and datum readings taken. Backfilling was then carried out behind the wall and measurements recorded. In order to investigate the walls behaviour strain gauges were attached to the model piles. From these measurements of strain an accurate calculation of the bending moment acting on the piles was achieved. From the bending moment distributions the shear forces and earth pressures could be inferred by single and double differentiation, respectively. These tests enabled engineers to gain a clearer understanding of the structural behaviour of sheet pile walls that had not been possible from previous research experiments.

Tschebotarioff effectively demonstrated that the reduction in bending moment was due to fixity below the level of excavation opposed to previous findings suggesting soil arching. This basically reduces the effective span of the wall and thus the resulting bending moment. Further modifications to the *fixed earth support*

method were developed as a result of his findings. Conclusions of these tests also showed no correlation between the depth of the point of contraflexure and the angle of friction in the soil, assumed by Blum's equivalent method.

2.2.2.1 Peter Walter Rowe

Rowe's work is consider by many as the most comprehensive work carried out to date to investigate the effect pile flexibility has on anchored sheet pile walls His work covered the geotechnical aspect of behaviour although it does not detail the structural aspects concerning the performance of U-pile sections. The first series of tests performed were experiments on anchored retaining walls (Rowe, 1951) and investigated the effect of soil arching similarly to Stroyer's work (1935) and the moment reduction due to fixity above anchor level discussed by (Tschebotarioff, 1949). He discovered similar results to both of the previous findings showing that bending moments could be predicted for a number of different cohesionless soils. Much of this work focused on wall flexibility and the effect of soil type on this flexibility. His findings identified a relationship between flexibility of the wall and the position of the resultant passive pressure; the more flexible, the higher the point of action of the resultant pressure. This effectively reduces the span of the wall and therefore significantly reduces the overall maximum bending moments and deflections.

Rowe's work has formed the basis of some of the more recent design codes still used today. His work was extended using modern facilities by (Bransby and Milligan, 1975). This work was based in a laboratory and used models in dry sand. Using an advanced method unavailable to Rowe, Bransby and Milligan used X-rays to record soil deformations. Many tests were carried out on different types of sand, but as with Rowe's work they concentrated on activity in the soil and not the behaviour of the structure. However this led to greater understanding of the passive and active soil pressures acting on the wall itself.

2.2.2.2 Finite element analysis

The earliest finite element model (FEM) of a sheet pile wall known was presented in 1972 by Bjerrum (Williams, 1989). This model was based on a wall conjured almost 15 years earlier by Edelman *et al.* (1958). This was an anchored

sheet pile wall 19m high with an embedded depth of 8m and a ground anchor at 6m from the head of the pile. This model was used to compare bending moments with those determined from Row's method. It was found that the bending moments calculated using this FEM were considerable higher than in Row's method, however the arching of the wall was found to be more stable than previous investigations had considered (Williams, 1989).

More current FE models and analyses have been presented using similar conditions to that of Bjerrum's analysis. Smith and Boorman (1974) using slightly different elements for the wall and soil found a good correlation with the previous investigations. However, further analysis suggested that the wall became unstable with medium stiffness wall and certain anchor yields. High yield anchors caused rapid increases in the bending moments in the wall well in excess of those measured by Row.

During the 1980s the design of retaining walls were investigated for the purpose of evaluating the accuracy of the current design methods. The then current design methods for propped walls were based on approximate limit equilibrium calculations. A factor of safety was used to ensure stability and to restrict wall movement to acceptable levels. However, no distinction at this time was made for the different types of retaining wall available or method of construction (Potts & Fourie, 1984) and dealt with stiffness more akin to concrete diaphragm walls. However, it is the following publication that provides more interesting analysis concerning steel sheet piling by investigating the effect of varying wall stiffness.

Potts and Fourie (1985) article concerning the effects of wall stiffness on the behaviour of a propped retaining wall used a FEM with an elasto-perfectly plastic soil model. This regards the elastic soil modulus as constant until yield stress is reached. No reference is directly made to RMA but a description of a 'rigid wall' and 'soft wall' are made with regards to a steel sheet piling and are given different bending stiffness. The results of the model suggest that rigid walls generate higher levels of stress compared to flexible walls with the soft wall and the *SSP* wall having similar stress levels along their length. The conclusion states that piles of the steel type that are flexible demonstrated that the predicted bending moments are much lower than those given by simple design calculations. However, it is suggested that the results also imply that stiff walls in stiff clays could exceed the design values for bending moments and prop loads based on the same design methods.

2.3 Monitoring of sheet pile walls

Due to the limited knowledge in field evidence in the performance of steel sheet pile walls two new anchored sheet pile walls were monitored. This exercise was to gain the complete stress history of the piles and tie-rods for comparison with expected results based on then conventional design approaches (Matich *et al.*, 1964). The work reported does not cover the period in which the wall experienced its full design load but it does provide valuable insight into the practical behaviour of a real sheet pile wall. However, a note is made by the author that the information is too limited to draw conclusions with regard to future design.

The two test situations consisted of a wharf and shipping channel extension located in Hamilton Harbour, Toronto. The soil conditions in the areas were natural soil of a granular consistency and dense sandy silt respectively. Instrumentation used to monitor the behaviour of the sections at both sites were Wilson slope indicators and stress measurements of the tie-rods. It is reported that out of the many readings taken on both projects only one case was found to be driven straight and vertical. Interestingly, Match *et al.* (1964) mentions that a 5^{o} plan rotation of a Z-section pile reduces the moment of inertia by 10% from the designed capacity. This makes driving the Z-piles accurately an important issue when designing with small factors of safety.

Direct comparison between theory and observed values of the bending moments in the wall were not possible. To compare these values would require knowledge of the amount of friction present in the interlocks. This noted by the author stating that derivation of the bending moments in not possible as the knowledge of the amount of friction generated in the interlocks is unknown. Thus an effective moment of inertia could not be determined. It is suggested that the degree of friction generated in the interlocks is dependant on the material entering and its ability to resist slippage.

In 1974 on the north coast of France at the Port of La Havre, construction of a steel sheet pile wall for a roll on-roll off ferry terminal was required. Engineers form the Technical studies department of the La Havre Port Authority used this opportunity to instrument a steel sheet piling wharf. The main objective of this study was to test measurement equipment giving the active and passive earth pressures.

However, in doing this work other observations were also taken and reported (Hebert *et al.*, 1978). The most interesting of these observations were those that indicated that interlocks of the U-section piles slipped relative to one another providing evidence that the modulus of inertia used for the pair of piles did not correspond to reality, reduced modulus action.

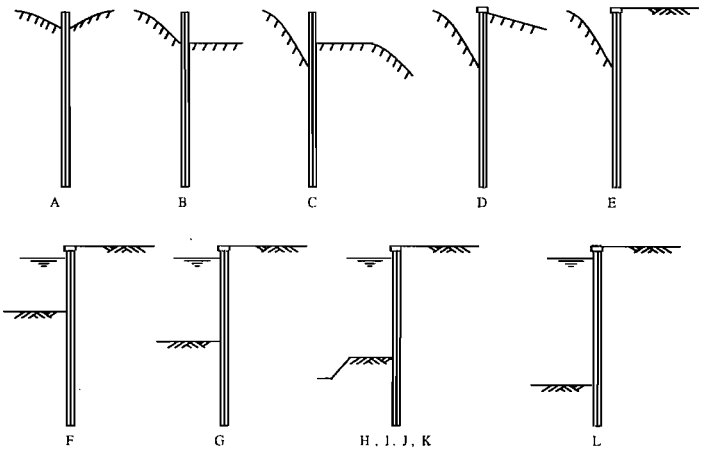

Fig. 2.1 Stages of work and measurement at La Havre

The section of the piling monitored was made up of Larssen 3 sections approximate 19m in length with tie-rods placed at 1 metre centres and 5m below the level of the concrete capping beam. One pile pair in the wall was monitored using a total of 10 Glötzl pressure gauges and 18 strain gauges. Gauges were fitted to the section before installation and all but one strain gauge survived the driving process. The gauges were situated on both the pile pan and the interlocks of the pile sections allowing for accurate stress distributions to be drawn. The measurements were taken over a period of 15 months of construction. The construction process and measurement program can be seen in Fig. 2.1. Fig. 2.1A represents the phase at which all gauges were set at zero and B through to L the phases in the construction where measurements were taken.

Presented in the paper is a figure of the stress distributions of the measured sections at each of the phases of construction at the three different depths (Hebert *et al.*, 1978). Although the author observes interlock slippage from the readings, looking closely at the stress distributions the extent of RMA is not within accordance of that suggested in Eurocode 3 part 5. The results suggest that interlock stress are

similar to pan stress and rarely exceed them by a factor of 1.6. Typically RMA produces interlock to pan stress ratios of 4.1 in extreme cases. Therefore this experimental data provides evidence that RMA is not as significant in practice as theory suggests. Hebert *et al.*'s (1978) investigation did not produce any deflection data other than topographical displacement of the capping beam thus the affect of interlock slippage on flexibility can not be assessed.

Although it was not the main aspect of the investigation of the steel pile wall to look at the effects of interlock slippage between adjacent piles strain measurement taken during the tests indicated that a significant amount of stress was observed at the interlock. This suggested the partial independence of the sheet piles in the wall. Herbert *et al.* produced a short simple mathematical investigation into the interlock slippage deriving an '*equivalent modulus*' calculation to compare with the specified Modulus of Inertia of the section profile. An assumption that the stress distribution is comprised three components a concept first encountered by Lohmeyer (1934). These were a specific moment, a complementary moment and an axial compressive load from the capping beam and friction. It was then assumed that the axial load equal zero and therefore the distribution and be split into two components. The first component called the *specific moment* representing the forces applied to each sheet pile individually and the *complimentary moment* representing the force applied to a pile pair assuming singularity. Using these components and analysing the experimental results the equivalent modulus is presented at two phases of the construction process.

The equivalent modulus calculated from the observation gave evidence to suggest that the piles showed a 25% to 50% reduction in strength. In conclusion the author expressed concern that the modulus of inertia of a pair of steel sheet piles does not correspond to reality.

2.4 Research into Reduced Modulus Action

Research on the subject of *RMA* in U-section *SSP*s is comparatively sparse. An acknowledgement made by Williams that there is limited work provides some evidence that there is little known about the effects of reduced modulus action (Williams and Little, 1996). This could account for the diverse approach to the treatment of this problem by design engineers.

2.4.1 Lohmeyer 1934

The earliest referenced work concerning the reduced bending strength caused by interlock slippage of U-section steel sheet piling was the *'Analysis of sheet-pile bulkheads'* by (Lohmeyer, 1934). The paper introduced a mathematical model that attempted to quantify the effects interlock slippage can have on the bending stress in piles. The theory and calculations were influenced by similar work carried out around the same time (Blum, 1931). Lohmeyer applied conventional elastic beam theory to U-section piles and examined the effect that the transfer of shear force at the interlock of the piles can have on overall bending strength. As discussed previously, two boundary cases for shear transfer were considered; firstly the condition of full shear transfer (a) and secondly the zero shear transfer condition (b). However, it was recognised that partial shear transfer (c) is more likely to occur than either boundary case. Lohmeyer's analysis provides an approach to quantifying how the transfer of shear force to adjacent piles is proportional to their strength.

The numerical model suggested that a single section in a sheet pile wall experiences two forms of loading. Firstly, direct load from the soil pressure and secondly, the effect of the shear force transfer from adjacent pile sections causing two longitudinal forces to act along either interlock. The model did not identify the causes of or whether RMA regularly occurs in U-section pile walls, these questions were left unanswered. Although the model fails to identify the causes, it is acknowledged that the most likely cause of interlock slippage is insufficient driving. Lohmeyer's observations explain that if the interlock friction cannot transmit the shearing force fully, then the extreme fibre stresses will increase. This paper did not consider the effects of locking up but mentions the potential for *'jamming'* of pile interlocks.

In conclusion, Lohmeyer suggested that the question of the strength of *SSPs* and, therefore the question of the section modulus is often over-estimated as compared with the careful examination of penetration. Lohmeyer's closing statement mentions that without exception, failures that do occur are not be because the wall is too weak, but because the piles have not been driven to a sufficient depth.

2.4.2 Williams and Little 1992

Williams and Little reintroduced and expanded Lohmeyer's 1934 method of analysing U-section piles, showing how the position of the neutral axis varies with the degree of shear transfer (Fig. 2.3). Their analysis of RMA was based on the testing of a 30m long retaining wall located close to the A1(M) in Hatfield on a site dominated by granular soil conditions. The data from this construction were obtained between 1985 and 1988 and were originally analysed and reported on by (Symons, 1987). Associated with the work was a report that investigated the anchorage (McNulty & Little, 1987), although the major analysis of RMA was carried out by (Williams & Little, 1992).

Data from the testing were obtained using various methods of instrumentation. Horizontal deflections and direct bending stresses were measured directly using inclinometers and strain gauges. Two different types of gauge were used: arc welded vibrating wire strain gauges, and spot-welded electrical resistance strain gauges. Horizontal deflections were measured at 500mm vertical intervals along the entire length of the wall. These provided a detailed analysis of the walls flexibility. However strain was only monitored on two pile pairs, of which both had gauges attached to the pile pans, enabling only extreme fibre stresses to be measured. To enable an accurate stress distribution to be drawn a second set of strain data measurements were needed. Unfortunately, only one pair of piles from the whole wall fulfils this criterion and Williams and Little have based their analysis around its measurements.

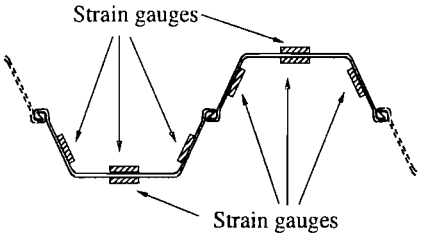

Fig. 2.2 Placement of Strain gauges of the Hatfield A1(M) investigation

Looking more closely at the monitoring of this single pair of piles, inspection of the positioning of the strain gauges shows potential problems. For optimum accuracy, a set of strain gauges would have been positioned at the interlocks, as well

as in the pans, since a reduced amount of interpolation would be required to define the full stress distribution. Unfortunately, the strain gauges located on the web of the piles were only 76–90mm away from the pan (see Fig. 2.2). This required data to be interpolated over a large section to produce a stress distribution for the whole pile pair. This in itself can be a source of inaccuracies, but coupled with the variation observed in the gauge readings, any error recorded would have been magnified. This variation or scatter in the gauge readings was considerable with only 71 to 78% of the gauges surviving the pile driving.

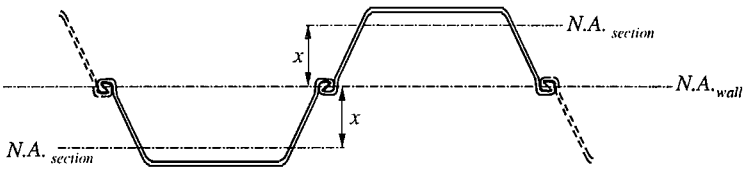

Fig. 2.3 Positions of neutral axis of individual sections, where X reduces with increasing shear transfer

Using the strain data from this pair of piles the applied moments and the corresponding effect of RMA was calculated. However, because of the above mentioned problems a further check for RMA was carried out based on deflection measurements. In calculating bending moments from deflected shape, $\frac{d^2v}{dz^2} = \frac{M}{EI}$ is used. Unfortunately both M and I were unknown. To create a solution the full composite section modulus of the piles was used. The resulting moments were then compared with those calculated from the strain data and, perhaps unsurprisingly, they were found to differ.

Table 2.1 Summary of previous research on steel pile walls

Author	Date	Pile section	Effective pile stiffness
Thompson & Matich	1961	Algoma	0.4-1.0
Matich et al.	1964	Larssen	0.4-1.0
Baumann	1934	Larssen	0.4-0.89
Bromborough Lock	1987	Larssen	0.32-0.41

The results showed that RMA reduced the moment of inertia by between 28 and 43% of the fully composite value. Although this fits in the range of stiffness values determined by other investigations (Table 2.1), it should be treated with caution because of the problems regarding the methodology. Williams and Little conclude

that the reduction in stiffness and associated reduction in strength is not critical when conservative design methods are used, for example, free earth support. Less conservative design methods (Rowe, 1952) do however cause concern as the reduction in performance due to RMA may have far greater significance.

2.4.3 Interlock friction analysis

More recently the analysis of steel sheet piling and the behaviour of the surrounding soil have entered the finite element (FE) analysis phase. Complex computer models made up of tiny elements. However, these conceptual models rely on experimental data in which they base the initial parameters. Relatively little is known about the effect of soil entering the interlocks of steel sheet piles and how it interacts with the structure. For the development of a FE model the amount of interlock friction in a steel sheet pile wall was investigated (Vanden Berghe *et al.*, 2001). The FE model was designed to evaluate the influence friction on the flexural stiffness of a sheet pile wall.

The friction in the interlocks was measured using two reduced scale pull out tests. These tests were not designed to analyse the behaviour of a sheet pile but to just provide parameters to be used in a FE model. To ensure the most accurate evaluation of the interlock conditions the sections were driven into sand using vibratory technique, the most commonly used method. It is suggested that the resistance in the interlocks is determined by the method in which the piling is installed. Found in a few test specimens, where pull-out forces were found to be high, were soil particles that had formed solidarity locking the interlocks. This phenomenon is likely to be a reason as to why practical pile walls do not exhibit RMA to such an extent as laboratory experiments have suggested (Schillings & Boeraeve, 1996).

Despite the advances this research has provided it still does not allow for the calculation of the friction that might be expected in full scale steel sheet piles under full loading from deep embedded depths. These tests carried out in small volumes of sand with little loading cannot provide a coefficient of friction that may be applied to larger sections. To provide this information a known applied load would be needed. However, this still does not allow for the complex deflected shape that may aid resistance to inter-pile movement.

2.4.4 Further research into U-section piling: oblique bending

The concern of the occurrence of RMA and the claims of the devastation affect it has on both strength and stiffness of the sections, guidelines have been made to crimp pairs together. This involves welding the common interlock of a pair of piles together to form a double U-section. This has considerable disadvantages especially in the handling and driving of the sections in hard ground conditions. However, it was initially believed to solve the occurrence of RMA in soft soil conditions (BSI, 1951).

More recently, investigation into U-section piling has moved away from the effects of RMA in singly installed piles to the behaviour of piles crimped in pairs. Research suggests that crimped or double U-piles do not as previously thought generate a full section modulus (BSI, 1994). This is due to a rotation of the neutral axis of each pair under loading (Schmitt, 1998). This effect is know as oblique bending and occurs because a crimped U-section pile is asymmetrical and the neutral axis lies oblique to the line of the wall (Fig. 2.4). This phenomenon has taken much of the focus for research away from RMA of singly installed U-sections. Schmitt suggests that oblique bending can in a worst case scenario cause deflections of twice that calculated using the manufacturer's data (Schmitt, 1998). Schmitt concludes that neglecting the effects of oblique bending when calculating the displacements and bending stresses leads to the unsafe design of the retaining structure. Crimped U-sections have been used as guided in BS8002, without the consideration of oblique bending and the phenomenon has rarely been observed in practice (Crawford, 2003).

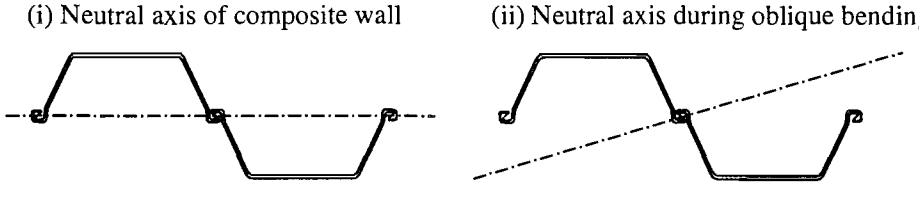

Fig. 2.4 Neutral axis assumed for a composite wall (i) and crimped pairs exhibiting oblique bending (ii)

Further to Schmitt's research on U-section steel sheet piling Byfield and Crawford (2002) investigated the effect of oblique bending. Experimental work

carried out on miniature piles in laboratory conditions looked at the effects of oblique bending in double U-section piling. Theory suggests that when oblique bending occurs, pairs of piles both twist and move laterally causing the whole wall to shift sideways. Arguably this lateral movement is prevented by the soil around the wall. It is the soil-structure interaction that is claimed to prevent this movement by Byfield and Crawford, (2002), '...piles restrained from lateral movement by soil-structure interaction... will not exhibit significant oblique bending'. Presented along side the experimental data is a numerical model predicting the behaviour of crimped U-section piles. In conclusion, if oblique bending is found to still occur due to lack of lateral restraint then a simple modification can be used to prevent oblique bending. The solution is by simply placing a single U-section between a series of crimped sections thus altering the direction in which the pile wants to move. This puts alternating series of crimped piles in the wall that act against each other and therefore prevent lateral movement. These single sections need only be placed sporadically in the wall therefore not allowing the wall to suffer from the apparent effects of RMA. As a result of this solution Crawford's PhD thesis suggests that reduction factors for crimped U-sections be taken as unity.

2.4.4.1 Full scale testing

At the same time as Crawford's and Byfield's laboratory based tests were being carried out, research in Europe also looked into the effects of oblique bending. As well as laboratory work, tests were also carried out on a full scale steel sheet pile wall. This wall was specifically designed to analysis the behaviour of steel sheet piles. This test wall was built in Rotterdam in a generally soft soil and peat layered ground with a Pleistocene sand at a depth of 16m. The wall formed a box with one set of facing walls containing the test sections. One wall was constructed of Z-section piles and the opposing wall of double or crimped U-sections. The aim of these test were to provide a benchmark for new models for the design of steel sheet pile walls in soft ground conditions. This experiment was known as the *Delft Sheet Pile Wall Field Test* and remains as one of the few full-scale field test to investigate the behaviour of U-section piling. It follows on from research carried out in sand using shortened steel piles retaining sand (Wolffersdorff, 1997). These earlier test

provided experience in the monitoring of sheet pile walls and soil-structure interaction.

The results of the field pile wall test aimed to justify the new European design rules being introduced for the safe design of sheet pile walls. However, engineers in some counties are finding that new design rules will lead to uneconomical designs (Byfield & Crawford, 2002) when using a U-section pile. The field test was also analysed by a PhD student D. A. Kort. His thesis looked at plastic design methods and the behaviour of U-section piling. Kort (2002) states in the introduction to the field test chapter that oblique bending is hardly ever observed in practice, a point reinforced by practicing engineers. Presented in the thesis are detailed results of the observed bending moments and deflection data comparing the action of the U-sections and Z-sections of the test walls. Oblique bending was observed in the wall in two U-piles. The variation in the occurrence of oblique bending is attributed to varying interlock friction. Oblique bending is considered to have a considerable effect on the strength and stiffness of U-section piles. The average values suggested by the research for the reduction in strength is 0.68 and for stiffness 0.73 of the composite section. This reduction may encourage the design engineer to choose Z-section piles over U-sections for economy and to avoid complex calculations. However, properties such as drivability and reusability must be key considerations in choosing the correct section (Kort, 2002).

2.5 Design codes for earth retaining structures

2.5.1 BS 8002: 1994 Code of Practice for Earth retaining structures

Tschebotarioff and Rowe were the pioneers for the first design methods in the UK, known as CP2 (BSI, 1951), but it was not until some 43 years later that The British Standard for the design of earth retaining structures, BS 8002 (BSI, 1994) was published. The new code adopts the philosophy of limit state design and does not specify specific design requirements such as overall and partial factors of safety. Previously CP2 imposed an overall factor of safety by reducing the passive resistance by approximately 1.5 to 2.0 or by factoring the shear strength parameters. Unfortunately this did not always result in the economical design of retaining walls.

Detailed in section 4.4 is the design of embedded retaining walls, including the design of steel sheet pile walls. Paragraph 4.4.4.3 makes specific reference to *Reduced Modulus Action*. The code assumes that U-section piles act as a composite structure if sections are driven to there full embedded depth and are not used in situations such as:

1. passing through soft clay or water;
2. prevented by rock from penetrating to the normal depth of cut-off;
3. used as a cantilever;
4. supported by props or struts but is cantilevered to a substantial distance above the highest waling or below the lowest waling.

For the conditions listed above the code recommends that the sections are welded or crimped in pairs to allow full transfer of shear between adjacent sections and to aid the development of the full composite moment of inertia. If this is not possible, then non-composite section properties should be used in design in accordance to the recommendations of the manufactures. Furthermore, no mention of made of the problem of oblique (biaxial) bending, although it is introduced into the Eurocode design guidance.

2.5.2 CIRIA Report 104

In the early 1980's research was carried out into the reduction of strength due to settlement with embedded walls in stiff clays and the various different design methods available for applying factors of safety to design against catastrophic failure or collapse. This research (Padfield & Mair, 1994) aimed to explain and compare the different methods available to designers. The four methods recommended were:

1. factor on embedment method (F_d);
2. factor of safety on shear strength (F_s);
3. factor of safety on moments (F_p);
4. factor of safety on moments after Burland-Potts (F_r).

The first method (factor on embedment) is probably the simplest of the four methods. Geometry, as in the anchor heights and arrangement of excavation are adjusted to satisfy equilibrium with fully-mobilised strength and is then readjusted to produce a margin of safety. This method is used considerably in the *British Steel* (Corus) *Piling*

Handbook (British Steel, 1997). The second method of applying a factor of safety is to reduce the strength parameters by a single factor of safety before the geometry of the wall is changed. This method is considered to be reliable and a consistent method for situations representation the greatest uncertainty (Padfield & Mair, 1984).

The final two methods covered involve adjusting the geometry of the design such that the restoring moments exceed the over turning moments by a predetermined margin using fully-mobilised strength parameters.

This CIRIA report also addressed the issue RMA, suggesting that in constructions located in stiff clays, full friction at the interlocks can be assumed and the full section modulus expected. The report notes that this in not accepted by all designers. The idea of welding the upper parts of the piles as they are exposed is advised to ensure full shear transfer but this depends upon the design life of the structure, since this presents problems when the wall is to be extracted as with temporary works.

2.5.3 Eurocode 3 - Part 5

In an attempt to remove barriers to free trade the European Commission has introduced a series of pan-European design codes for construction. These were named 'Eurocodes' and consisted of eight volumes covering separate design and construction aspects. Important to this subject is *Eurocode 3: Design of steel structures* but more specifically *Part 5: Piling*. This was not published with the original document but in March 2000 a final draft was released accompanied by the *NAD* (Nation Application Document) which contains country specific references in support of the design methods. This provides each individual state with the freedom to adjust what are termed "boxed-values" to their own specific requirements. They also allow for the incorporation of additional information and guidance specific to individual nation states. The research to support the design code was carried out by an amalgamation of interested parties, under the guidance of the *European Coal and Steel Community* (ECSC) and involve research establishments from the, Belgium, Netherlands, Germany and UK.

2.5.3.1 Development of Eurocode 3 part 5

Under guidance of the ECSC initial research was carried out to develop an understanding for the effects RMA on U-section steel sheet piles (Schillings & Boeraeve, 1996). The tests carried out at CRIF in Liege, Belgium aimed to quantify the effect of friction in the interlocks on the bending strength of single U-section piles.

Sheet piles are very difficult to test in laboratory conditions at full size. Therefore the sections tested in Liege were not full pile sections. Interlocks from Larssen piles were removed and welded on to either flat steel plates (Fig. 2.5) or H-sections. In addition, the specimens were only 1m in length and were tested in 3-point bending under a variety of interlock conditions.

Fig. 2.5 Schillings & Boeraeve (1996) sample of a test specimen.

Four types of specimen were tested; free interlocks, interlocks containing sand, lubricated interlocks and welded interlocks. The influence of sand in the interlocks was found to increase in stiffness by between 2 and 12%. It was thus concluded that the presence of sand in the interlocks did not increase friction enough to significantly prevent the development of RMA.

It can be argued that these tests did not provide a realistic loading arrangement, in particular:

- The size of the specimens tested where small, only 1m long whereas a typical *SSP* is 15m in length. Section depth was also noticeable less than found in practice. This combination produces shallow deflections and the relative moment between piles was less than 1mm. This is in contrast to the several centimetres of movement that would be expected form full-scale piles subjected to RMA. Moreover, these comparatively low movements may be insufficient to generate the full frictional force available from the sand.
- The tests used 3 point bending. Typical loading conditions for a retained *SSP* wall are significantly different, with the active and passive pressure

distributions producing two or three points of contraflexure. The maximum shear forces in 3 point bending are located adjacent to the free ends of the specimen, whereas the maximum shear force is typically located away from the ends of the piles under normal conditions. Therefore, 3 point bending may present a situation more conducive to RMA than found in practical pile walls.

- Capping beams are commonly formed from reinforced concrete at the head of the piles. These will prevent of inter-pile movement at this point. The tests carried out provided no assessment as to the effect this may have on the strength of the structure.
- Soil-structure interaction was not modelled. The effect of soil on the surface of the piles could help to prevent inter-pile movement and influence the development of RMA.
- The effect of corrosion in the interlocks on the transmission of shear between the piles was not considered.

Therefore, this investigation may have provided a lower-bound estimate of the strength of U-piles. Despite this potential conservatism these tests were used as the basis for Eurocode 3 part 5.

The most influential work as regards to Eurocode 3 comes from the doctoral thesis of Hartmann-Linden, (1996). The work was carried out using full-scale pile sections but reduced in length to 4m span. Hartmann-Linden analysed three section arrangements commonly used in practice; *single U-profile, double U-profile and triple U-profile*, and showed that each section arrangement demonstrated a reduction in moment of inertia (see Table 2.2).

Table 2.2 Reduction in I for zero shear transfer

Profile	**Reduction factor of I**
Single U-section	0.3
Double U-section	0.5
Triple U-section	0.9

Within the European Union a number of conflicting approaches to *reduced modulus action* had to be considered in producing the Eurocode. In Germany, it is usual to drive piles in crimped or welded doubles in normal conditions. Moreover, shear force transmission is checked when piles are situated in hydrostatic or soft soil

conditions or where lubrication was applied before installation. In contrast, the UK approach is to design sheet pile walls without consideration of RMA in situations other than those specifically identified as prone to RMA in BS8002: 1994. The UK manufacturers of U-sections, Corus, suggest that reducing the modulus of the section even under the condition outlined in BS8002 is not necessary based on past experiences with design using full modulus values (Piling Handbook British steel, 1997). French engineers have no official guidelines to the use of U-sections and often install single section with no consideration for reduction of the section modulus.

The generally soil conditions of each nation have a large impact on the importance of reduced modulus action. In the UK it is often difficult to drive sections and anecdotal evidence suggest that there is little occurrence of RMA but in the Netherlands where soil conditions are generally soft, RMA is a problem. The national standards recommend using reduction factors of 0.6 for section modulus and 0.35 for the moment of inertia when using single sections. It is only when triple sections are employed that full section properties are recommended.

2.6 Summary

The brief review of the past research surrounding sheet piling has shown that geotechnical based research has been developed further than the structural research into retaining wall design. It has only been within recent years that in depth research has been carried out regarding the effects of reduced modulus action although the problem has been identified many years before. Whilst there has been much understanding of sheet pile wall behaviour there is still ambiguity surrounding the effect of the transfer of shear across interlocks in single U-section walls. A more comprehensive understanding of the mechanisms of shear transfer would be of great advantage to establishing a complete design method for steel sheet piling.
Prior laboratory tests into RMA may not have accurately modelled the conditions found in full-scale pile walls. The difference between the performance of U-piles under laboratory conditions and their performance in practice may be due to the simplified modelling of loading and section details.

3 Experimental testing of scale model piles

The following chapters describe experiments carried out to investigate the influence reduced modulus action has on the bending strength of U-section piles. The results will subsequently be used to develop a mathematical model to predict the behaviour of these sections. Through further investigation and development this model may in time be applied to full-scale steel sheet pile sections to provide an accurate estimate of the influence RMA has on strength in practical piles for designers.

U-sections steel sheet piles are amongst the largest hot rolled products available. At full scale a typical section would be between 10m and 20m in length and 600mm wide. In addition, piles are arranged in panels often hundreds of meters long and are provided with at least partial restraint against RMA by the friction generated by soil-structure interaction. Furthermore, interlocks are restrained against local buckling by the connection to adjacent piles. Simulating these conditions of restrained and scale found in practice presents a significant challenge. Previous investigations have used piles fabricated from H-sections welded to pile interlocks (Schillings & Boeraeve, 1996). This overcomes the lateral restraint problems, because no interlocks are free to buckle. Unfortunately, the specimens tested were only 1m in length, therefore, uncertainty exists about the transferability of the findings to the much longer elements found in practice.

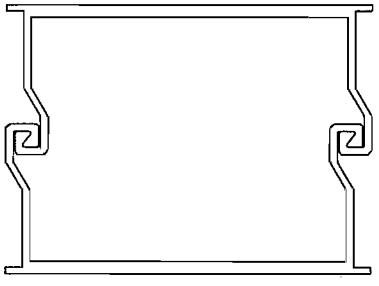

Fig. 3.1 Cross sectional view scale model piles

In order to overcome the problems of scale and restraint that are associated with full-scale testing the investigation reported in this thesis involved the testing of scale model piles. The model piles were extruded from aluminium and simulate a

1/8th scale pile, see Fig. 3.1. The piles form a box section, rather than the corrugated profile usual for steel sheet piling. This arrangement was selected because each pile provides mutual restraint to the interlocks of the connected section. This ensures that all the interlocks are restrained against local buckling. This was considered important because previous tests using miniature U-piles showed that the edge piles would buckle due to this lack of restraint (Crawford & Byfield, 2004). Whilst visually the box section is substantially different to the usual open profile, the sensitivity to RMA would remain unchanged because the tests will be represented relatively, one aluminium section to another. Therefore, it will be the change in strength and stiffness that will be recorded. A problem with using aluminium extrusions is that the surface finish is smooth in comparison with the rough finish found in hot-rolled sections. This may produce a lower bound estimate of strength in comparison with tests carried out on full-scale piles, although the practical benefits of using miniature piles out weight this relatively minor problem.

A further problem with using aluminium extrusions is that the elastic modulus is approximately 1/3rd that of steel. Whilst this difference is not significant to the development of RMA, it will affect the development of local buckling. For this reason and because the slenderness of the web and pan of the extrusion differs from that of full-scale piles, it is not possible to classify the sections in terms of their susceptibility to local buckling, i.e. plastic, compact, semi-compact etc. Therefore, these tests are only suitable for assessing the effect RMA has on the elastic bending strength of U-piles.

The choice of the aluminium sections present further limitations. However, it is necessary to have this size of section due to laboratory space, only allowing for a length of 2500 mm to be tested and hence providing the scale at which to test. Aluminium is a very ductile material and has its limitations when compared to the behaviour of steel. However, due to the nature of the scale of the tests a metallic material that could be extruded into small detailed sections with tight radii was required. The sections would also only be able to provide answers to the effect of soil-structure interaction within the interlocks and not skin friction from soil around the piling. Despite these drawbacks, the material and profile provide a straight forward and economical solution to a complex problem of testing steel sheet piles in laboratory conditions.

3.1 Calculation of material and geometric properties of test specimens

The material and geometric properties of the extruded sections are shown in Fig. 3.2 and listed in Table 3.4. These were determined using a parametric solid modelling software package (Pro Engineer). Young's Modulus (E) for the extrusions had to be determined, because the manufacturers quoted value was insufficiently accurate for research purposes. Young's Modulus was measured using a series of tensile and bending tests and a total of three independent tests where performed before an accurate and consistent measure of E could be established. It is not possible to define a precise yield point for aluminium, although the tests indicated that the yield stress was approximately 200 Nmm^{-2}, although it was decided that a limiting stress of 140Nmm^{-2} would be adopted during the tests in order to ensure that the tests remained elastic. The value of E was taken as the slope of the stress strain curve up to a stress of 120 Nmm^{-2}.

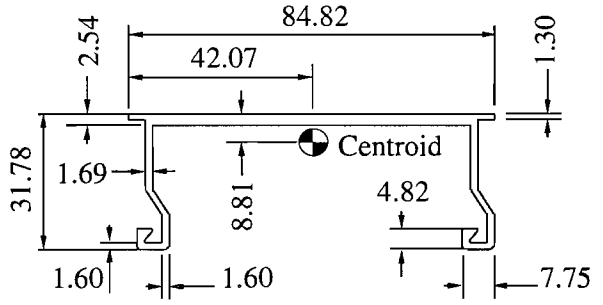

Fig. 3.2 Key dimensions (in mm) of single section

3.1.1 Primary tensile tests

A total of 3 tensile test coupons were fabricated made from the pan of the extruded aluminium section. To one side of each coupon a strain gauge was attached using M-2000 bonding agent and appropriately wired. These coupons were then tested in tension with the strain at the mid-section measured. Analysis of the results from each test showed that the variation in the Young's Modulus from coupon to coupon was greater than that for simple gauge error. E was recorded as 66000, 64000 and 56000 Nmm^{-2}, giving standard deviation of 5300. The standard gauge error is significantly less than this deviation. This error was due to poorly attached strain

gauges, combined with the errors due to single sided application of gauges. When attaching strain gauges precision is paramount and strict procedures and guidelines have to be followed. Even when these methods are followed inevitably a strain gauges mounted by hand can incur errors and any slight rotation or misalignment of the gauge could cause a significant error in the readings.

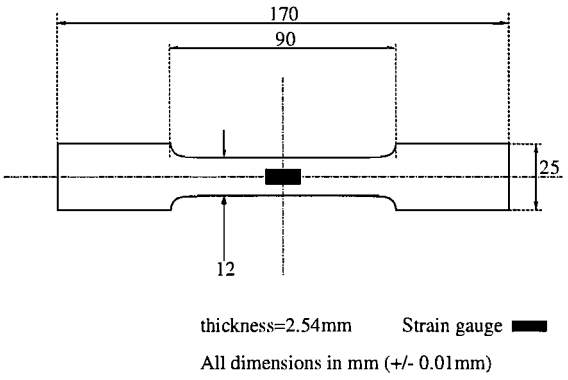

Fig. 3.3 Extensometer test specimen (coupon)

3.1.2 Further tensile tests

To overcome the inaccuracies of previous tests a second strain gauge was place on the opposite side of the coupons. Taking the average reading of these gauges would help minimise error due to gauge misalignment. More importantly, the average stress taken from both sides of the coupon removes the effects of small bending moments that may be present in the test specimen. Each specimen was tested up to a 5kN applied load and then released.

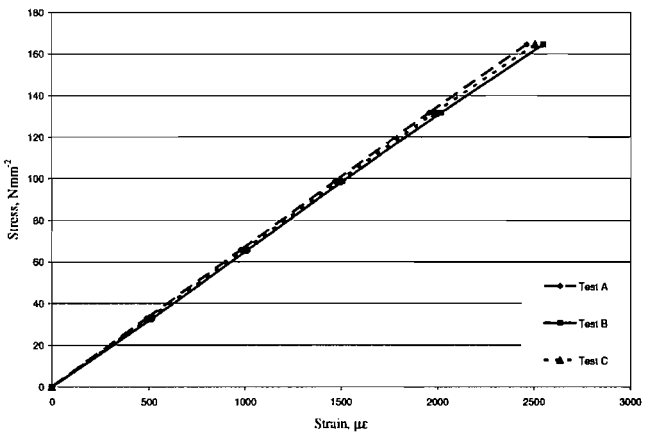

Fig. 3.4 Stress vs. Strain for second series of tensile tests

On inspection of the stress vs. strain curve (Fig. 3.4) it can be seen that all three coupons performed consistently and remained elastic throughout the tests. The calculated value of Young's modulus from each coupon can be seen in Table 3.1.

Table 3.1 Summary of the second series of tensile tests

Coupon	Young's modulus, $kNmm^{-2}$
Test 1	67.228
Test 2	64.783
Test 3	65.996
Average	**66.002**

All three tests specimens gave results with 5%. Taking an average reading from the data gives a Young's modulus of $66.0kNmm^{-2}$.

3.1.3 Deflection test

A simple deflection test was carried out to provide an independent check on Young's modulus using a single section of the extruded aluminium. The beam was tested in 4-point bending (Fig. 3.5). Deflection was recorded via a centrally placed dial gauge. The load applied to the beam was measured using a steel proving ring load cell and the beam was supported on roller supports in order to prevent the development of frictional forces.

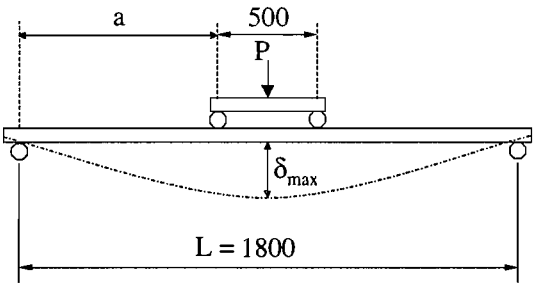

[all dimensions in mm]

Fig. 3.5 Four-point loading arrangement for beam deflection test

Knowing the dimensions of the loading arrangement the test specimen, together with the recorded displacement, Young's Modulus could be calculated using equation 3.1 (SCI, 1994), where the terms are defined in Fig. 3.5.

$$E = \frac{PL^3}{6\delta_{max} I}\left[\frac{3a}{4L} - \left(\frac{a}{L}\right)^3\right] \quad ...(3.1)$$

The results of the beam deflection test are shown in Table 3.2. The results show a solid consistency with a slight variation of approximately 1.5% between the minimum and maximum values of the Young's Modulus.

Table 3.2 Beam deflection test results

Applied Load, N	Mid-span deflection, mm	Young's modulus, Nmm^{-2}
130	5.17	66060.99
220	8.76	65979.77
310	12.24	66538.42
400	16.04	65516.07
Average Young's Modulus		**66023.81**

It can be concluded from this set of data the Young's modulus, E is 66.0$kNmm^{-2}$ pending confirmation from further tensile testing presented in the next section. The result from the previous two tests, beam deflection and tensile tests (3.1.2), a close correlation of Young's modulus has been developed. It can therefore be assumed for further testing that Young's modulus for the extruded aluminium section is given below.

Young's modulus = 66.00$kNmm^{-2}$

3.1.4 Final check of material and geometric properties

A second section was tested under a similar 4-point loading arrangement. In addition to the deflection measurements this specimen had strain gauges attached at the mid-span. The strain gauges where bonded to each interlock and the pan of the section (Fig. 3.6). The purpose of this test is to enable a cross reference of the newly determined Young's modulus. Using a theoretical stress distribution independent of Young's modulus and comparing the results of the measured stress in the specimen will provide verification of an accurate value of the Young's modulus. The results of this test and the comparison of the stress distributions can be found in Table 3.3.

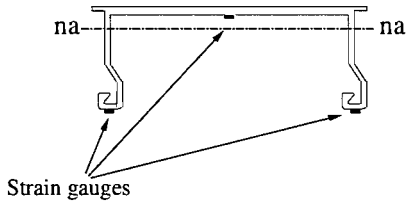

Fig. 3.6 Strain gauge positions on test specimen

The variation in the interlock values shown in Table 3.3 could be due to twisting of the section caused by the applied load not being exactly central. However the average of the two interlock stresses can accommodate for any minor twisting. The average value of the interlock stresses is 39.56Nmm^{-2}. This value corresponds exactly with the theoretical interlock stress and readings of stress in the pan also provide extremely close comparisons. Thus, the material and geometric properties of the test listed in Table 3.4 are shown in independent checks to be accurate.

Table 3.3 Theoretical and experimental stress distribution at 220N applied load

	Interlock (1)	**Pan (2)**	**Interlock (3)**
Theoretical stress, Nmm^{-2}	39.56	10.95	39.56
Experimental stress, Nmm^{-2}	40.65	10.96	38.47

Table 3.4 Geometric and material properties of extruded aluminium section

Properties	**Single**	**Combined Composite**
Section length (mm)	2500	2500
Area of x-section (mm^2)	341.57	683.15
Second moment of area (mm^4)	41390	339441
Elastic section modulus (mm^3)	1807	12011.7
Young's modulus (Nmm^{-2})	66,000	66,000

3.2 Preparation of test specimens

To investigate the effects of RMA three test series of different loading arrangements are presented in this thesis. The specimens for each test were prepared with varying interlock conditions. Two specimens were designed to produce the upper bound and lower bound conditions for interlock friction. The remaining tests investigated the effects of varying degrees of interlock friction. The interlock friction was varied by the introduction of sand into the interlock to simulate post driven conditions.

3.2.1 General Preparation

Each specimen had to undergo a procedure before any specific preparation was done. The extruded sections where cut to various lengths depending on the nature of the test arrangement. After cutting to length sections tended to have burred edges and fragments of aluminium caught in the interlocks. Specimens were thoroughly checked for any signs of structural inconsistencies such as dents or warping. Burred edges and debris were removed from within the interlocks. Strain gauges were attached according to the preparation and bonding guides set out by the Measurements Group (Vishay, 1999) before assembly of the sections. The methods of interlock preparation are described below:

3.2.1.1 Plain sections

The *plain sections* contained no additives in the interlocks and were simply pushed together.

3.2.1.2 Lubricated sections

The lower boundary case for friction was tested with interlocks lubricated with Castrol LMX (lithium based grease). The lubricant was applied to each interlock using a long bristled brush in order to push the lubricant into the interlocks. The individual sections were then assembled and excess lubricant was removed.

3.2.1.3 Sand filled interlocks

Placing sand in the interlocks before assembly was not possible due to high friction. Therefore, sand was introduced into the interlocks by coupling two extrusions together to form a tube, which was filled with sand and then sealed. The specimen was then placed on a shaking table for 10 minutes. Penetration was observed by signs of smaller particles of sand appearing on the outside of the specimen. However, the interlocks of the specimens were formed relatively tight; therefore very few particles of sand were able to penetrate through the interlocks. Strain gauges were attached to the test specimen after assembly, with the surfaces where gauges were to be attached were protected during shaking to prevent any surface deformation or pitting.

3.2.1.4 Composite sections

Three composite specimens were used during the testing program: glued, riveted and welded. Each specimen underwent a different procedure of preparation and each is detailed as follows.

- *Glued or bonded interlock:* two different types of adhesive were tried in an attempt to provide a strong enough bond to resist the shear force between the interlocks. Loctite 330 multi-bond adhesive was used originally by suggestion of the Loctite technical advisors (Loctite, 2002a). Early experimental tests of these sections showed significantly higher deflections that would have been expected for full composite action. Thus, a two part epoxy resin known as Loctite 3421 A & B was tried (Loctite, 2002b). Despite the long curing time (24-36 hours) this provided a much improved bond, however, bending tests still showed an insufficiently close match between the observed and experimental values of deflection. Therefore an alternative shear transfer mechanism was sought.
- *Riveted sections:* sections were riveted together using 3.2mm diameter pop rivets passing through 3.2mm holes. The rivets were located on both interlocks and spaced at 100mm centres. This provided an adequate resistance to shear between the interlocks. However, previous research studies (Crawford and Byfield, 2002) have shown that slippage will occur between shear connectors in composite members connected together at discrete points along their length. Therefore, whilst riveting provided a simple and effective means of achieving composite action, a more complete shear connection method was sought.
- *Welded interlocks:* Sections were welded together along the entire length of the specimen. A small gap of 100mm either side of the gauge area was left without weld. This was to prevent the weld interfering with the strain gauges. The heat built up during welding thin materials can cause ripples or warping of the surfaces and care was taken not to over heat the sections. Despite this some parts of the section suffered from localised damage.

The final stage of preparation for all specimens was to attach the necessary wiring to the strain gauges. Tri-core wire was used and soldered to the terminals of the gauges and M-bond's polyurethane protective coating for strain gauges was

applied and for addition protection wires were held in position using strong all-purpose tape.

3.3 General bending moment-stress relationship

The following experiments measure the direct stress at points across the section of a beam in bending. From the distribution of stress the bending moment can be determined. For this method of measuring the bending moment a few classical assumptions must be made:

- The material obeys Hook's law
- Plane sections remain plane
- Stress is distributed linearly across the section.

By making these assumptions, the neutral axis can be found from the stress distribution. Knowing the distribution of area around the newly found elastic neutral axis and the level of stress at each point Fig. 3.7 the bending moment can be determined.

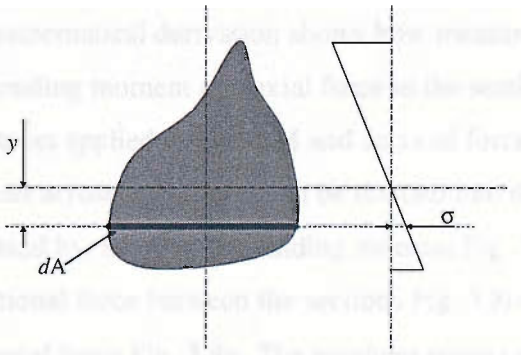

Fig. 3.7 Area of cross-section and related stress distribution

The bending moment from the stress distribution and area is determined by the sum of the area x stress x distance to that area, this is simply expressed in equation (3.2).

$$BM = \int_A \sigma_z y \, dA \qquad \text{...(3.2)}$$

3.4 Verification of test data

The testing arrangements used in this thesis are all statically determinate. Therefore the bending moment at any point in the test specimen can be calculated since both the load and load positions are known. Furthermore, if the material and geometric properties of the test specimen are known, together with a knowledge of the strain distribution (from strain gauges), it is also possible to evaluate the moment at a cross-section. Thus, two independent checks of bending moments provide a verification, or otherwise, of the test data.

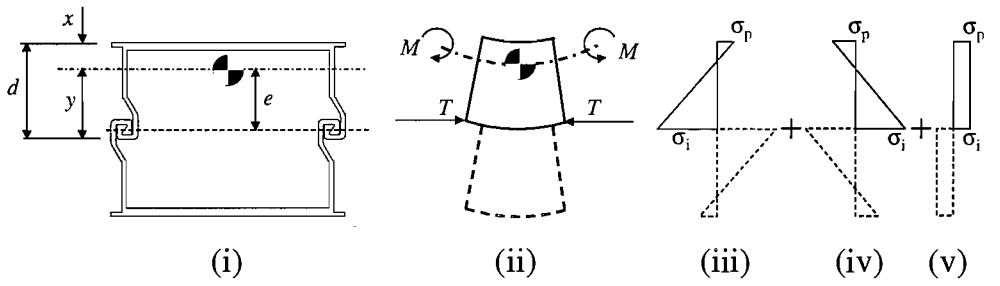

Fig. 3.8 Top section of specimen showing notation used in following equations

The following mathematical derivation shows how measured strain data can be used to calculate the bending moment and axial force in the section. Consider a single section subject to an applied moment M and an axial force T due to friction. The distribution of stress across the section can be divided into three component stress distributions caused by: the applied bending moment Fig. 3.8iii, the eccentricity of the frictional force between the sections Fig. 3.8iv and the axial loading from the frictional force Fig. 3.8v. The resultant stress in the pile pan (σ_p) and in the interlocks (σ_i) can be expressed as:

$$\sigma_p = \frac{-Mx}{I} + \frac{Tex}{I} - \frac{T}{A} \qquad ...(3.3)$$

$$\sigma_i = \frac{My}{I} - \frac{Tey}{I} - \frac{T}{A} \qquad ...(3.4)$$

Isolating M from both equations gives:

$$M = Te - \frac{\sigma_p I}{x} - \frac{TI}{Ax} \qquad ...(3.5)$$

$$M = Te + \frac{\sigma_i I}{y} + \frac{TI}{Ay} \quad \text{...(3.6)}$$

Therefore:

$$Te - \frac{\sigma_p I}{x} - \frac{TI}{Ax} = Te + \frac{\sigma_i I}{y} + \frac{TI}{Ay}$$

Simplifying:

$$T = -\left[\frac{Ax\sigma_i + A\sigma_p y}{x + y}\right] \quad \text{...(3.7)}$$

Furthermore, isolating T from both equations gives:

$$T = \frac{\sigma_p AI + MxA}{exA - I} \quad \text{...(3.8)}$$

$$T = \frac{-\sigma_i AI + MyA}{eyA + I} \quad \text{...(3.9)}$$

Therefore:

$$\frac{MyA - \sigma_i AI}{eyA + I} = \frac{\sigma_p AI + MxA}{exA - I}$$

Isolate M and simplifying:

$$M = -\left[\frac{-\sigma_i I + \sigma_i Aex + \sigma_p Aey + \sigma_p I}{y + x}\right] \quad \text{...(3.10)}$$

Using this equation (3.10) and applying it to the strain values measured during testing will provide a measured value of bending moment.

3.5 Reduction Factors

The reduction in performance due to RMA can be represented in terms of the β-values incorporated into Eurocode 3 Part 5 (CEN, 1997), with β_b representing the loss of strength and β_d stiffness. The experimental tests reported in this thesis have

been used to determine values for these factors. Two slightly different methods have been used to calculate these factors. In the first, β_b and β_d are calculated with reference to the experimentally observed value for composite action, i.e.:

$$\beta_b^1 = \frac{stress\ from\ composite\ test}{maximum\ obseved\ stress} \quad ...(3.11)$$

$$\beta_d^1 = \frac{deflection\ from\ composite\ test}{observed\ deflection} \quad ...(3.12)$$

This method is advantageous, because experimental errors that occur in all the tests, such as frictional effects, can be largely eliminated. An alternative approach is to calculate the β-factors on the basis of the values of stress or deflection that are theoretically expected for full composite action, i.e:

$$\beta_b^2 = \frac{theoretical\ stress\ for\ composite\ action}{maximum\ obseved\ stress} \quad ...(3.13)$$

$$\beta_b^2 = \frac{theoretical\ deflection\ from\ composite\ action}{observed\ deflection} \quad ...(3.14)$$

Where superscripts are:

1. β – values normalised against composite experimental result.
2. β – values normalised against expected composite result.

3.6 Initial experimental testing (test series A)

An initial series of experimental tests were carried out in order to provide a simulation of the tests previously carried out to investigate RMA by Schillings & Boeraeve (1996). As discussed in Chapter 2, these tests represent a relatively poor simulation of the loading setup found in practical pile walls. In particular, the span to depth ratio was low and 3-point loading was used. The test series reported herein utilised a very similar loading configuration, a photograph of which can be seen in Fig. 3.9.

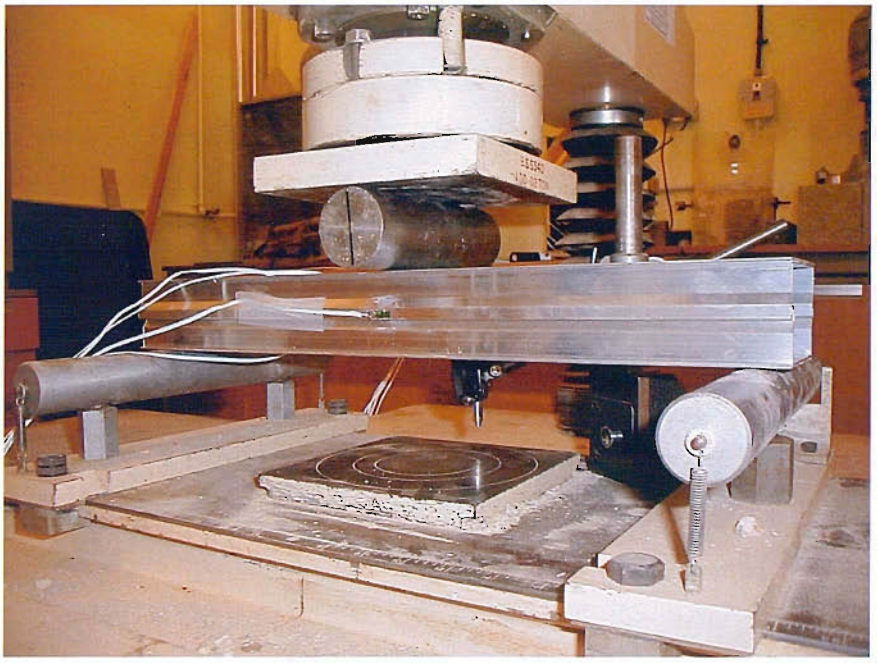

Fig. 3.9 Photograph of the general arrangement of test series A

The general arrangement and dimensions of the test set-up are shown in Fig. 3.10. Load was applied to the specimen via a mild steel roller. The roller needed to sit over a strain gauge attached to the upper pan of the specimen. This was achieved by filing a groove in the roller preventing any mechanical interference between the roller and the gauge (see Fig. 3.11).

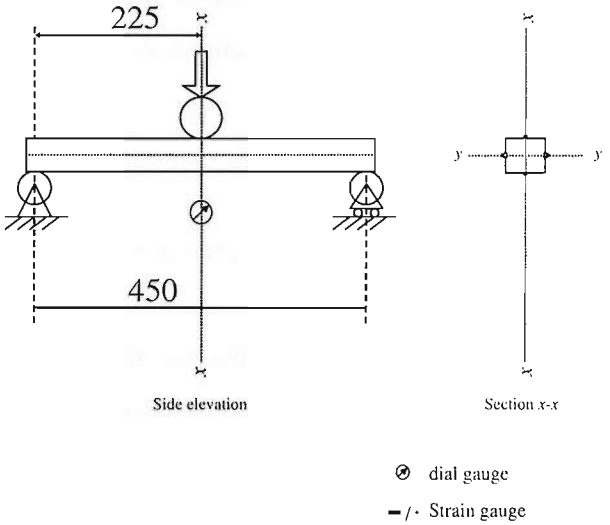

Fig. 3.10 General arrangement and Instrumentation used in test series A

The parameters recorded during this series of tests consisted of applied load, mid-span displacement and strain. Load was recorded using the Denison loading

apparatus accurate to ±0.01kN. Displacement was measured using a dial gauge and was measured from the vertical movement of the load-applying roller due to space restrictions around the loading apparatus. The roller was in direct contact with the test specimen therefore giving the displacement reading of the test specimen. The four strain gauges used where attached using M-bond 200 and catalyst and where attached to each interlock and pile pan and can be seen in the photograph of the test set-up (Fig. 3.9) and in the schematic in Fig. 3.10.

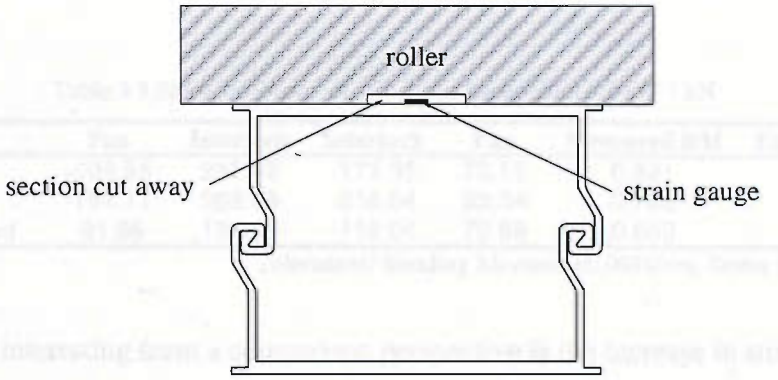

Fig. 3.11 Specially modified roller arrangement for test series A

The specimens tested were as follows:

C 1 - Sand filled interlocks

C 2 - Plain interlocks

C 3 - Lubricated interlocks

3.6.1 Results

The strain gauge data obtained from these tests are presented in Table 3.5. The comparison between the observed moment and that expected from the applied load shows a reasonable agreement. Although observed bending moment and applied moment show good correlation the data retrieved from the strain gauges displayed varied results.

Due to the cross section of the composite specimen being symmetrical about its centre of area, top and bottom sections should have provided equal but opposite measurements of stress. Each test demonstrated significantly more stress in the top-section than the bottom and it is because of this few conclusion can be drawn from

the data sets. However, a generalised view can be formed in a comparative sense, but supporting figures put to these findings are open to interpretation.

The results suggest that the presence of sand in the interlocks caused a reduction in stress in the section of approximate 11.8% over the plain section. Interestingly the lubricated section provided the lowest readings for stress against all expectations. However, the strain data collected cannot provide a solid basis to draw conclusions on the effects of sand in the interlocks of U-section piles due to the large scatter of the results.

Table 3.5 Stress in N/mm^2 distributions for applied load of 7 kN

Section	Pan	Interlock	Interlock	Pan	Measured BM	Expected BM
A1. Sand	-109.55	287.92	-173.35	73.11	0.821	0.788
A2. Plain	-151.11	289.83	-218.04	93.34	0.788	0.788
A3. Lubricated	-91.66	194.25	-119.04	70.98	0.650	0.788

Tolerances: Bending Moment ±0.001kNm, Stress ±0.01 Nmm^{-2}

More interesting from a comparison perspective is the increase in stiffness due to interlock friction, see Table 3.6. Friction increased stiffness by only 12% and 2% for the plain and sand in the interlocks respectively. These findings are consistent with the original tests by Schillings & Boeraeve (1996) in which interlock friction was observed to increase stiffness by between 2-12%. Interestingly, the test with sand in the interlocks had a lower observed stiffness than the plain sections. In larger sections deflection is far greater allowing for greater movement of the sand particles. The small movement of the sand may not be enough to generate the friction as with larger sections. Thus these tests confirm the findings of previous researchers.

Table 3.6 Deflection data for an applied load of 7 kN (test series A)

Section	Deflection (mm ±0.1)
Sand	-3.32
Plain	-3.01
Lubricated	-3.39

4 Experimental testing of simulated cofferdam (test series B)

A loading system was designed in an attempt to simulate the relatively complex loading arrangement experienced in practical retaining walls. The system developed aims to simulate the loading arrangement found in typical cofferdam situations, such as that sketched in Fig.4.1. To date this form of loading has not been investigated in laboratory conditions. The chosen situation was a cofferdam subjected to the triangular distribution of load generated either by active pressures in soils or hydrostatic loads. In this commonly occurring situation, propping is provided at the head of the piles, with a relatively small embedment of the piles into the soil providing the base support. A series of points loads (Fig.4.2) were used to approximate to the triangular distribution. This series of test will be referred to as *test series B.*

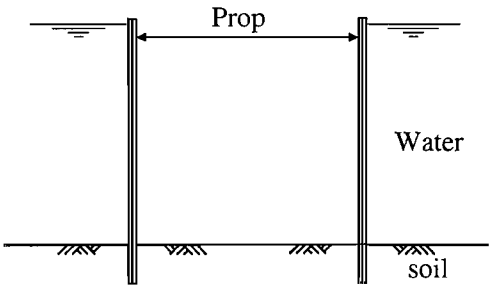

Fig.4.1 Cofferdam under hydrostatic load

Many pile walls have the option of installing capping beams. A capping beam sits on the head of the pile wall and its functions include distributing vertical loads across a pile groups or to provide a finished surface for the wall top, such as a harbour wall. However, capping beams has the added advantage of tying the pile heads together and potentially preventing differential pile movement. It is expected that a capping beam will aid the development of full modulus action because of it providing a point of fixity stopping relative pile movement and preventing the development of RMA. Investigation into the possibility that capping beams aid full modulus action has been allowed for in the following test series. As a capping beam

effectively provides a point of zero movement at the pile head, sections will be set up with and without restricted movement at that pile head and then results compared.

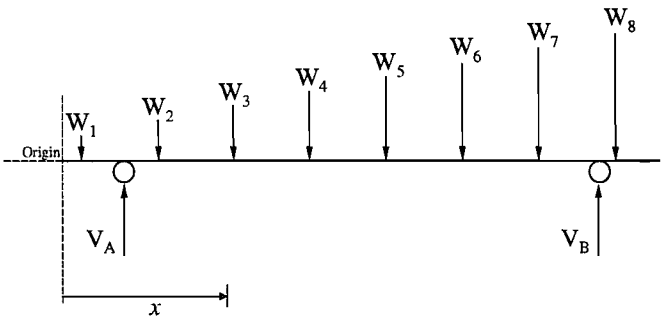

Fig.4.2 Loading arrangement for test series B

4.1 The test arrangement

The general arrangement of the test series is sketched in Fig. 4.3. Load was applied to the primary loading beam, which was supported by two secondary beams, both of which had poly vinyl chloride (PVC) reaction points. In practical frames, the friction between the soil and the wall would help to restrain the generation of RMA. However, the present tests aim to simulate what could be considered as a worst case scenario, in which frictional restraint to movement was not available. Therefore, low friction *poly tetrafluoroethylene* (PTFE) bearings were used as the interface between the loading assembly and the test beam. This arrangement delivered a triangular distribution of load. This loading configuration will be referred to as the '*upper loading arrangement*' and remains unchanged throughout the subsequent test series reported in this thesis. Following several configurations and modifications of the testing arrangement, the final set up is sketched shown Fig.4.4.

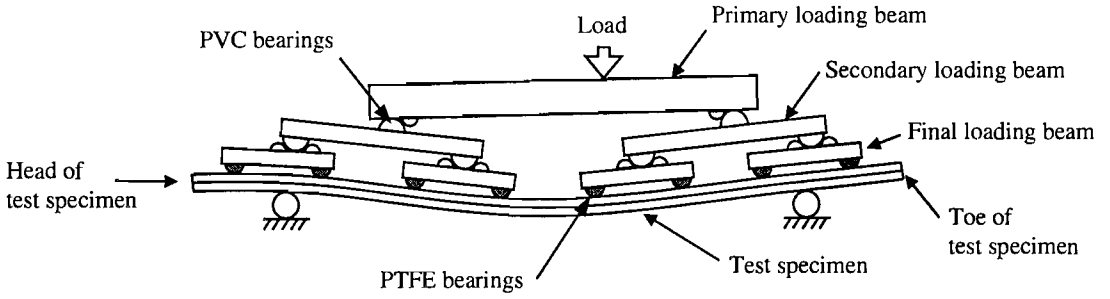

Fig. 4.3 General arrangement used during test series B

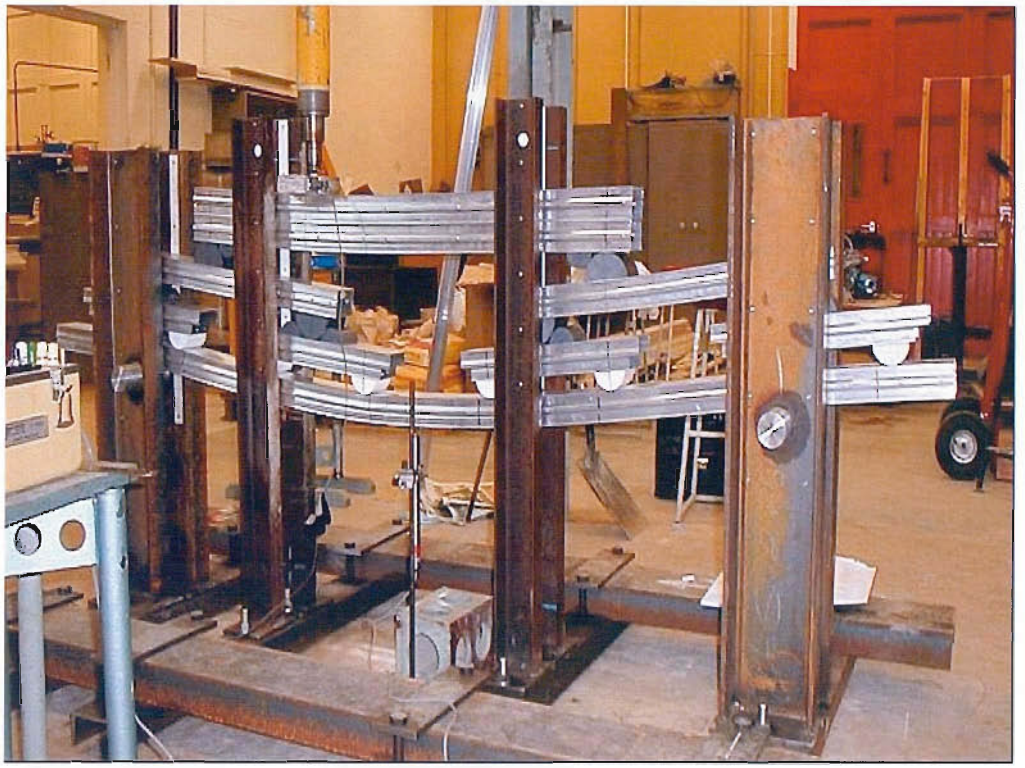

Fig.4.4 Photograph of the general arrangement of test series B

The key features and the modifications made to the testing arrangement are as follows:

- The primary spreader beam shown in Fig. 4.5 is loaded via a load cell and hydraulic jack.
- The loading arrangement is statically determinate. This was considered as vital, so that the bending moment at any cross-section along the beam could be calculated from the knowledge of the frame and loading geometry and the out-put from the load cell. Second-order inaccuracies due to change of geometry at large deflections would occur. Therefore all the tests were carried out at relatively low loads in order to ensure second order effects were insignificant.

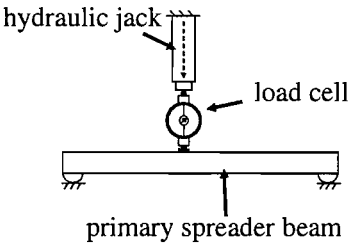

Fig. 4.5 Application of load to the primary spreader beam

- In order to maintain the relative positions of the load points, the spreader beams were connected together via a system of PVC pinned joints (Fig. 4.6). This was found necessary after initial tests showed that the beams slid at the connections, thus introducing second-order inaccuracies. Initial attempts to produce a pinned support included a series of steel hinges, unfortunately these buckled under load. This problem was solved using PVC half round rods.

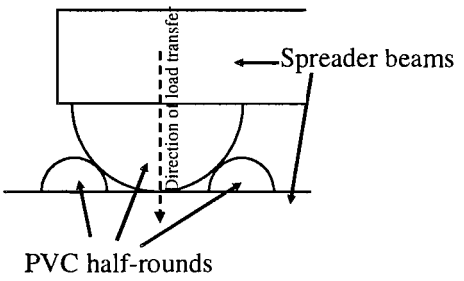

Fig. 4.6 Pinned joints using PVC half round rods

- Every effort was made to reduce friction at the interface between the loading beam and test specimens. Thus PTFE roller bearings were used. Comparison between the observed moments and moments calculated from strain gauges showed inaccuracies. These were reduced by introducing thin sheets of PTFE between the specimen and the roller bearings, where the interface was lubricated using a silicone based grease (Fig. 4.7). Thus, an extremely low friction support system was achieved. Prior to this arrangement of PTFE a PVC roller, mounted on a steel spindle set in to an aluminium housing was used. Due to the high loads used during testing these failed during early tests.

- Friction between the machined aluminium support points and the test specimen was reduced again using PTFE. A strip of PTFE was placed over the roller to provide the low friction interface.

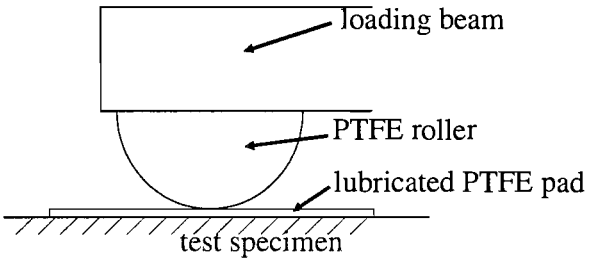

Fig. 4.7 PTFE roller bearings and lubricated pads

- The loading system comprised of a hydraulic jack, load cell and a series of spreader beams was potentially unstable. Thus lateral restraints were installed to ensure safety and maintain vertical alignment. Providing this lateral restraint presented the problem of introducing friction into the system. To prevent this from occurring thin strips of PTFE were attached to the contact surfaces. The loading beams were all fabricated from the test specimens and therefore a tight fit was achieved between lateral restraints and loading system.

4.2 Instrumentation

The parameters recorded during this test series consisted of applied load, displacement, relative slip and strain. Load was recorded using a steel proving ring placed in series between the hydraulic jack and the test specimen. Using a simple conversion factor the displacement of the steel ring provided an accurate measurement of the applied load (Fig. 4.5). Displacement was measured using dial gauges, manufactured by Batty, accurate to 0.02mm. Five dial gauges were used along the length of the test specimen. Relative slip between the top and bottom sections was measured using Vernier callipers.

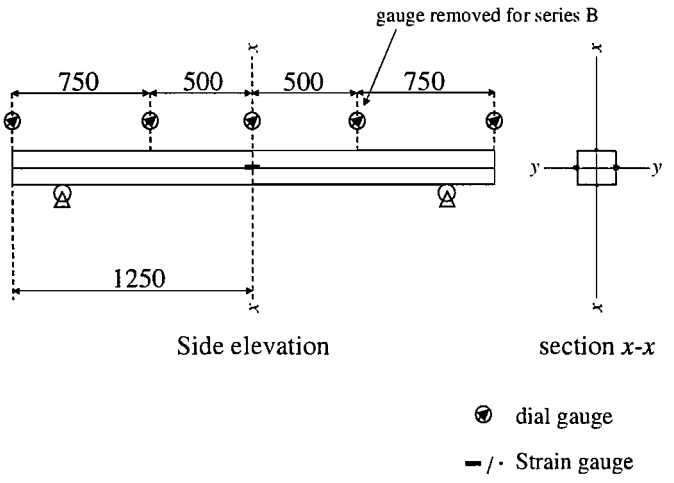

Fig. 4.8 Instrumentation used for test series B and C

Strain measurements were obtained using FLA-6-23 strain gauges attached to the specimens using adhesive. Aluminium requires special adhesives to provide a strong enough bond to prevent the gauge from detaching during testing. The surface of the metal was degreased using acetone. The adhesive used to attach each gauge was M-bond 200 and appropriate catalyst, and after application and soldering a polyurethane coating was applied to provide addition protection. Placement of the instrumentation can be seen in Fig. 4.8

4.2.1 Distribution of load

The distribution of the load has been provided by the spacing of the supports at the ends of each of the loading beams. From static equilibrium of the forces the distribution of load can be calculated. These loads provide a linear increase along the length of the test specimen producing a triangular distribution of point loads and are shown in Table 4.1 for the following test series.

Table 4.1 Distribution of point loads used in test series B and C in N for a 1kN applied load

Point Load	Load (*N*)
W1	28.1
W2	55.7
W3	83.7
W4	111.0
W5	138.9
W6	165.7
W7	194.2
W8	222.7

4.3 Results

A series of specimens each with different interlock conditions were tested (B1 to B5). The tests were repeated (B6 to B11), with the support position varied in order to investigate what effect tie rod position has on RMA. The interlock conditions of the sections tested were as follows:

B 1, B6 & B12 – Welded interlocks

B 2, B7 & B13 – Sand filled interlocks

B 3, B8 & B14 – Sand filled interlocks with simulated capping beam

B 4, B9 & B15 – Plain interlocks

B 5 , B11 & B16 – Lubricated interlocks

B 10 Lubricated interlocks with simulated capping beam

The lubricated sections (B5, B11 and B16) provide minimal friction between sections, and thus allow RMA to develop fully. Conversely, the welded sections (B1, B6 and B12) represent the upper-bound strength condition, in which full modulus action is generated.

4.3.1 Results from test series B1 - B5

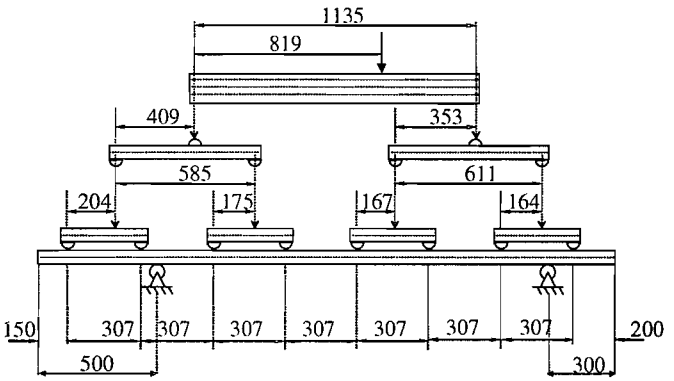

Note: all dimensions in mm

Fig. 4.9 Dimensions for test series B1-B5

The dimensions of the loading arrangement used in series B1-B5 can be seen in Fig. 4.9. A considerable cantilever is present at the head of the piles. Thus, this test represents the case of relatively low level for the positioning of the top supports.

Table 4.2 shows the values of stress distributions recorded at the mid-span of location for each test. The loading at which these data were recorded was well within the elastic limits of the cross-section. Therefore, a complete range of linearly increasing load deflection data is not presented. Rather, a single sample of data, normalised to show the stresses at 1 kN of applied load are presented, for ease of comparison. The analysis of the testing arrangement shows that this load generates a theoretical bending moment of 0.137 kNm at the strain gauge position. Inspection of Table 4.2 shows that this bending moment calculated from the geometric arrangement of the loading apparatus corresponds well with the bending moment calculated from the strain gauge data. This cross-reference provides verification that the data recorded are reliable. The comparison does however show a slight reduction in the observed bending moment. This is due to friction present in the loading system. Friction generated between the rollers and pivots causes a slight restraining effect. More importantly is the restraining effect of the friction between the load apparatus and the test specimen. All attempts were made to reduce this friction and are explained in section 4.1. These previous tests resulted in a more pronounced error in the observed and theoretical bending moments. This error was reduced to within 1.5% with the introduction of additional PTFE sheets and grease between the PTFE bearings and the test specimen, as described in section 4.1. The combined section is symmetrical and should therefore produce an equal but opposite stress distribution in the top and bottom sections. It can be seen from the data that the stress developed in the top section is mirrored in the bottom section of each specimen, thus providing further evidence of the accuracy of the strain measurements.

Table 4.2 Experimentally observed stress data in Nmm^{-2} for1kN applied load with bending moments (BM) in kNm

Section	Pan	Interlock	Interlock	Pan	Measured BM	Expected BM
B1 Composite	-10.92	0.00	-0.66	11.64	0.134	0.137
B2 Sand	-11.08	2.66	-3.36	11.74	0.133	0.137
B3 Sand & capping	-12.24	12.02	-12.01	12.52	0.134	0.137
B4 Plain	-13.82	23.80	-22.04	13.62	0.137	0.137
B5 Lubricated	-14.21	26.93	-29.11	14.16	0.137	0.137

Tolerances: Bending Moment ±0.001kNm, Stress ±0.01 Nmm^{-2}

Fig. 4.10 shows the observed stress distributions presented graphically. Importantly, the tests provide conclusive evidence that piles with high friction in the interlocks from sand have considerable reduced bending stresses, in comparison with

sections with lubricated interlocks. The stress distribution in the section containing sand in the interlocks is similar to that for the composite section, demonstrating similar pan stress and having nominal interlock stresses. Interestingly, the section containing sand in the interlocks and a simulated capping beam at the head of the pile, produced higher levels of stress in the interlocks than just sand filled interlocks without a capping beam. This indicates that capping beams are not important in the prevention of reduced modulus action.

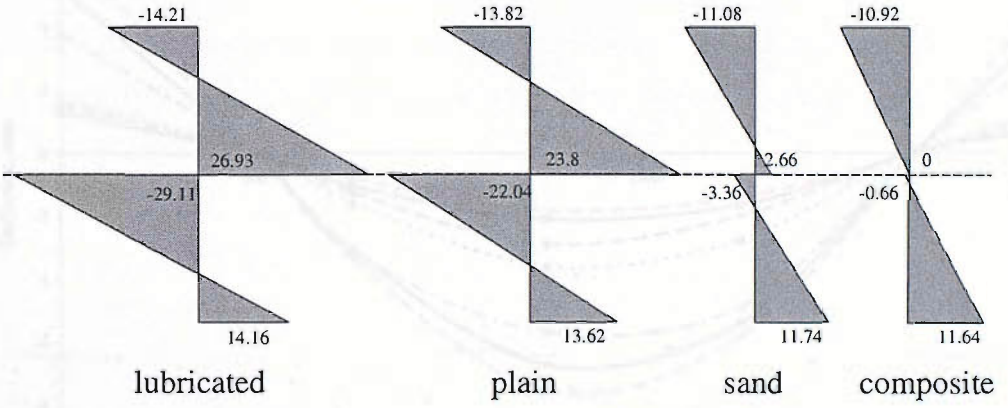

Fig. 4.10 Stress distributions for test series B1-B5 in Nmm^{-2}

The deflection data is presented in Table 4.3 and a graphical comparison of all these data is presented in Fig. 4.11. This figure also shows deflections predicted from the basic theory, assuming full modulus action and reduced modulus action. All experimental deflections remained within the boundaries expected from the theoretical analysis. Sections performed as expected with stiffness increasing with interlock friction with the surprising exception of the simulated capping beam section with sand in the interlocks. This particular section was not as stiff as expected producing greater deflection than test B2: sand filled interlocks.

Table 4.3 Deflection in mm from 1 kN applied load

Dial gauge No.	**1**	**V_a**	**2**	**3**	**4**	**V_b**	**5**
Gauge Position	**0mm**	**500mm**	**750mm**	**1250mm**	**1750mm**	**2200mm**	**2500mm**
B1 Composite	1.25	0	-1.07	-2.10	-1.67	0	0.60
B2 Sand & capping	1.72	0	-1.58	-3.58	-2.75	0	1.09
B3 Sand	1.47	0	-1.28	-2.88	-2.01	0	0.72
B4 Plain	3.76	0	-3.12	-5.67	-4.87	0	2.66
B5 Lubricated	5.22	0	-3.05	-6.71	-5.37	0	3.43

Tolerances: Deflection ±0.01mm

The introduction of sand into the interlocks produced lower deflections in between 57% and 48% in comparison with the section with lubricated interlocks. Perhaps surprisingly, the test with sand filled interlocks and a simulated capping beam was less stiff, being only 46% stiffer than the lubricated test specimen.

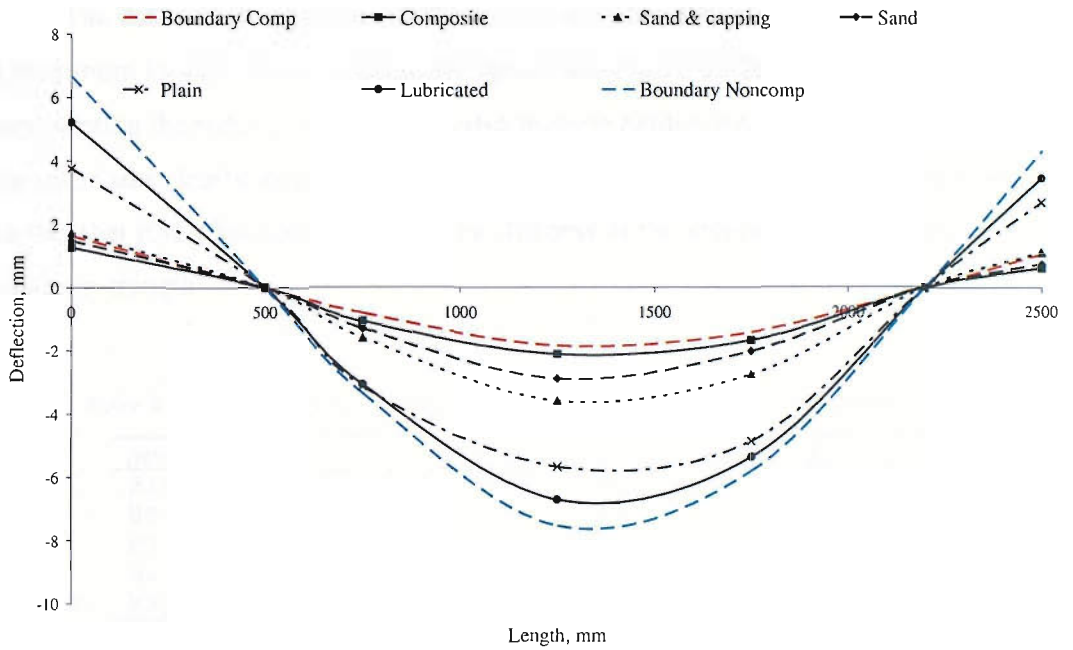

Fig. 4.11 Deflection for 1 kN applied load to specimens B1-B5

4.3.1.1 Calculation of β-factors

The effect that RMA has on bending strength can be represented in terms of the β-factors discussed in section 3.4. Table 4.4 shows these factors calculated using the experimentally observed strength and stiffness of the composite section hence the β-factor is 1.0 for the welded section (B1). As discussed previously, the comparison between the applied moment and the moment calculated from the strain data revealed that tests B1-B5 generated low bending moments. By deriving the β-factors from the composite test results, these consistent errors are reduced. It can be seen when comparing the values in Table 4.5 that when the results are compared to the theoretical data, the resulting β-factors are considerably smaller particularly in reference to stiffness.

Table 4.4 Average β-factors for specimens, normalised against test B1

Section tested	β_b^1	β_d^1
B1 Composite	1	1
B2 Sand	0.990	0.814
B3 Sand & capping	0.956	0.629
B4 Plain	0.474	0.324
B5 Lubricated	0.457	0.323

The data presented reveals that sand has a dramatic effect on RMA, resulting in a maximum loss in elastic bending strength of less than 5%. The β_d-factors representing the reduction in stiffness also provide evidence that the presence sand in the interlocks clearly increases the stiffness. It can also be seen from the reduction factors that RMA has more effect on the stiffness of the section than the elastic bending strength.

Table 4.5 Average β-factors for specimens, normalised against theoretical behaviour

Section tested	β_b^2	β_d^2
B1 Composite	0.951	0.801
B2 Sand	0.948	0.643
B3 Sand & capping	0.906	0.498
B4 Plain	0.448	0.275
B5 Lubricated	0.382	0.254

The effect of RMA becomes obvious when sand is not present in the interlocks of the sections and inter-pile movement is not restricted. The strength and stiffness are considerably reduced in these conditions. These reductions are more in keeping with Eurocode 3 Part 5 guidelines but it can be argued that these situations are highly unlikely as in normal driving conditions material will inevitable enter the interlock providing higher coefficients of friction.

4.3.2 Results from test series B6 - B11

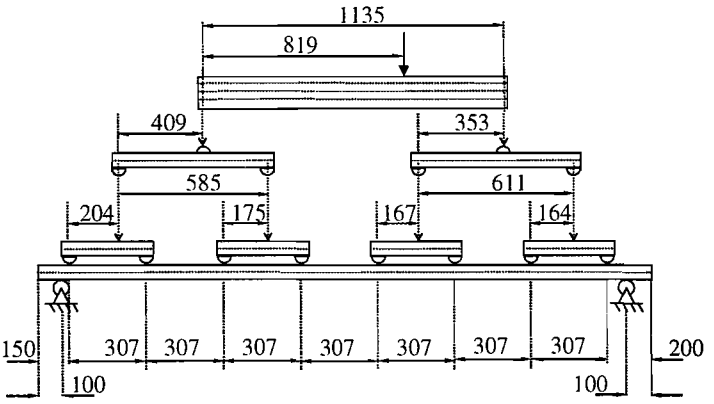

Note: all dimensions in mm

Fig. 4.12 Dimensions for test series B6-B11

This series is identical to B1 to B5 except that the left hand support shown in Fig. 4.12 is only 100mm from the head of the piles. This represents the more commonly offering high positioning of the restraining system. Table 4.6 presents the stress data recorded from strain gauges attached to the specimens. The data show that the moment observed from the strain data is consistently higher than that expected from the applied loading. This error is consistent between all the tests. In addition, the stress observed in the upper sections closely mirrors that observed in the lower sections, thus providing a reassurance that the strain data are reliable. Thus a consistent error is observed in the loading setup, although the error is relatively low the average error being under 6% of not a cause for concern. From the data the distribution of stress at the mid-span of the section can be plotted. The distributions from tests B6, B7, B8 and B11 can be seen in Fig. 4.13. It can been seen from the distributions that the influence of sand in the interlock plays a significant role, reducing the maximum stress in the section from 63.03 Nmm^{-2} to 24.19 Nmm^{-2} for 1 kN of applied load.

Table 4.6 Stress data in Nmm^{-2} for1kN applied load with bending moments (BM) in kNm

Section	Pan	Interlock	Interlock	Pan	Measured BM	Expected BM
B6 Composite	-24.70	0.97	-1.39	25.56	0.299	0.2730
B7 Sand & capping	-23.68	8.20	-4.00	24.19	0.279	0.2730
B8 Sand	-24.04	9.01	-7.34	25.46	0.286	0.2730
B9 Plain	-29.89	51.69	-56.70	29.53	0.291	0.2730
B10 Lub & capping	-29.33	58.00	-55.62	29.96	0.288	0.2730
B11 Lubricated	-30.48	61.18	-63.03	31.43	0.297	0.2730

Tolerances: Bending Moment ±0.001kNm, Stress ±0.01 Nmm^{-2}

As already observed, the first test series (B1-B5) showed that the capping beam reduced strength and stiffness. However, this data set (B6-B11) show different trend, in which the capping beam produces a small reduction in stress, in comparison with the equivalent test without a capping beam. However, the differences are small.

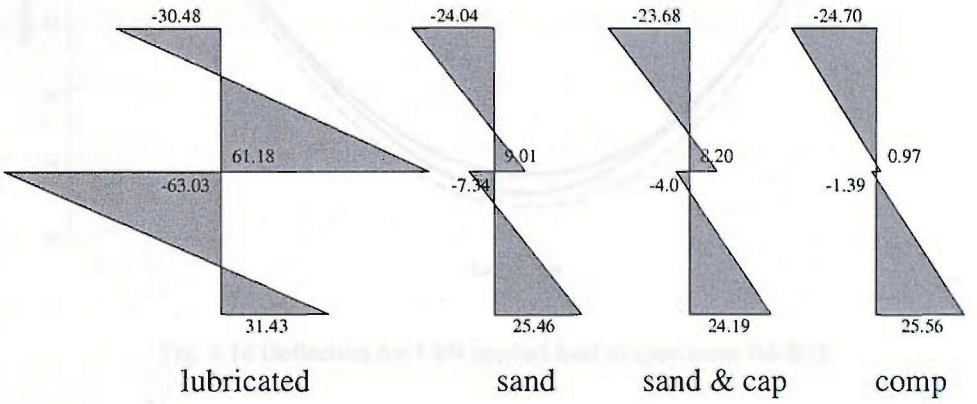

Fig. 4.13 Stress distributions for test series B6-B11 in Nmm^{-2}

The data from the deflection measurements for a 1 kN applied load can be seen in Table 4.7 and are represented graphically in Fig. 4.14. It is evident from the graphical representation of the deflection readings that the introduction of sand into the interlocks has a significant effect on the stiffness of the section. The specimens behave similarly to the composite expected deflections. Conversely, the specimens containing no sand in the interlocks behaved similarly to non-composite expected deflections. The capping beam reduced the deflection only slightly. This difference aside, the influence of sand produced a 65% increase in stiffness over the lubricated section.

Table 4.7 Deflection from 1 kN applied load

Dial gauge No.	**1**	**V_a**	**2**	**3**	**4**	**V_b**	**5**
Gauge Position	**0mm**	**100mm**	**750mm**	**1250mm**	**1750mm**	**2400mm**	**2500mm**
B6 Composite	0.35	0	-5.83	-7.49	-6.03	0	0.72
B7 Sand & capping	0.73	0	-6.03	-8.29	-7.26	0	0.55
B8 Sand	0.73	0	-6.25	-9.31	-7.75	0	0.48
B9 Plain	n.a.	0	n.a.	-25.71	n.a.	0	n.a.
B10 Lub & capping	3.04	0	-19.19	-25.41	-20.46	0	3.19
B11 Lubricated	4.11	0	-19.77	-26.79	-20.70	0	4.18

Tolerances: Deflection ±0.01mm

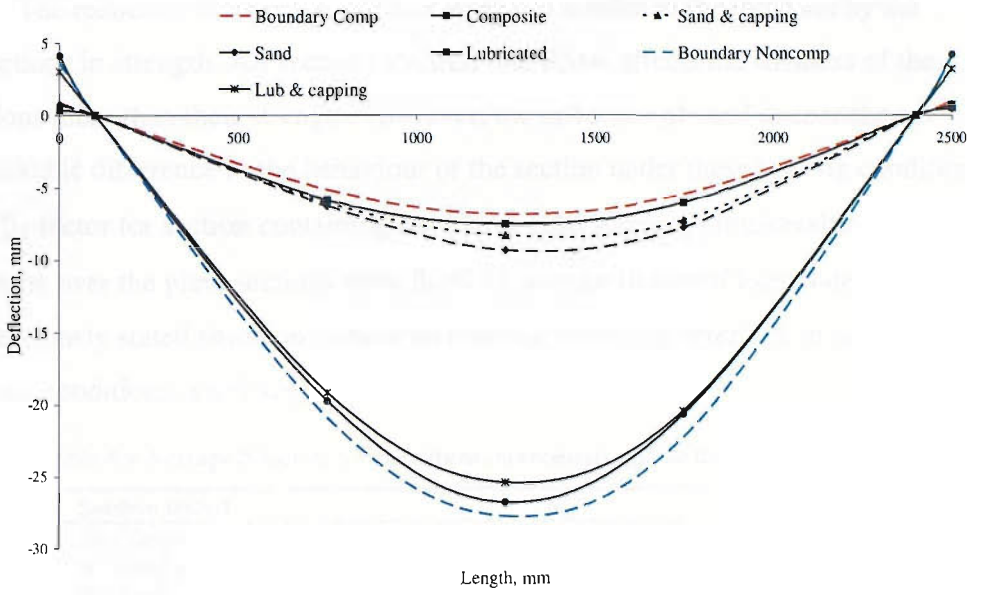

Fig. 4.14 Deflection for 1 kN applied load to specimens B6-B11

4.3.2.1 Calculation of β-factors

The repeated tests (B6 – B11) where the position of the prop load was placed higher up the sections provided lower reduction in stiffness and elastic bending strength. Table 4.8 shows the reduction factors normalized to the experimental data of the composite test (B6). The β_b-factors for sections containing sand in the interlock are 1.0. No increases in maximum stresses were found in either of these two test specimens. However in plain sections RMA was more apparent suggesting reduction factors of β_b=0.48. Calculating the reduction factors from the theoretical data also provided similar results give β_b=1.0 for sections containing sand and β_b=0.48 for plain sections (Table 4.9).

Table 4.8 Average β-factors for specimens, normalised against test B6

Section tested	β_b[1]	β_d[1]
B6 Composite	1	1
B7 Sand & capping	1	0.90
B8 Sand	1	0.838
B9 Plain	0.481	0.317
B10 Lub & capping	0.441	0.298
B11 Lubricated	0.405	0.289

The reduction factors for stiffness were not similar to the trend set by the reductions in strength. All sections showed that RMA affects the stiffness of the sections more than their strength. However, the influence of sand does make a remarkable difference in the behaviour of the section under these loading conditions. The β_d-factor for section containing sand were 0.83 showing considerable increase in stiffness over the plain sections were β_d=0.32, similar to that of Eurocode 3 part 5 but as previously stated situations where no material enters the interlock in normal driving conditions is unlikely.

Table 4.9 Average β-factors for specimens, normalised against theoretical behaviour

Section tested	β_b^2	β_d^2
B6 Composite	0.881	0.896
B7 Sand & capping	1	0.908
B8 Sand	1	0.892
B9 Plain	0.481	0.412
B10 Lub & capping	0.441	0.364
B11 Lubricated	0.405	0.363

4.3.3 Results from test series B12 – B16

This series of results reports experiments performed prior to tests B1 to B11. These early tests were initially reported in a paper presented at Eurosteel 2002 (Byfield and Mawer, 2002), although the paper was selected for publication in a special issue of the Journal of Steel Constructional Research (Byfield & Mawer, 2004). The instrumentation used for these tests consisted of a single point measure of the deflection at the mid-span and the load applied. No strain gauges where attached to the specimens and each specimen was tested to complete failure. These tests highlight the elastic limits of the section and provide an outline to their ultimate strength. The tests arrangement used can be seen in Fig. 4.15. The section regarded as welded (B12) for these tests had been riveted and not welded as with the previous tests. The sections were riveted using 3.2mm diameter rivets passing through 3.2mm holes drilled through the interlocks on both sides at 100mm centers.

The load vs. deflection responses recorded during the tests are shown in Fig. 4.16. Furthermore, the ultimate bending strengths and stiffnesses (recorded during the initial linear elastic region) are listed in Table 4.10. A brief inspection of these results shows that a significant improvement in stiffness has been achieved by the

addition of sand into the interlocks. In addition, RMA did not significantly affect ultimate bending strength.

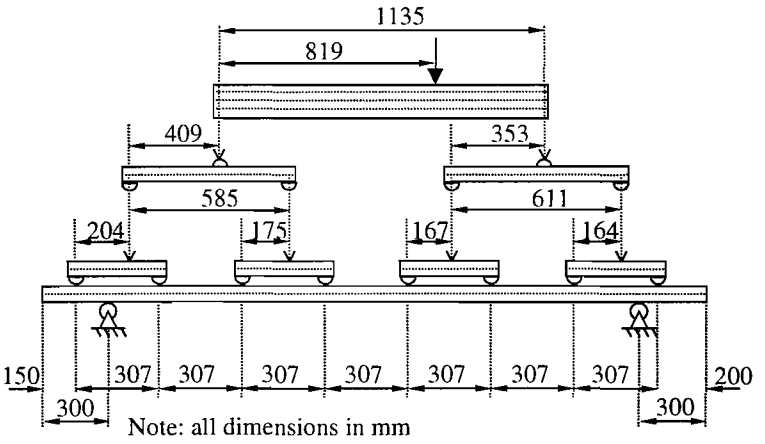

Fig. 4.15 Dimension for test B12 – B16

Test B16 (greased interlocks) provides the benchmark test. Comparison between the expected and observed deflections showed that the grease was successful in removing interlock friction, thus allowing the full effects of RMA to develop. Test B15 was carried out on plain (ungreased) aluminium piles. Whilst the piles were free to slide along the interlocks, friction was responsible for a 16% increase in stiffness (in comparison with B16). Tests B13 and B14 were carried out with sand introduced into the interlocks. Test B13 showed that the sand increased the bending stiffness by 20%. Test B14 was carried out with the interlocks riveted at the head of the piles to simulate the effect of a capping beam and stiffness was observed to be 60% higher than that for Test B16.

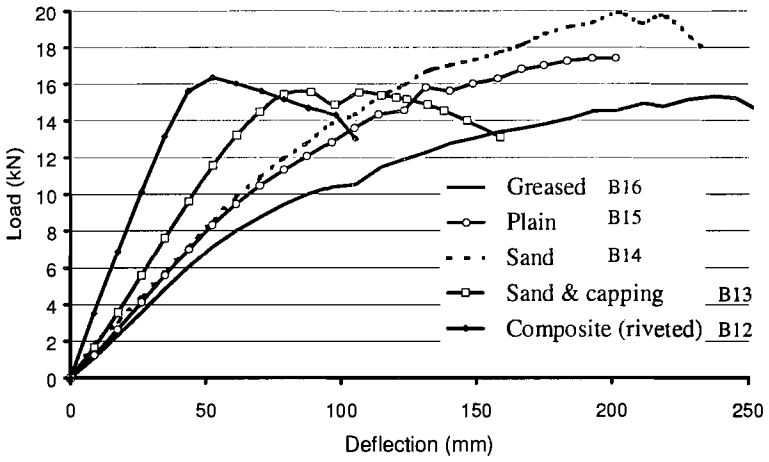

Fig. 4.16 Load vs. deflection: tests B12 – B16

Table 4.10 Series B12 – B16 Test results

	Load/displacement (Nmm^{-1})	Ultimate load capacity (kN)
B12 Riveted interlocks	386.12	16.35
B13 Sand filled interlocks	164.61	19.87
B14 Sand and rivets at pile head	220.04	15.54
B15 Plain interlocks	159.92	17.40
B16 Greased interlocks	137.68	15.33

As would be expected Test B16 (greased sections) showed the lowest ultimate bending strength of all the tests. Test B15 (plain sections) showed a 13.5% increase in ultimate bending strength. Test B13 (sand filled interlocks) produced the highest ultimate bending strength, showing an increase of 30% over the greased sections. However, both Tests B14 and B12 produced similar bending strengths to that for Test B16. The sections tested were relatively slender in cross-sections and failed due to local buckling of either the flange or web. U-section piles are generally class 1 or 2 in classification. It is therefore not possible to make direct conclusions concerning the effect of RMA on the plastic moment of resistance. Generally the specimens showed a overall failure with no formation of plastic hinges or signs of local buckling except for the composite section. The modes of failure observed from the test cannot provide any conclusions for plastic behaviour of SSPs due to the difference of the section shape. However, RMA should have reduced the bending strength of the test piles because the ratio between the elastic bending strength of the pair of piles acting compositely vs. the non-composite elastic strength of the pair is 3.3 to 1 (see Table 3.4). Therefore, RMA should theoretically have led to significant reduction in strength. The absence of any significant strength reduction may help explain why RMA has a clear impact in theory, but has rarely been observed in practice.

4.4 Conclusions

The loading arrangement used for this test series demonstrated that for the first time RMA is to a large extent mitigated by the presence of sand in the interlocks. Plain interlocks showed a pronounced reduction in strength and stiffness suggesting that RMA could be a problem in hydrostatic conditions where no soil-structure interaction takes place in the interlocks. However, the extruded aluminium was by

nature polished allowing for a lower coefficient of friction with the grain runs parallel to the movement expected in the interlocks of the sections. A Rolled steel clutch would be much less susceptible to movement due to its naturally rough surface giving a higher coefficient of friction.

Friction between the loading system and the specimen was observed to reduce the bending moments in the section substantially. Considerable effort was required to reduce the skin friction (between wall surface and soil) to provide accurate bending moment comparisons for applied and measured results. Soil-structure interaction causing increased skin friction in a practical situation can therefore be expected to have a substantial effect on RMA. Thus the tests reported herein can be regarded as a worst case scenario.

RMA was also influenced by the position of the prop load situated near the head of the pile. If the prop is placed lower down the pile leaving a large cantilever above the top prop load then RMA can be expected to be more of a problem. Reducing the cantilever at the pile head by placing the prop higher up provides a reduction in the effect of RMA. Small cantilevers above the prop load are generally more common in practical walls.

The effect of the capping beam as a measure to help prevent RMA has been regarded as not important in the test series herein. In the series of tests in which a large cantilever was present at the head of the piles (B1 to B5) the capping beam increased the effect of RMA. However, the subsequent tests (B6 to B11) , in which no significant cantilevering of the head of the piles was used, RMA was shown to be reduced by the presence of a capping beam. In both cases the overall factor was small providing no great advantages or disadvantages. Thus it can be concluded that the inclusion of a capping beam will not significantly affect the development of RMA. In the cases with no capping beam it was observed in all tests containing sand in the interlocks that no interlock slippage occurred at the toe or head of the piles.

The previous tests, carried out to assess the effects of interlock friction on the development of RMA showed that sand introduced into the interlocks is capable of increasing the bending stiffness by between 2 and 12% (Schillings and Boeraeve, 1996). Tests B13, B14 and B15 may have demonstrated higher stiffnesses because of the triangular distribution of load used during the tests, which more accurately models the loading commonly found in practice, in which the active and passive pressure distributions may in effect help to "clamp" the base of the piles.

This clamping effect will raise the reactions between the piles and therefore generate relatively high friction forces. This conclusion is justified from observations made during the tests. No interlock slippage was observed at the toe of the piles during Test B15, although significant inter-pile movement was observed at the pile head. Furthermore, zero movement in the interlocks was observed at either the head or toe of the specimen during Test B14. Thus, the tests presented herein provide an explanation as to why the tests carried out in support of the development of Eurocode 3 part 5 showed only a marginal impact on RMA from interlock friction.

If these tests are considered as being representative of full-scale steel sheet piles a recommendation for β_b could be 0.95 for sand, and 0.5 for plain sections. The β_d factors recommended would be 0.8 and 0.4 for sand and plain sections respectively.

5 Experimental testing of simulated propped cantilever wall (test series C)

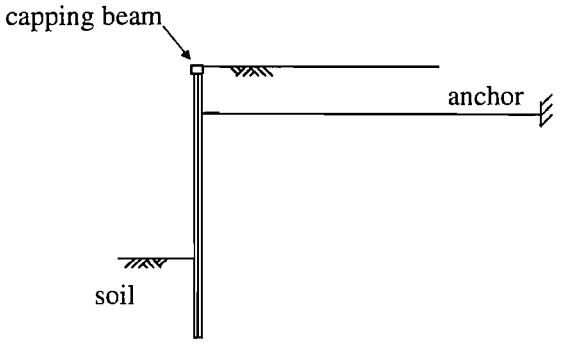

Fig. 5.1 Typical propped cantilever wall

The loading system used in series B was modified to simulate the behaviour of piling under a similar loading arrangement to that found in a propped cantilever (fully restrained *SSP*) wall (Fig. 5.1). The simulation of active pressure used was identical to that in test series B, with pinned joints and spreader beams providing a series of point loads of increasing intensity (Fig. 5.2). The passive pressure generated in front of a sheet pile wall can also be considered as a triangular distribution and for this test series a *lower loading arrangement* has been developed to provide this distribution. At the head of the pile a simple support was used to simulate a prop load.

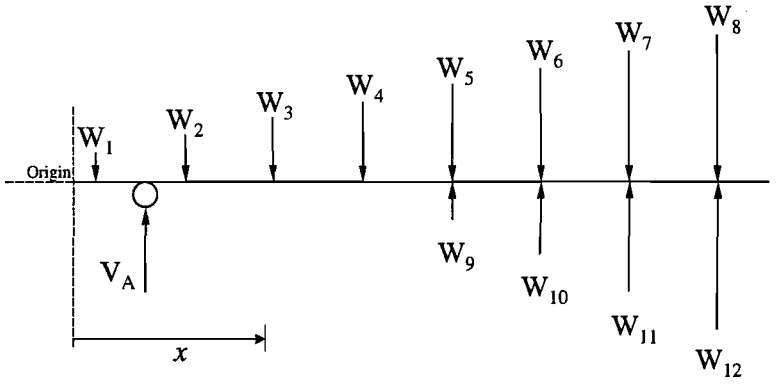

Fig. 5.2 Loading arrangement for test series C

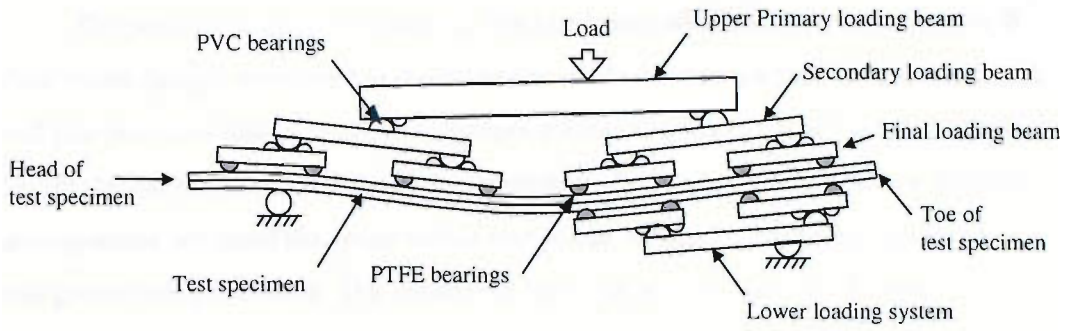

Fig. 5.3 General arrangement used during test series C

The general arrangement of the test set up is sketched in Fig. 5.3, with a schematic diagram of the loading shown in Fig. 5.2. The apparatus are as the previous experiment with adjustments made to the supports in order to achieve the correct loading situation and to allow for the passive resistance or *lower loading arrangement* to be inserted. As with series B PTFE half rounds and lubricated pads where used to provide low friction bearings for each load point in contact with the test specimen. PVC pinned joints we used to provide the pivots for the spreader beams as with the upper loading arrangement.

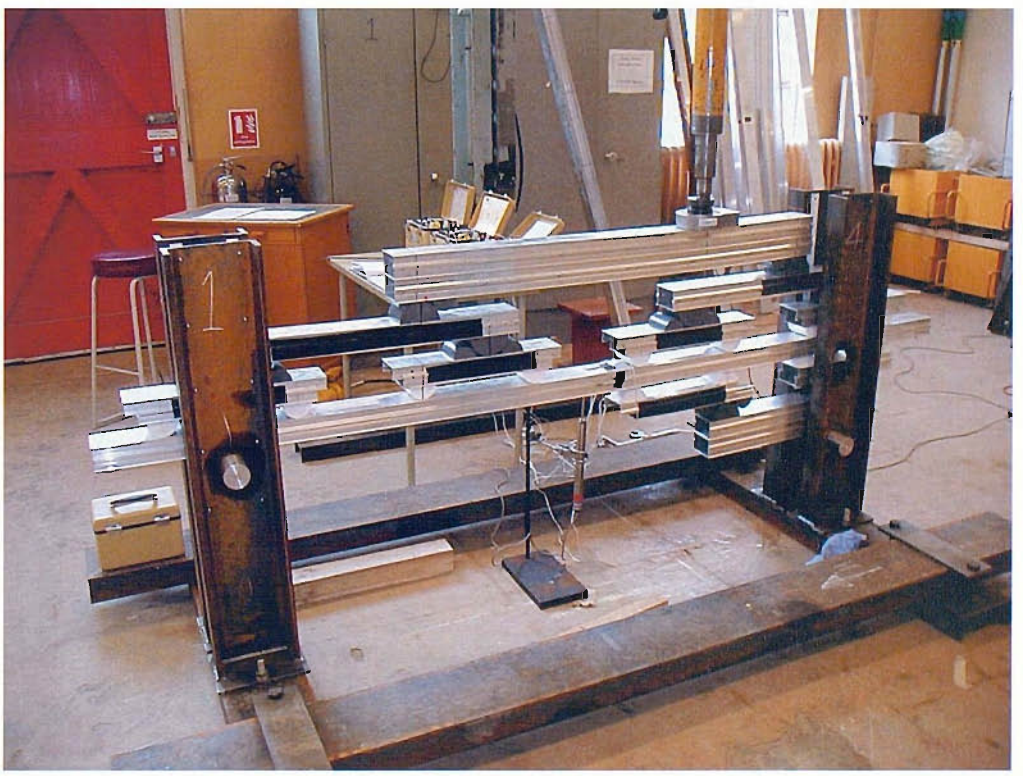

Fig. 5.4 Photograph of the general arrangement of test series C

The parameters measured during this test series where similar to test series B. Four strain gauges were used at the mid-span of the section located on each interlock and pile pan as in test series B. Dial gauges measured the deflection along the section length similar to series B but with the exception of one gauge, as the *lower loading arrangement* occupied the space where one gauge would be positioned resulting in this gauge being excluded. The remaining four dial gauges were used along the length of the section (Fig. 5.5).

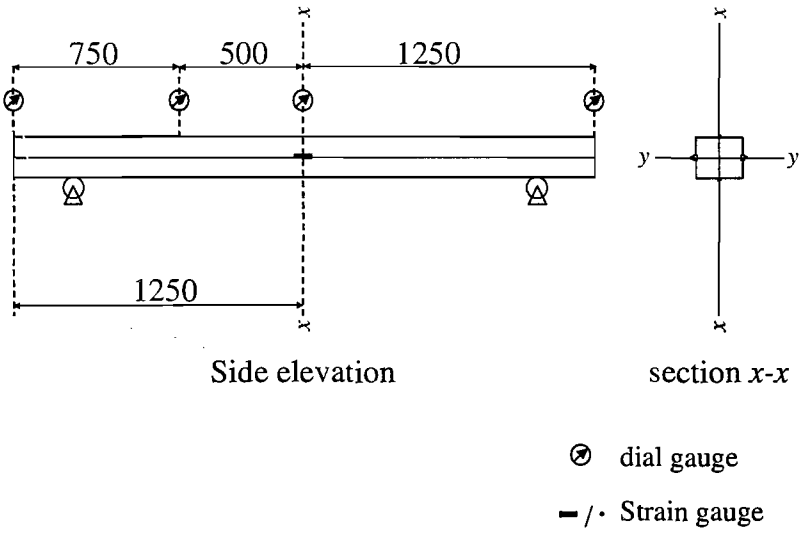

Fig. 5.5 Instrumentation used for test series C

5.1 Results - series C

A series of tests were carried out on specimens with different interlock conditions, (C1 – C5). The tests were repeated with the support position varied to investigate what effect the tie-rod position has on RMA during active-passive loading conditions, (C6 – C10). The results presented herein contain the following interlock conditions:

C1 & C6 - Welded interlocks

C2 & C7 - Sand filled interlocks

C3 & C8 - Sand filled interlocks with simulated capping beam

C4 & C9 - Plain interlocks

C5 &C10 - Lubricated interlocks

The welded sections (C1 & C6) provide the upper bound limits for the test series, in which full modulus action is achieved with no inter-pile slip. Whereas the lubricated sections (C5 & C10) provide minimal friction at the interlock, and thus allow for full development of RMA.

The dimensions of the testing arrangement are shown in figure Fig. 5.6. The position of the tie-rod (V_a) will be given in the following sections contain the relevant results.

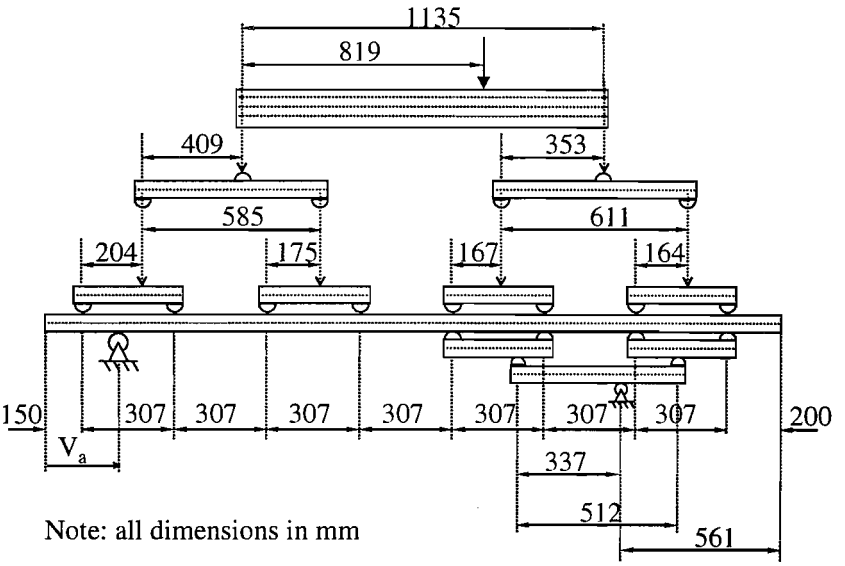

Fig. 5.6 Dimensions of test arrangement for test series C

5.1.1 Results from test series C1 – C5

The position of the tie-rod denoted by V_a in Fig. 5.6 was set at 100 mm from the pile head. A small cantilever is present at the head of the piles therefore these tests represent the case of a relatively high level of tie-rods.

Table 5.1 shows the values of stress recorded at the mid-point of the pile sections. The loading at which these data were recorded was well within the elastic limits of the cross-section. Therefore, a complete range of linearly increasing load deflection data is not presented. However a single sample of the data normalised to show the stress at 1 kN of applied load is presented. This allows for comparisons to be made easily. Calculating the bending moment applied at the mid-point of the section from the geometry of the loading arrangement gives a theoretical bending moment of 0.088 kNm from 1kN of applied load. Inspection of Table 5.1 shows that this bending moment corresponds well with the bending moment calculated from the

strain gauge data. This cross-reference provides verification that the data recorded are reliable. The comparison, similar to test series B, shows a minor reduction in the observed bending moment. This reduction is due to friction within the loading system. Friction generated between the rollers and the pivots causes a slight restraining effect but more importantly this is the restraining effect of the friction between the loading apparatus and the specimen. The methods used to reduce the friction to the minimum are explained in section 4.1; previous tests showed more pronounced errors before these methods were applied. The reduction in the observed bending moment is generally greater than that of test series B and this is due to the increased number of pivots in the whole system with the addition of the *lower loading arrangement*. It can be seen from the data in Table 5.1 that the stress in the top section and stress in the bottom section of each specimen provides an equal and opposite distribution thus providing further evidence that the strain gauge were recording accurate data.

Table 5.1 Experimental stress data in Nmm^{-2} for 1kN applied load

Section	**Pan** Nmm^{-2}	**Interlock** Nmm^{-2}	**Interlock** Nmm^{-2}	**Pan** Nmm^{-2}	**Measured BM** kNm	**Expected BM** kNm
C1 Composite	-6.57	-0.49	-0.10	6.47	0.0781	0.088
C2 Sand & capping	-6.61	3.86	-2.18	7.40	0.0801	0.088
C3 Sand	-6.20	4.05	-4.64	6.73	0.0721	0.088
C4 Plain	-6.51	9.18	-11.15	6.71	0.0670	0.088
C5 Lubricated	-6.40	13.01	-15.21	6.91	0.0630	0.088

Tolerances: Bending Moment ±0.001kNm, Stress ±0.01 Nmm^{-2}

Fig. 5.7 shows the observed stress distributions of the four tests presented graphically. They show strong evidence that piles with sand filled interlocks have considerably reduced bending stresses in comparison with lubricated interlocks. The stress distribution of the section containing sand in the interlocks with a simulated capping beam demonstrates similar stresses to the composite section, showing almost identical pan stresses with nominal interlock stresses. Conversely to test series B the effect of the simulated capping beam at the head of the pile produced lower stresses in the interlock compared to the same section without a capping beam. The effect is small and relatively insignificant compared to effect of increased friction from plain interlocks to sand filled interlocks, thus indicating that capping beams do not provide any great advantage to the prevention of RMA.

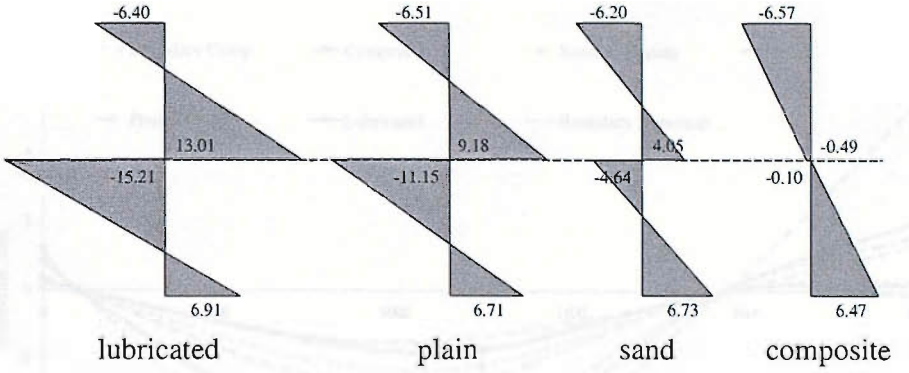

Fig. 5.7 Stress distributions for test series C1 – C5 in Nmm^{-2}

Table 5.2 shows the deflection data collected from tests 1 to 5 and a graphical representation can be seen in Fig. 5.8. This figure also shows the predicted deflections from basic theory, for full modulus action and reduced modulus action. All the experimental deflections remained within the boundaries expected from theoretical analysis. Each section performed as expected with stiffness increasing with interlock friction.

Table 5.2 Deflection in mm from 1 kN applied load

Dial gauge No.	**1**	**Va**	**2**	**3**	**4**
Gauge Position	**0mm**	**100mm**	**750mm**	**1250mm**	**2500mm**
C1 Composite	0.21	0	-1.46	-1.76	0.19
C2 Sand & capping	0.16	0	-2.04	-2.21	0.32
C3 Sand	0.38	0	-2.53	-2.60	-0.16
C4 Plain	1.18	0	-3.92	-3.99	1.63
C5 Lubricated	0.85	0	-4.15	-4.61	2.05

Tolerances: Deflection ±0.01mm

The introduction of sand into the interlocks provided a 40% increase in stiffness over the lubricated section and a 35% increase over the plain sections. Interestingly the sand and capping beam section (B2) produce a higher stiffness than the sand section (B3) contrary to the results of test series B. The capping beam provided an increase in stiffness of 19% over the sand section and 51% over the lubricated sections. It has also been observed that the base of the sections curved over more than expected showing a point of contraflexure not obvious in the expected deflections.

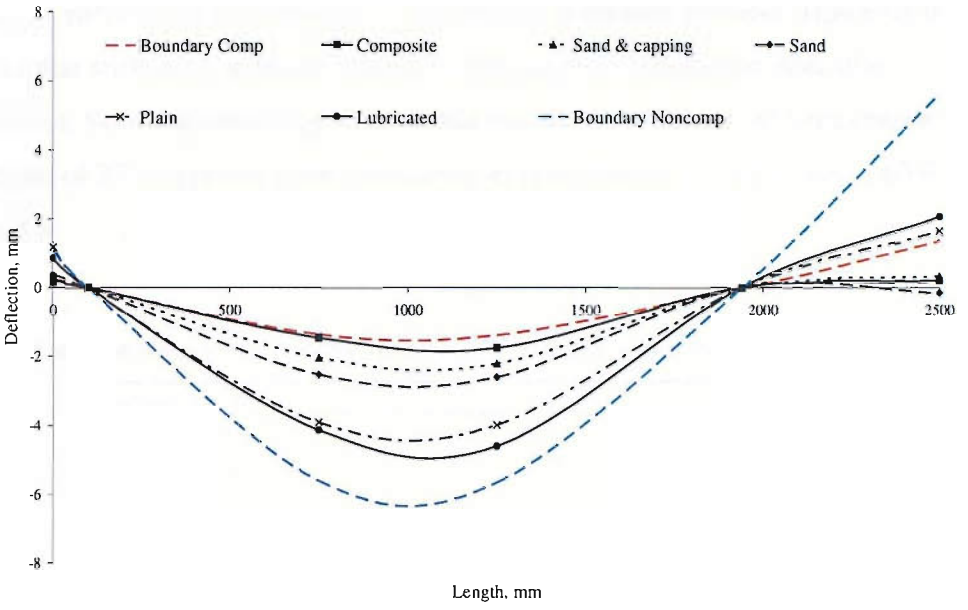

Fig. 5.8 Deflection for 1 kN applied load for tie rod at 100mm from pile head

5.1.1.1 Calculation of β-factors

Section 3.4 discusses the calculation of β-factors to represent the effect of RMA on bending strength and flexibility. Table 5.3 shows these factors calculated using the experimentally observed strength and stiffness of the welded section (C1) hence the β-factor is 1.0 for the composite test. As previously discussed in section 4.3.5 deriving the β-factors with this method reduces the consistent errors between the observed and theoretical bending moments. However, the β-factors compared to the expected data have also been presented and can be seen in Table 5.4.

Table 5.3 Average β-factors for specimens, normalised against test C1

Section tested	$\beta_b{}^1$	$\beta_d{}^1$
C1 Composite	1	1
C2 Sand & capping	0.89	0.75
C3 Sand	0.97	0.63
C4 Plain	0.58	0.41
C5 Lubricated	0.43	0.37

The data shown in Table 5.3 demonstrates that the presence of sand significantly effects the development of RMA. Sections with sand contained in the interlocks showed that inter-pile movement resulted in a maximum loss in elastic bending strength of 11% under these loading conditions. The β_d-factor represents the

change in stiffness and as previously sand clearly increased stiffness. However it is evident that stiffness is affected more than bending strength due to inter-pile movement. Sections containing sand within the interlocks produced a maximum reduction of 37% opposed to the lubricated sections showing a reduction of 63%. Table 5.4

Table 5.4 Average β-factors for specimens, normalised against theoretical behaviour

Section tested	β_b^2	β_d^2
C1 Composite	1	0.81
C2 Sand & capping	0.93	0.63
C3 Sand	1	0.51
C4 Plain	0.59	0.33
C5 Lubricated	0.45	0.29

The effect of RMA becomes more apparent when sand is not present in the interlocks of the sections and inter-pile movement is not restricted. Both strength and stiffness are considerably reduced in these conditions and the values are similar to those presented in Eurocode 3 part 5's guidelines. As with the previous discussion of reduction factors (section 4.3.1.1) it can be argued that these situations are highly unlikely in normal driving conditions as material will enter the interlock providing higher coefficients of friction.

5.1.2 Results from test series C6 – C10

The position of the tie-rod denoted by V_a in Fig. 5.6 is set at 350 mm from the pile head for specimens C6 to C10. This series of tests has a considerable cantilever above the top support and therefore these tests are representing the case of low level of tie-rods.

Table 5.5 shows the distributions of stress measure at the mid-point of the specimens. As with the previous results these tests remained well within the limits of elastic behaviour. A sample of the data normalised to show the stress at 1 kN of applied load are provided for ease of comparison. The theoretical bending moment calculated from the geometric arrangement is 0.067 kNm at the strain gauge position. Inspection of Table 5.5 shows that this bending moment corresponds well with the measured bending moment from the strain gauges providing verification that the data are reliable. As reported in previous tests the measured bending moment is slightly

reduced in comparison with the expected result and again is due to the restraining effect of the friction present in the loading arrangement. Further evidence to support the reliability of the data is that the strain recorded in the upper section is close to equal and opposite of the strain in the lower section.

Table 5.5 Deflection in mm from 1kN applied load

Section	Pan Nmm^{-2}	Interlock Nmm^{-2}	Interlock Nmm^{-2}	Pan Nmm^{-2}	Measured BM kNm	Expected BM kNm
C6 Composite	-4.60	-0.64	-0.73	4.83	0.0563	0.067
C7 Sand & capping	5.25	3.14	-6.53	6.30	0.0670	0.067
C8 Sand	-5.07	3.95	-5.99	5.38	0.0566	0.067
C9 Plain	-5.09	7.57	-8.07	5.24	0.0525	0.067
C10 Lubricated	-4.87	10.31	-11.18	5.57	0.0498	0.067

Tolerances: Bending Moment ±0.001kNm, Stress ±0.01 Nmm^{-2}

Fig. 5.9 presents the observed stress distributions in graphical form. Examination of the data reveals that interlock stress has decreased with increasing levels of interlock friction. It can be seen from this figure that the influence of sand has a considerable effect on reducing the effect of *reduced modulus action*. Stress in the pile pans remained similar but interlock stress is reduced considerably with the increased level of friction. This has been the trend with all tests series carried out. This particular set of data showed sand in the interlocks gives a 47% reduction in interlock stress compared to the lubricated specimen and a 36% decrease from the plain specimen.

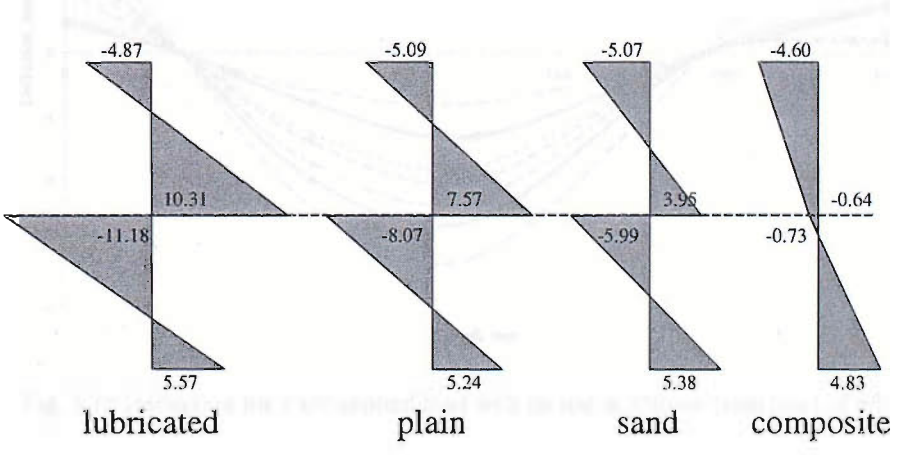

Fig. 5.9 Stress distributions for test series C6 – C10 in Nmm^{-2}

Deflection data can be seen in Table 5.6 showing the deflection for a 1 kN applied load and is represented graphically in Fig. 5.10. It is evident from the graphical

output of deflection readings that the influence of sand in the interlocks has significantly increased the stiffness of the section. However, this increased stiffness due to the sand is not as dramatic compared to series C1 to C5. The capping beam (C7) increased stiffness by 10% over the sand (C8).

Table 5.6 Deflection in mm from 1 kN applied load

Dial gauge No.	**1**	**Va**	**2**	**3**	**5**
Gauge Position	**0mm**	**350mm**	**750mm**	**1250mm**	**2500mm**
C6 Composite	0.45	0	-0.80	-1.30	0.73
C7 Sand & capping	0.56	0	-1.28	-1.78	0.31
C8 Sand	0.98	0	-1.41	-1.99	0.16
C9 Plain	1.29	0	-1.74	-2.29	0.23
C10 Lubricated	1.61	0	-1.99	-2.62	0.76

Tolerances: Deflection ±0.01mm

Overlooking the influence of the capping beam the introduction of sand into the interlocks provided an increase of 24% and with the addition of a capping beam 32% increase over the lubricated section. As with the first series (C1 - C5) specimens tended to curve over at the base of the pile more than expected.

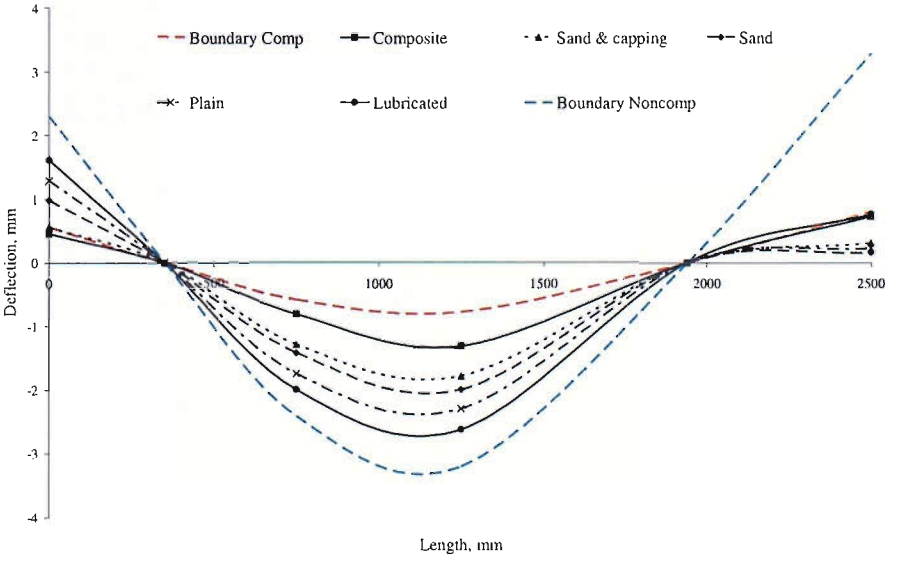

Fig. 5.10 Deflection for 1 kN applied load with tie rod at 350mm from head of pile

5.1.2.1 Calculation of β-factors

Expression of the reduction values by means of the β-factors can be seen in both Table 5.7 and Table 5.8. Table 5.7 shows these factors normalised to the

composite experimental values (C6), while Table 5.8 represents the reduction factors compared to expected composite behaviour derived from basic theory. Interestingly these values (Table 5.8) from the reduction in bending strength are less than those calculated in Table 5.7. Conversely when considering the reduction in stiffness the reduction factors normalised to test C6 produced a smaller reduction.

Table 5.7 Average β-factors for specimens, normalised against test C6

Section tested	β_b^1	β_d^1
C6 Composite	1	1
C7 Sand & capping	0.71	0.68
C8 Sand	0.77	0.61
C9 Plain	0.55	0.52
C10 Lubricated	0.50	0.45

Considering the reduction factors it is evident that the influence of sand has partially prevented the onset of RMA allowing for a β_b-factor of only 0.7 and a β_d-factor of 0.6 (allowing for experimental normalisation).

Table 5.8 Average β-factors for specimens, normalised against theoretical behaviour

Section tested	β_b^2	β_d^2
C6 Composite	1	0.63
C7 Sand & capping	0.78	0.43
C8 Sand	0.83	0.40
C9 Plain	0.62	0.319
C10 Lubricated	0.50	0.27

The findings of the lubricated sections conform well with the reduction factors found in Eurocode 3, where no friction is present in the pile interlock bending strength and stiffness can be severely effected demonstrating reductions factors as low as 0.5 and 0.3. However, such a situation where no material enters the interlock could be considered as highly unlikely in normal driving conditions.

5.2 Conclusions

The tests reported herein have demonstrated interlock friction caused by sand can mitigate the effects of RMA. However, plain sections showed pronounced RMA as with previous test results. This reduction in stiffness and strength where no soil-structure interaction takes place suggests that hydrostatic conditions are worst effected. However, the aluminium used in the experimental tests has different surface

properties to that of rolled steel as explained previously in section 4.4. The higher friction generated in the clutches of rolled steel section would make them less prone to inter-pile movement.

Friction generated between the test specimens and the load applicators caused a considerable reduction in the bending moment in the section. This effect of skin friction was reduced to a minimum in all experiments to provide accurate bending moment comparisons between measured and expected results. Therefore soil-structure interaction causing increased skin friction can be expected to have a critical effect on RMA and the test series reported should therefore be regarded as a worst case situation.

Reported in test series B was the effect of the position of the prop load and its effect on the development of RMA, these findings were reinforced in this test series (Series C). If the prop is placed lower down the pile allowing for a large section of piling to be cantilevered above this load then RMA can be expected to be more significant than if the prop is place at a higher position. Reducing the cantilever at the pile head by placing the tie-rod higher up provides a reduction in the effect of RMA.

This series of tests showed that capping beams have little effect on RMA when the tie-rod was placed near the head of the pile. It caused a slight reduction in bending strength and flexibility. However, when the tie rod was positioned lower down the pile the influence of the capping beam was advantageous providing an increase in stiffness and reducing the overall bending stresses. This is contrary to the findings in test series B. Therefore it is not possible to draw firm conclusions about the influence of capping beams in mitigating the effects of RMA.

If these tests are representative of full-scale SSP*s* these results could justify recommendations for reduction factors. The following reduction factors may be assumed as β_b=0.9 for sand with a high position of prop load and β_b=0.55 for plain sections. The reduction in stiffness could also be recommended as β_d=0.7 for sand and β_d=0.5 for plain. From the data it could be argued that Eurocode 3 Part 5 β–factors are conservative when considering sections with high interlock friction.

6 Experimental testing of interlock friction (Tests series D)

As discussed in previous chapters the full section modulus is mobilised when adjacent piles act as a single unit. This only occurs when longitudinal shear stress is transferred between the sections. In practical pile walls this is provided by friction within the interlocks, skin friction with surrounding soil and any form of mechanical transfer such as capping beams. However the only mechanism for this to occur in the experiments reported herein is the friction generated in the pile interlocks. Thus the tests provide a situation relatively conducive to the development of reduced modulus action. Determining the coefficient of friction in the interlocks provides a vital step into understanding the previous experimental test results and for the understanding of the effects of *reduced modulus action* in full-scale sheet pile walls. However, the conditions within sheet pile interlocks vary considerably from site to site and providing an accurate model of these conditions can prove extremely difficult. The following method has been employed to quantify the values of friction that could occur in pile interlocks. The series of tests reported in this chapter will initially estimate the friction developed in the scale piles made of aluminium reported previously and secondly at the interlock friction developed in real steel pile interlocks.

6.1 Friction tests with Aluminium Specimens

To establish the amount of friction developed between the interlocks of the model pile sections a series of test were designed. These tests consisted of short lengths of aluminium extrusion loaded in 4-point bending while simultaneously being pulled apart (Fig. 6.1). The details of the geometry of the extrusions can be found in detail in section 3.1. Using this method the load applied allows for the calculation of the reaction between the specimens and by measuring the force required to initiate inter-pile movement, the coefficient of friction within the interlocks can be determined under specific loading and interlock conditions.

6.1.1 Test arrangement

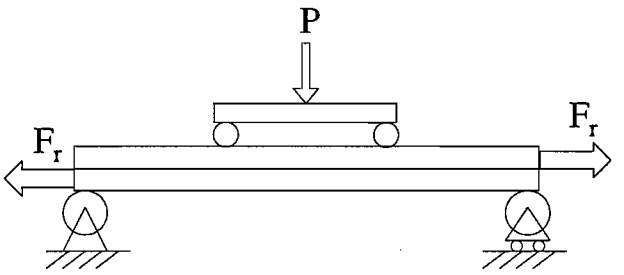

Fig. 6.1 Loading arrangement

The general arrangement of the test apparatus is shown in Fig. 6.1 and Fig. 6.2 with the exact dimensions of the tests provided in Fig. 6.3. Load was applied to a primary spreader beam, which transferred load to two steel bearings providing a 4-point loading arrangement. The lower section of the specimen was held in place while the top section was pulled sideways using a hydraulic jack reacting off the side of the testing frame. The specimens were 350mm long and were subjected to loads ranging from 0N to 600N. While under vertical load the sections where loaded horizontally. The horizontal load was increased until the point at which the sections moved. The horizontal load at this point was recorded. This recorded the force at which static friction was overcome.

A series of specimens with different interlock conditions were examined. Each interlock condition was tested under varying vertical loads. Given the results of the different loads a plot of the frictional force against internal reactions could be generated. This provided a best fit line of which can be used to calculate the coefficient of friction. However, it is likely when sand is in the interlock that the frictional force at a reaction of zero will not equal zero, due to the sand provided a mechanism for 'locking up' the tight space of the scale pile interlocks.

Fig. 6.2 Photograph of test set-up

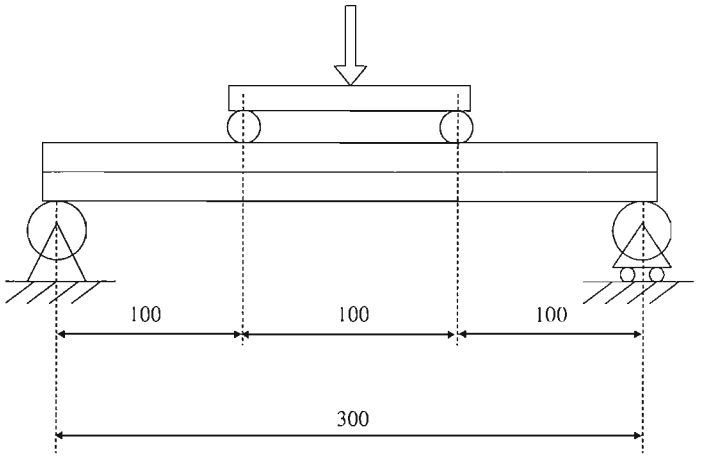

Fig. 6.3 Dimensions of friction test set-up

The following key features where incorporated into the test apparatus:

- Vertical load was applied using a set of hanging weights suspended from beneath the test specimen. Using this arrangement as apposed to a hydraulic jack allowed for the continuously applied load to translate with the specimen (Fig. 6.4) and thus avoided the introduction of frictional between the load bearing points and the test specimen.

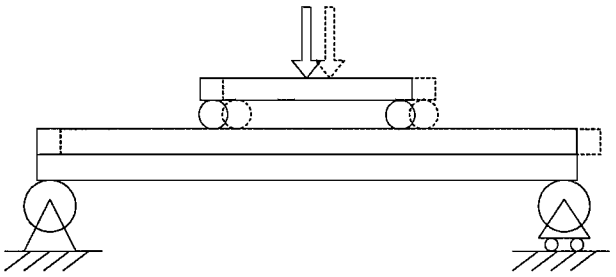

Fig. 6.4 Loading applicator moves with top section to prevent unwanted friction

- The lower section of specimen was horizontally placed using steel rods riveted to the legs of the pile section. These stabilised the test specimen and provided lateral restraint.
- The upper section of the specimen was connected to the hydraulic jack using steel ties riveted to the legs of the pile section. The hydraulic jack provided the force to mobilise the top section. This force was measured to enable the calculation of the coefficient of friction within the interlocks.
- To avoid introducing bending moments into the specimen due to an eccentric applied axial load, the steel rods connecting the top and bottom sections to the hydraulic jack and loading frame respectively were riveted along the neutral axis of the individual sections. This connection was paramount as any misalignment of theses forces would change the reactions between the sections therefore effecting the calculation of the coefficient of friction.

6.1.2 Instrumentation

For this series of tests the only measurements required were the vertical and horizontal loads. The vertical load was applied using mass weights. Each weight was checked before using in order to confirm that its markings were true. The horizontal force was measured using a load cell integrated into the hydraulic pump, see photograph Fig. 6.2.

6.1.3 Preparation of test specimens

Two interlock conditions were used in this test series: plain interlocks and sand filled interlocks. The plain interlock specimens used new sections cut to length.

However, the sand filled interlock specimens used short sections of previously tested miniature piles. Sections from test series B and C were cut to length and were used to provide sand filled interlock specimens for this test series. This provides a level of friction that relates to that experienced during the previous series of tests.

Many of the short lengths of extruded aluminium contained substantial burring on the cut ends. This burring, if not removed, would impede movement, therefore burring was removed using a small metal file to produce clean finished surfaces. During the cutting and filing process it was inevitable that some shards of aluminium would run into the interlocks of the sections. To remove any such obstructions a special tool was fabricated using a section of interlock removed from a scale pile wrapped in cloth and passed the entire length of the test specimens several times. This was the most effective way of cleaning unwanted material form the interior of the interlocks. However, for the sand filled interlocks the sections could not be separated after cutting and filing. Due to the nature of these specimens the sand prevented filings from entering the interlocks; therefore the section ends could be cleared of burs without affecting the integrity of the specimens.

6.1.4 Results

Generally the specimens acted as expected with the frictional force increasing with the applied load. Specimens with sand filled interlocks provided significantly higher levels of friction than specimens with plain interlocks.

6.1.4.1 Plain interlocks

Table 6.1 provides a comprehensive list of the results of test series D with plain interlocks. The table shows the load applied to each specimen and the force required in initiating inter-pile movement and the corresponding coefficient of friction.

Table 6.1 Experimental data obtained from plain interlock friction tests

Applied Load (*N*)	Frictional Force (*N*)	Coefficient of Friction
0	0	
80	50	0.625
80	50	0.625
120	80	0.667
120	100	0.833
160	100	0.625
160	100	0.625

200	100	0.5
200	200	1.0
300	200	0.667
300	180	0.6
400	200	0.5
400	200	0.5
500	250	0.5
500	250	0.5
500	240	0.48
600	400	0.667
600	400	0.667
	Average Coefficient of Friction:	**0.631**

The overall average coefficient of friction for the plain sections is 0.631. It can be seen from the coefficient of friction for different applied loads and in Fig. 6.5 that there is a comparatively small amount of scatter in the data. These small variations were expected due to material variations and a large sample size at varying loads was taken to minimise any error generated from these inconsistencies.

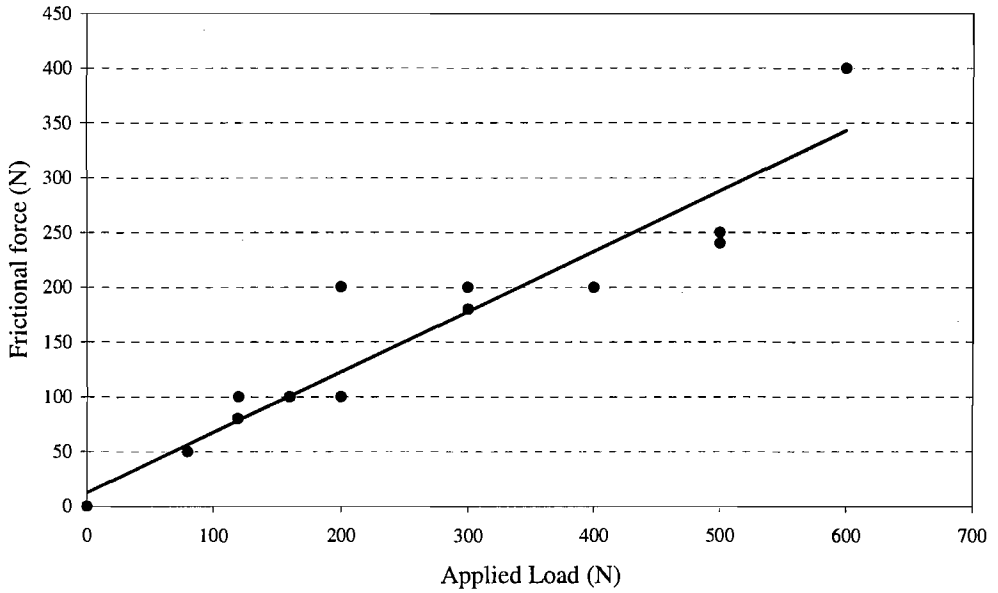

Fig. 6.5 Plain interlocks

6.1.4.2 Sand filled interlocks

Table 6.2 details the results of the tests series containing sand in the interlocks. The table presents the applied load, the frictional force required to initiate inter-pile movement and the corresponding coefficient of friction in each case.

Table 6.2 Experimental data obtained from friction tests with sand filled interlocks

Applied load (*N*)	Frictional Force (*N*)	Coefficient of Friction
0	100	n.a.
0	100	n.a.
0	100	n.a.
80	100	1.25
80	100	1.25
120	130	1.083
120	140	1.167
160	160	1.0
160	180	1.125
200	200	1.0
200	200	1.0
200	200	1.0
300	300	1.0
300	280	0.933
300	1050	3.5
400	1300	3.25
400	400	1.0
400	380	0.95
400	400	1.0
500	500	0.925
500	400	0.8
500	480	0.96
600	600	1.0
600	600	1.0
600	600	1.0
600	400	0.667
600	500	0.833
600	600	1.0
	Average Coefficient of Friction:	**1.19**

The graph shown in Fig. 6.6 shows the test data but it should be noted that the line representing the coefficient of friction does not pass through the origin. This observation is confirmed with the results from three tests with zero applied vertical load, each of which required 100N of horizontal force to initiate inter-pile movement. As the coefficient of friction, μ is the gradient of this line working out the coefficient at each given point does not represent the true value. For this instance a value of μ is required with the addition of a residual frictional force, which can be referred to as soil adhesion. The overall average coefficient of friction for the specimens containing sand in the interlocks is 1.19. However, this value is the average gradient of the individual points on the graph. The true gradient of the line presented in Fig. 6.6 is gained by looking at the equation of a line, $y = mx + c$. This gives a friction force equal to the effective coefficient of friction multiplied by the applied load plus soil adhesion (f_{ad}L):

$$f_R = \mu P + f_{ad} L \qquad ...(6.1)$$

The adhesion factor can be described as force per unit length required to move the surfaces against another under zero normal force.

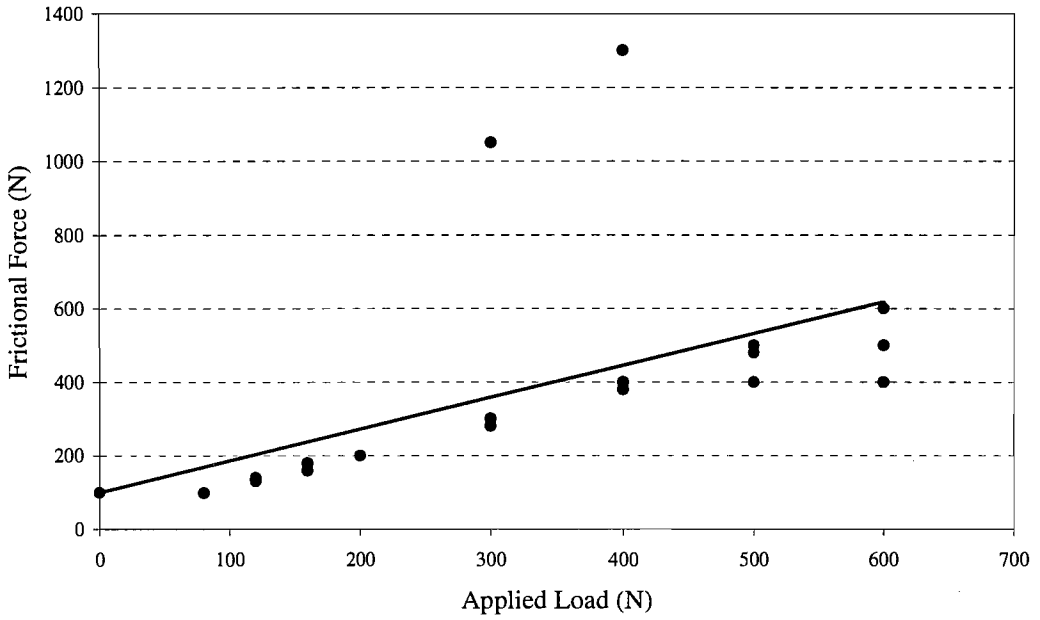

Fig. 6.6 Sand filled interlocks

From Table 6.2 and the graph Fig. 6.6 it can be seen that this adhesion force is 100N over the full length of the specimen. Substituting this value in equation 6.1 the gradient of the line can be found. The gradient of the line is 0.77. This value can be considered as an affective coefficient of friction as it can only be used in this form when used in equation 6.1.

The sticktion is likely to be a progressive build up of friction within the interlock due to the particles of sand present. The progression can be expressed as a force per unit length; the longer the specimen the more force is required to induce inter-pile movement. This effect provides evidence to suggest that testing short lengths of pile section would not provide the same level of friction as a full scale pile and would therefore not be able to produce the transfer of longitudinal shear stress needed to produce *full modulus action.* From the tests provided in this section a value for the soil adhesion can be calculated by dividing the residual force by the length of

the specimen. This provides a useful coefficient that can be used in further analysis. Therefore these experiments have provided three useful constants that can be applied to the aluminium sections, these coefficients are:

Aluminium with plain interlocks coefficient of friction, $\mu = 0.631$

Aluminium with sand filled interlocks coefficient of friction, $\mu_{eff} = 1.2$

Adhesion factor, f_{ad}=285Nm^{-1}

For example an aluminium section of a 350mm length under a 400N applied load with sand in its interlocks would require a force of:

$$0.770 \times 400N + 285Nm^{-1} \times 0.350m = 407.75N$$

6.2 Friction tests with steel specimens

Similar to the aluminium friction tests described previously in this chapter where the coefficient of frictions were evaluated with different interlock conditions, tests using actual Corus LX 20 pile interlocks have been carried out. These tests will provide insight into the levels of friction developed in steel sheet piles (*SSP*s). *SSP*s are hot rolled steel and have very course grained surfaces that are topped with mill scale, a thin flaky layer of blue/black iron oxide found on hot rolled steel (Larousse, 1995). Whilst mill scale is generally not removed in sheet piles unless they are painted for special applications, such as underground car parks or bridge abutments. There is difficulty in measuring accurately the level of friction that can be expected in a *SSP* wall due to unknown conditions of interlocks post installation. Levels of oxidation are not known, and can take a long time to prepare in the laboratory environment; the angle at which adjacent piles are installed may produce unknown forces within interlocks. Therefore the short section tests reported herein are likely to provide a lower bound estimate of the friction values.

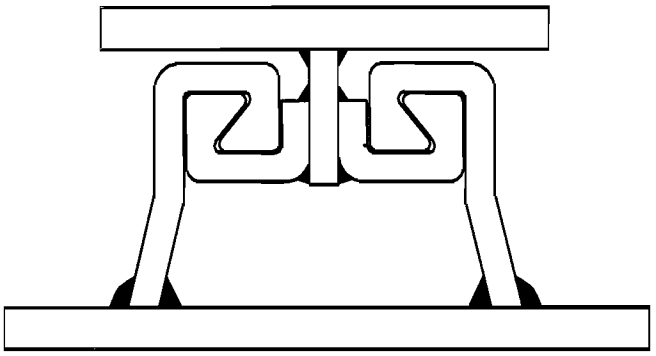

Fig. 6.7 Cross-section of steel test specimens

The sections used for this test series were cut from U-section piles that had been through an installation-extraction process. The cut interlocks were cleaned of soil but still showed slight signs of oxidation. The cut interlocks were then mounted on steel plates in order for them to sit in a test rig that provided a vertical and horizontal load. The general cross-section of the complete test specimen can be seen in Fig. 6.7. Each steel test specimen was 500mm in length and comprised of two pairs of interlocks, thus representing the friction developed in the interlocks of a single pile in the middle of a wall.

6.2.1 Test arrangement

The general arrangement of the test can be seen in Fig. 6.8 and in a photograph of the apparatus (Fig. 6.9). The exact dimensions of the loading arrangement can be seen in Fig. 6.10. Load was applied using a hydraulic jack that was set up to apply a constant load during each test phase. The test loads varied in each phase from 5kN to 25kN. This load was applied through a ball pivot joint to a spreader beam that applied load to the specimen through four roller bearings to provide an evenly distributed load along the length of the test specimen.

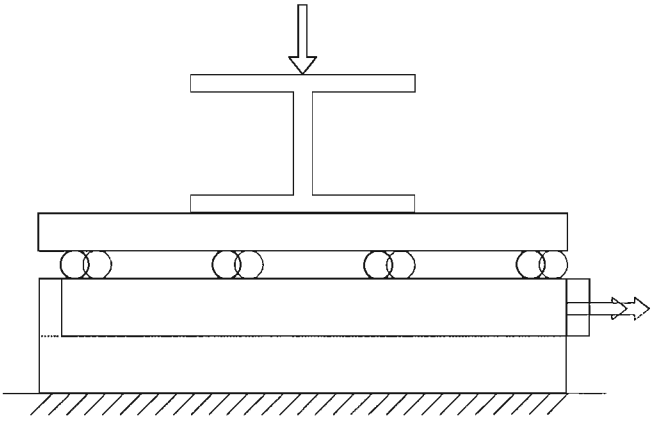

Fig. 6.8 Test arrangement: load applied through four roller bearings

The four roller bearings provide a low friction interface between the spreader beam and the test specimen. This allows the upper section of the specimen to move independently of the vertical loading jack while retaining a constant load and the lower section remains fixed in position to the testing platform. The upper section was connected via a series of pivots to a horizontally mounted hydraulic jack that was attached to the testing platform (Fig. 6.9). These pivots were used to prevent any bending moment in the horizontal loading system being transferred to the specimen. The horizontal loading mechanism was also mounted along the neutral axis of the sections so as not to induce any moment in the section due to eccentric axial loading.

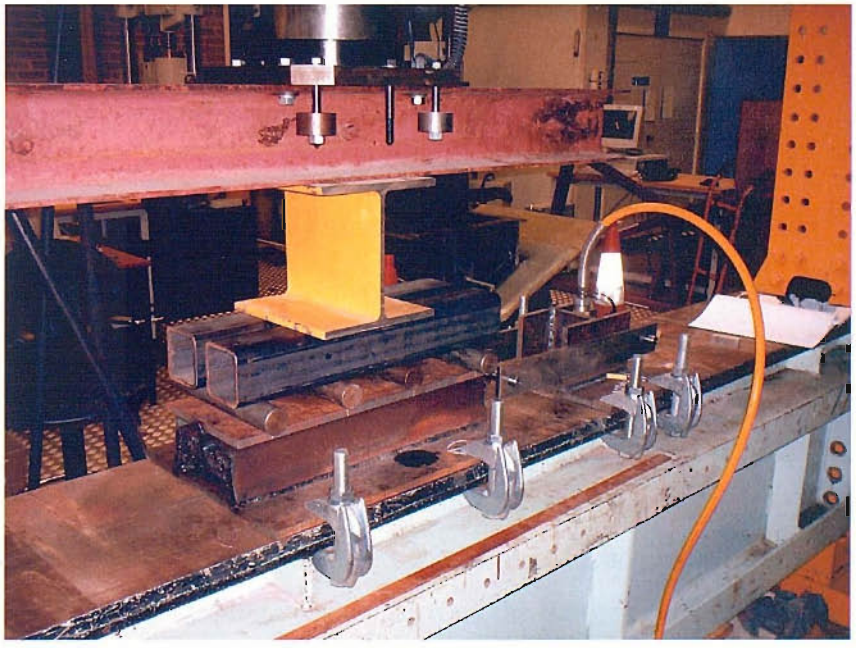

Fig. 6.9 Photograph of the test arrangement

The lower section of the test specimen and horizontal loading jack where mounted to the testing platform using high yield cast aluminium clamps. This allowed the apparatus to be mounted to the platform at any point and without the need for drilling series holes through the specimens or laboratory facilities and provided an adequate reaction for the test procedure to function.

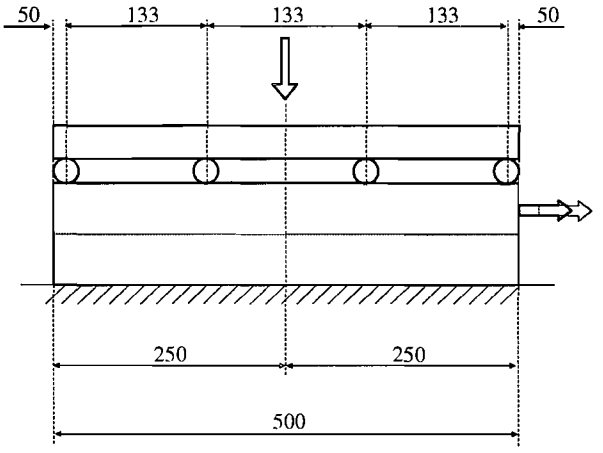

Fig. 6.10 Dimensions of test arrangement

6.2.2 Instrumentation

Two parameters were monitored during this test procedure. Firstly the applied vertical load was measured using a load cell integrated with the hydraulic jack and secondly the horizontal load was measured using the pressure gauge fitted to the hydraulic pump used to operate the jack.

6.2.3 Preparation of test specimens

A total of three specimens were required for this series of four tests; two with sand filled interlocks and one with plain interlocks. For the fourth test the plain interlock section was reused with wet interlocks. This preparation was completed by flooding the interlocks of the plain section with water prior to the (wet) test.

For the initial preparation the plain sections were cleaned of any debris from the manufacturing process and slid together to form the ready to test specimen. The specimens with sand filled interlocks underwent the following process to ensure that the interlocks were filled consistently with sand. Firstly the sections were cleaned of

debris and slid together as with the plain sections. Secondly a seal was placed around the sides and one end of the interlocks, creating a cavity containing the open interlocks. This cavity was then filled with sand, sealed and then placed on a shaking table and vibrated for twenty minutes. Every five minutes the specimen was rotated in order for the sand to penetrate throughout the interlocks. The seals around the interlocks were then removed and the excess sand discarded providing a ready to test specimen.

Each test specimen was lightly sanded with emery paper and cleaned with white spirit to provide a smooth surface for the roller bearings. Chalk lines were marked on the top and sides of the specimens to provide a guide for the positioning of the rollers.

Each test specimen was placed on the test platform, comprising a solid surface comprising of a large rolled I-beam connected to the floor. The specimen was then clamped to the test platform using cast aluminium clamps to prevent movement of the lower section of the specimen. The upper section of the specimen was attached to the horizontally mounted hydraulic jack. Load was applied from above using the vertically mounted hydraulic jack. Once the vertical load was set the horizontal load was increased gradually until inter-pile movement was initiated. The peak horizontal load was recorded in order to calculate the coefficient of friction. Each specimen was tested under several different vertical loads to establish an average value of the coefficient of friction.

6.2.4 Results

Generally the specimens behaved as expected with the sand filled interlocks producing higher levels of friction than the plain interlock specimens requiring greater forces to initiate inter-pile movement. The outcomes of the various interlock conditions are presented below.

6.2.4.1 Plain interlocks

The results of the plain interlock tests can be seen in Table 6.3. The results shown are the friction force generated for each applied load and a graphical representation of the results is presented in Fig. 6.11. The friction force increased

with the applied load giving a wide range in values for the coefficient of friction ranging from 0.5 to 0.95.

Table 6.3 Steel friction results with plain interlocks (dry)

Applied Load (*kN*)	Frictional Force (*kN*)	Coefficient of Friction
0	0	n.a.
10	10	1
10	8	0.8
10	10	1
20	15	0.75
20	12	0.6
20	10	0.5
20	15	0.75
25	20	0.8
25	18	0.72
25	20	0.8
25	21	0.84
	Average Coefficient of Friction:	**0.78**

Interestingly the plain interlocks under wetted conditions showed only a very slight reduction in the coefficient of friction of 7.5% with individual values overlapping those of the dry sections (Table 6.4). The close correlation of the wetted and dry plain interlock specimens suggests that water does not significantly reduce the friction in the interlocks of steel pile sections. However, generally the wetted tests show a slightly lower coefficient of friction than the dry conditions.

Table 6.4 Steel friction results with plain interlocks (wet)

Applied Load (*kN*)	Frictional Force (*kN*)	Coefficient of Friction
0	0	n.a.
10	8	0.8
10	9.5	0.95
15	11	0.73
15	10	0.67
20	14	0.7
20	13	0.65
25	18	0.72
25	17	0.68
	Average Coefficient of Friction:	**0.76**

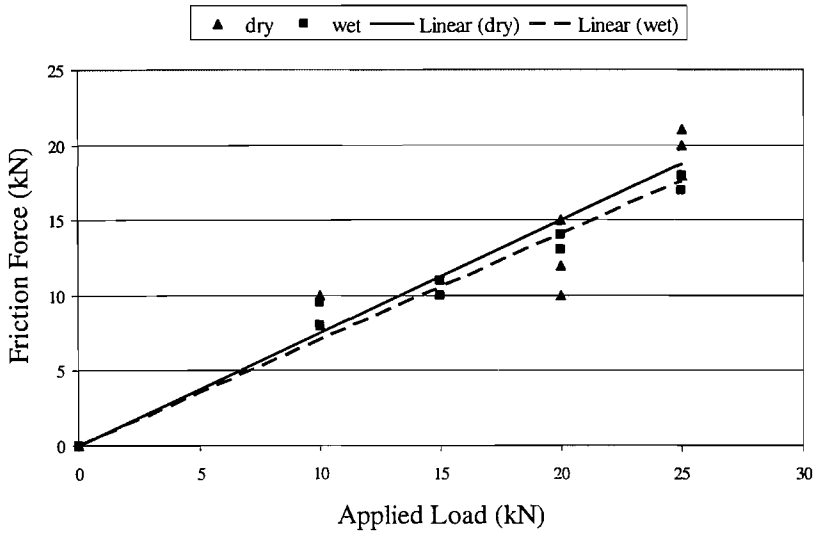

Fig. 6.11 Plain interlocks (wet and dry results)

The results for the test specimens with sand in the interlocks can be seen in Table 6.5 and is represented graphically in Fig. 6.12. The results from the sand filled interlocks provided a greater variation in frictional force than the plain interlocked sections. This was to be expected as the material is inconsistent and the distribution throughout the interlocks is difficult to reproduce with great accuracy.

Steel interlocks (plain and dry) $\mu = 0.78$

Steel interlocks (plain and wet) $\mu = 0.76$

6.2.4.2 Sand filled interlocks

The results of the sand filled interlock tests are detailed in Table 6.5 with a graphical representation of the results shown in Fig. 6.12. Unlike the plain interlock results there is a greater standard deviation in the values gained. The maximum and minimum coefficients of friction from different vertical loads varied considerable by 52% when considered individual values of applied load and frictional force. The general trend of the results shows that the frictional force increases with increasing load.

Table 6.5 Steel interlock results with sand filled interlocks

Applied Load (*kN*)	Frictional Force (*kN*)	Coefficient of Friction
0	n.a.	n.a.
5	10	2.0
5	5	1
5	7	1.4
5	10	2.0
5	10	2.0
10	21	2.1
10	15	1.5
10	12	1.2
	Average Coefficient of Friction:	**1.65**

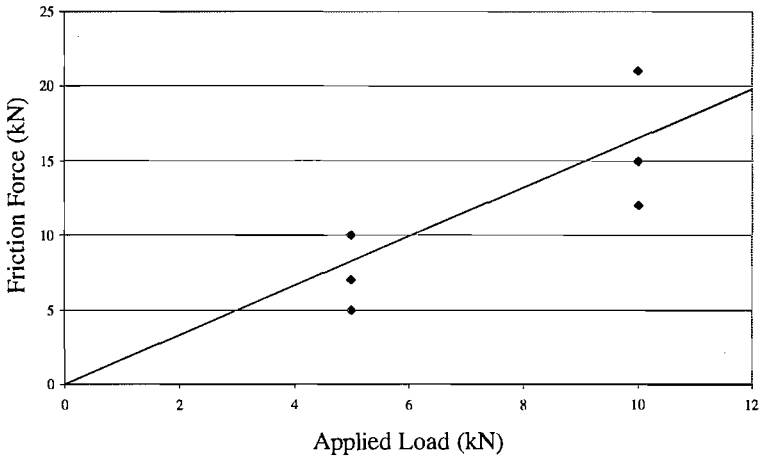

Fig. 6.12 Sand filled interlocks

The overall average coefficient of friction calculated using individual results of the tests of specimens with sand filled interlocks is considerable higher than the plain sections showing an increase of 53% giving a value of $\mu = 1.65$. This provides a general result for any given result and accounts for any adhesion that was expected through the sand. Fig. 6.12 shows the results of the test performed with sand filled interlocks and the line represents the average coefficient of friction. However, it can be seen that the results were varied under similar loads and suggests that interlock friction is not easily predicted even under controlled conditions. This average value of friction can be regarded as conservative for a soil filled interlock due to the method of placing the sand in the interlocks.

Steel sand filled interlocks coefficient of friction, $\mu = 1.65$

6.3 Conclusion

The tests presented in this chapter provide evidence to suggest that soil based material present within the interlocks of U-section piles provides an increase in the value of the coefficient of friction. In both cases of aluminium and steel interlocks the increase in coefficient of friction due to the presence of sand is approximately 30%. Interestingly the steel sections behaved similarly to the softer aluminium specimens. The sand in the aluminium sections scored the surfaces of the interlocks during inter-pile movement thus providing a higher coefficient of friction, this scoring was not expected in the steel interlocks and thus the effect of sand should not have been so evident. However, the effect of sand was equal in both cases but on inspection of the surfaces of the steel interlocks there was evidence of abrasion but not deep scratching from the grains of sand. The most interesting outcome of this series of experiments is that friction was aided by a background effect or adhesion between specimens containing sand. A force was required to separate sections even under zero load providing evidence to suggest that longer section would build up more adhesion over the longer length making inter-pile movement increasing difficult. This effect is not so apparent in full scale interlocks. The jamming may be an effect of scale, the small interlocks are more susceptible to jamming because they are closer fitting therefore become stuck by the relatively large grains of sand. This suggests that the accuracy of the friction analysis is more accurate for the real scale pile sections. A summary of the μ-values obtained from the experiments can be seen in Table 6.6.

Table 6.6 Summary of friction coefficients and adhesion factors

Material	**Interlock condition**	μ	f_{ad} (Nm^{-1})	μ_{eff}
Aluminium	Plain	0.63	n.a.	n.a.
Aluminium	Sand	1.2	285	0.77
Steel	Plain	0.78	n.a.	n.a.
Steel	Sand	1.65	n.a.	n.a.

7 Development of a mathematical model to predict the behaviour of U-section steel sheet piles

The ability to accurately predict the behaviour of steel sheet pile walls in the field is essential to achieve the full structural and economic potential of U-section piling. In response to this problem this chapter presents a method of predicting the behaviour of U-section sheet piles with inter-pile movement.

7.1 Outline of the model

The material and geometric properties are essential to the development of the mathematical model are as follows; second moment of area, elastic section modulus, Young's modulus, cross-sectional area, section depth, length, yield strength, interlock friction and position of the neutral axis of a single section. The applied load is a known quantity and provides the starting point of the analysis of the wall. From the general applied load, the bending moment and shear forces can be calculated along the length of the sections. For this analysis the load applied is not a continuously distributed load but a series of increasing point loads that approximate to a triangular distribution. This is to allow comparison with the tests reported in earlier chapters.

7.1.1 Limitations of the model

The following model is based on the internal soil-structure interaction. That is the soil contained in the interlocks. This interaction developed is analysed for U-section sheet piles in two particular situations commonly used in construction of retaining structures. However, there are many other aspects surrounding U-section piles that have not been incorporated into the model, this allows for the quantification of the effects of interlock friction. Although this provides detailed information with regards to interlock friction it may limit the model in other aspects of predicting behaviour.

The model does not consider the effects of soil surrounding the wall and the effects of time, such as oxidation within the interlocks. These particular aspects are

considered, by many authors, to aid the development of high bending strength and stiffness. This therefore suggests that the model presents a lower bound estimation of both strength and stiffness. There is a significant difficulty in modelling both skin friction and oxidation; firstly the effect of surrounding soil would require very large containers or external trial pits to be prepared and in turn this would present many difficulties the monitoring of behaviour of both soil and pile that hindered many previous experiments. Secondly, the effects of oxidation would require using full scale sections and allowing for enough time to rust. These were both have been extremely difficult with the given time and facilities available during the program of this research.

These limitations in the model give the likelihood for the underestimation of the full capacity of the situations analysed but present a relative study of performance considering only the friction generated in the interlocks.

7.1.2 Calculation of bending moment along the section

The distribution of bending moments (Fig. 7.2) along the single section is calculated using Macaulay's method. Although this produces a relatively lengthy equation (equation 7.1), it is an effective way of programming for discrete point loads (Fig. 7.1), since the method allows for the integration of discontinuous functions.

$$M_z = \frac{P_n z}{2}\langle z - z_n \rangle + \frac{P_{n+1} z}{2}\langle z - z_{n+1} \rangle \ldots \qquad \ldots(7.1)$$

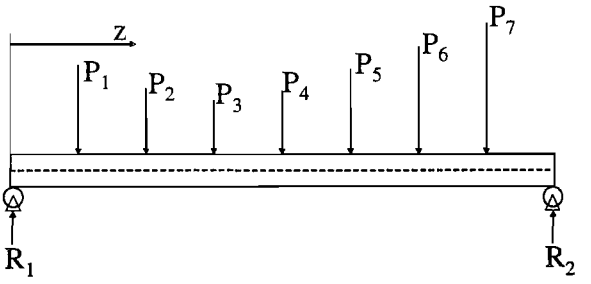

Fig. 7.1 Distribution of load along pile section

Double integration of the curvature $\frac{M}{EI}$ will be required to calculate the deflection of the pile sections. The combined moment of the top and bottom sections can be easily quantified at any cross-section because the load setup adopted during the testing was statically determinate. However, reduced modulus action reduces the effective I. Therefore the curvature at any cross-section cannot be calculated directly due to the unknown interaction between the upper and lower sections. Further knowledge of the interaction between the sections is required before curvature distributions can be established.

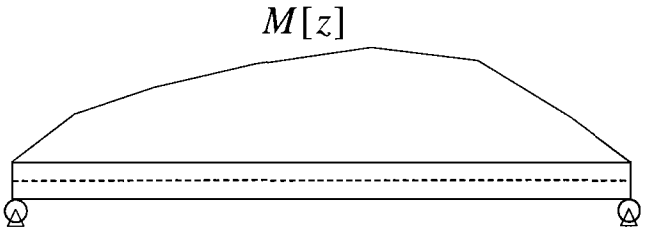

Fig. 7.2 Distribution of bending moment along pile section

The distribution of shear forces along the section can be determined form the loading arrangement as the set up is statically determinate, see Fig. 7.3.

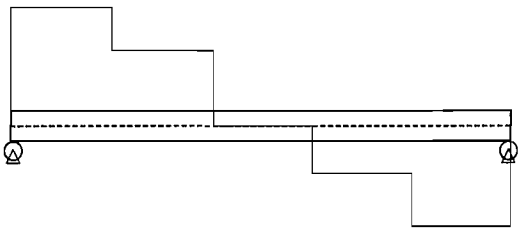

Fig. 7.3 Example distribution of shear force along pile section

7.1.3 Distribution of slip

To establish curvature, the distribution of stress across the section including the effects of friction must be determined. The simple model of friction states that the frictional force is the product of normal force and coefficient of friction. By definition, the frictional force acts in the opposite direction to the direction of slip. In the case of piling the motion is the direction of slip of the pile sections relative to one

another. This is dependent upon whether there is a capping beam or not in the wall construction because any capping beam will define the position of zero slip.

Before further analysis of the section can progress, more information is required about the mechanics of the interaction between the two pile sections. Unlike a single entity there is discontinuity across the surface of contact. For a U-section pile this is the interlock which is located along the centre-line of the wall. For any interaction to occur i.e. composite action, then longitudinal shear force must be passed across the interlock, this force is passed in the form of friction and therefore is in equilibrium with of the externally applied load.

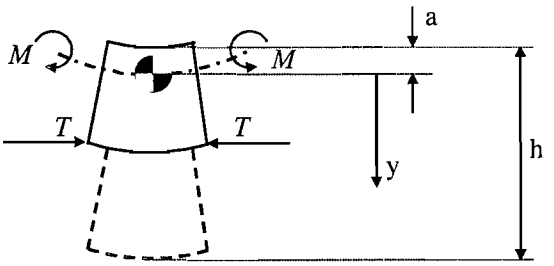

Fig. 7.4 Internal forces and moments experienced due to applied bending moment

The two adjacent sections of a retaining wall can be considered as two beams, one on top of another connected together via the interlocks which are represented as a contact surface, with a given coefficient of friction depending on interlock conditions. At any position along the section an applied bending moment and an axial load from the friction between the interlocks is experienced. Fig. 7.4 shows the forces acting on the top section. The applied bending moment is known because the loading arrangement is statically determinate. However, the axial load is not known as it depends on the frictional force developed between the interlocks. The frictional force developed in the interlocks depends on the coefficient of friction and the distribution of slip between the sections. Slip is the differential movement between the upper and lower sections of the combined pile section. Consider that one section is the reference point and remains stationary and that only the upper section can move. This assumption is based on no frictional force acting between the specimens. The effect of friction will be considered and added later.

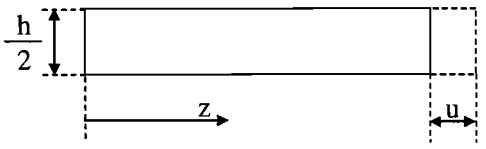

Fig. 7.5 Slip, u at any given point along a single section, z.

The slip, u along the length of a section, z is therefore the change in length in comparison to the lower section. Thus slip along the length of a section is a function of strain, ξ and furthermore, the classical definition of strain is given by the rate of change of position, i.e.:

$$\xi = \frac{\partial u}{\partial z} \qquad ...(7.2)$$

The slip along the length of the section must be given in terms of the applied bending moment. From the engineers' beam equation, strain can be defined as:

$$\xi = \frac{My}{EI} \qquad ...(7.3)$$

Therefore:

$$\xi = \frac{\partial u}{\partial z} = \frac{My}{EI} \qquad ...(7.4)$$

The distance from the neutral axis to the inter lock, $y = (\frac{h}{2} - a)$, therefore the rate of change of slip along the pile section is given by:

$$\frac{\partial u}{\partial z} = \frac{M}{EI}(\frac{h}{2} - a) \qquad ...(7.5)$$

The integral of Equation 7.5 (using the position of zero slip as the boundary condition) provides the distribution of slip along the pile section, from which the direction of slip can be calculated. Knowing the direction in which the sections want to move relative to one another allows for the determination of the direction in which the frictional force will act. The direction of slip depends on the construction of the sheet pile wall. Fig. 7.6 shows the distribution of slip along the top pile section when

a capping beam is placed at the head of the pile. The graph represents the accumulation of slip along the entire length of the section. No slip occurs at the head as the capping beam, which effectively fixes the top and bottom sections together.

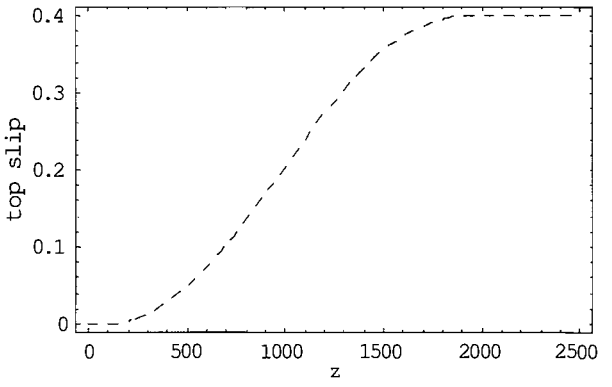

Fig. 7.6 Distribution of slip (mm) along pile length, z (mm)with capping beam in place

The direction of slip is calculated from the distribution of slip and can only be zero or unit positive or negative. A positive distribution of slip provides a positive direction and vice versa. For example the distribution of slip show in Fig. 7.6 translates to a direction of friction shown in Fig. 7.7. At this point the addition of the axial force due to friction can be added in t the calculation.

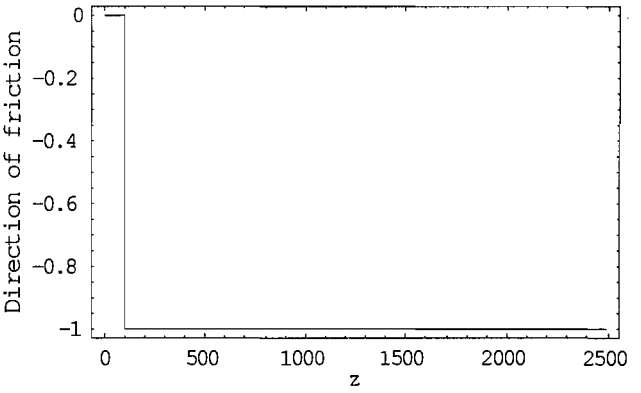

Fig. 7.7 Direction of slip with along pile length, z (mm) with capping beam in place

7.1.4 Frictional force within the interlocks

Frictional force is proportional to the normally applied load. However, frictional force can only be determined if the sections are at a point of limiting

friction, that is at the point where they are just about to move. For this model it is assumed that the sections are at a state of limiting friction when under loading. Assuming that each section carries an equal share of the bending moment it follows that each section also takes an equal share of the applied load. Thus, generally the internal distribution of normal force is shown in Fig. 7.8.

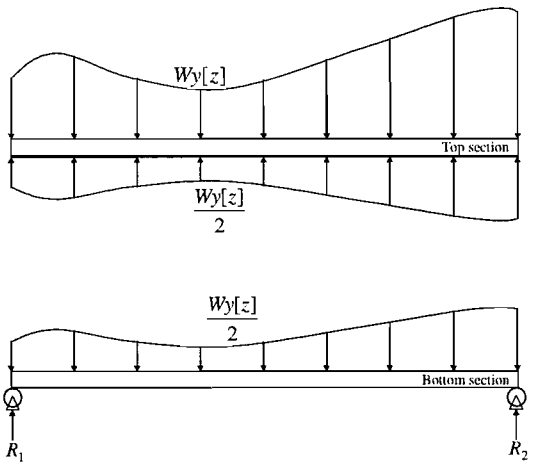

Fig. 7.8 Distribution of normal forces along the upper and lower surfaces of the sections

An approximation of the distribution of internal axial forces due to friction can be determined by using the coefficient of friction method. This point of the analysis presents an ambiguity concerning the adhesion properties of earth materials. For a plain section, the assumption is that friction does not act along the entire length of the specimen but at discrete points under each load point, but for the sand filled interlocks this is not so easily defined. The tests presented in Chapter 6 suggest that adhesion of the sand in the scale pile provides a residual friction requiring a separation force under no vertical load. This residual friction can be represented as a force per unit length along the specimen and from herein will be known as the adhesion factor. The coefficient of friction and the adhesion factor are constants for given materials and for the purposes of the mathematical model have been determined in experiments carried out and reported in Chapter 6. This method used to determine the axial load generated by the frictional force acting between the two sections is straight forward. It requires applying the effects of the residual force due to the adhesion of the sand within the interlocks in addition to the effects the coefficient of friction. This method implies that the length of a specimen has a positive effect on the force required to initiate inter-pile movement.

The data presented in Chapter 6 provides both factors of friction and adhesion. To predict the behaviour of the pile sections the values used in the model for adhesion and the coefficient of friction are $f_{ad} = 285 Nm^{-1}$ and $\mu = 0.77$ respectively (for sand in miniature piles). Addition of the two functions together provides the distribution of frictional force along the length of the interlocks. An example of this distribution can be seen in Fig. 7.9 for miniature piles with a capping beam.

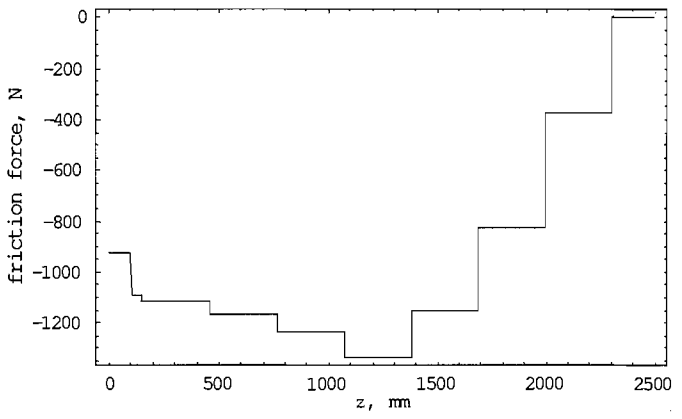

Fig. 7.9 Distribution of frictional force

For the plain sections adhesion is not considered as there is not soil based material causing the interlocks to bind together. The coefficient of friction used to calculate the friction force in the interlocks of the plain section is μ=0.65 as reported in Chapter 6.

7.1.5 The method for determining the direct bending stresses

The total stress across the sections is a combination of three stress distributions. Those distributions are formed from the applied bending moment and the axial load generated from the interaction between the interlocks provided by friction. The general stress distributions are shown in Fig. 7.10 where distribution (i) is the stress caused by the externally applied bending moment, (ii) is the secondary bending stress cause from the eccentricity of the axial frictional force and (iii) the direct axial stress from the frictional force.

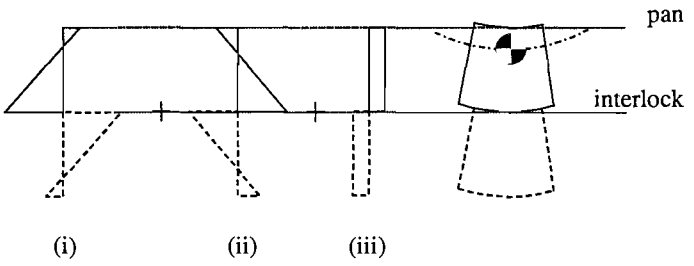

Fig. 7.10 Stress distributions across pile

The three distributions can be expressed as individual equations and added together to form the total stress across the pile sections. The distribution for stress due to the applied bending moment is represented in equation 7.6, the stress from the eccentricity of the axial load is represented in equation 7.7 and the stress from the axial load across the cross-sectional area is given in equation 7.8.

$$\frac{My}{I} = \sigma_m \qquad ...(7.6)$$

$$\frac{F_r ey}{I} = \sigma_{f1} \qquad ...(7.7)$$

$$\frac{F_r}{A} = \sigma_{f2} \qquad ...(7.8)$$

A general example of the various components and the overall stress distribution across both sections is shown in Fig. 7.11.

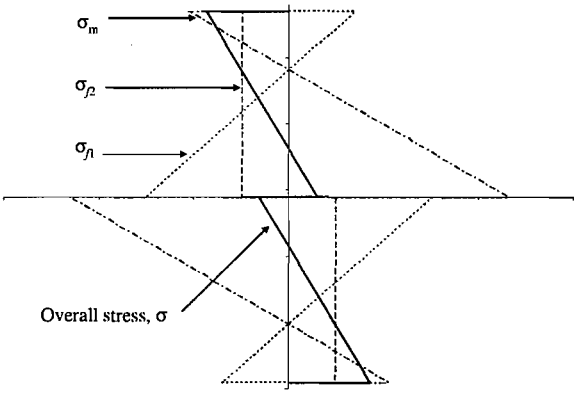

Fig. 7.11 General distribution of stress across pile sections under load

7.1.6 Method for calculating load vs. deflection

To calculate the distribution of the deflection the curvature of the beam or section must be determined from the distribution of stress. Knowing the curvature of the section caused by both the moment and axial friction allows for the calculation of the deflection by double integrating the curvature along the length of the section using the support positions as boundary conditions.

$$\frac{M}{EI} = \frac{1}{R} \qquad ...(7.9)$$

$\frac{1}{R}$ is the curvature, κ. Curvature is given by the rate of change of slope and is shown in elementary texts on structural mechanics as:

$$\frac{1}{R} = \frac{\frac{\partial^2 v}{\partial z^2}}{\left\{1+\left(\frac{\partial v}{\partial z}\right)^2\right\}^{\frac{3}{2}}} \qquad ...(7.10)$$

When deformation is assumed to be small, $\frac{\partial v}{\partial z}$ remains small and secondary effects of $\left(\frac{\partial v}{\partial z}\right)^2$ can be disregarded, giving:

$$\frac{1}{R} \approx \frac{\partial^2 v}{\partial z^2} = \frac{M}{EI} \qquad ...(7.11)$$

Using equation 7.11 and from the engineer's beam equation:

$$\frac{My}{EI} = \xi = \kappa y \qquad ...(7.12)$$

Therefore the strain in the outer most fibre of the section divided by $\frac{h}{2}$ gives the curvature of the section in radians (Fig. 7.12). Double integration using both supports to provide boundary conditions provides the deflection.

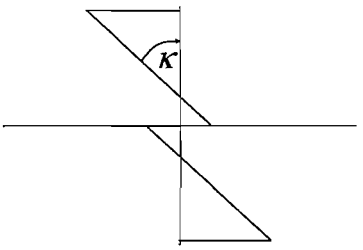

Fig. 7.12 Distribution of strain

By substituting the moment equation used to calculate the overall stress in the section divided by the flexural rigidity provides the correct terms for integration. Integrating the complex moment along the length of the section is relatively easy using modern symbolic or numerical integration techniques.

$$\frac{M}{EI} = \kappa = \frac{\partial^2 v}{\partial z^2} \qquad ...(7.13)$$

The flexural rigidity of the section is a constant therefore it can be taken out of the integration calculation (equation 7.14), where M is the moment derived from the overall curvature of the sections. Thus giving the overall deflection.

$$\frac{1}{EI}\iint M\ dz = v \qquad ...(7.14)$$

The graphically representation in Fig. 7.13 shows the output a deflection calculation represented by the solid line, the dotted lines represent the maximum and minimum deflections possible through complete shear transfer between sections and total reduced modulus action and the discrete points represent experimental data.

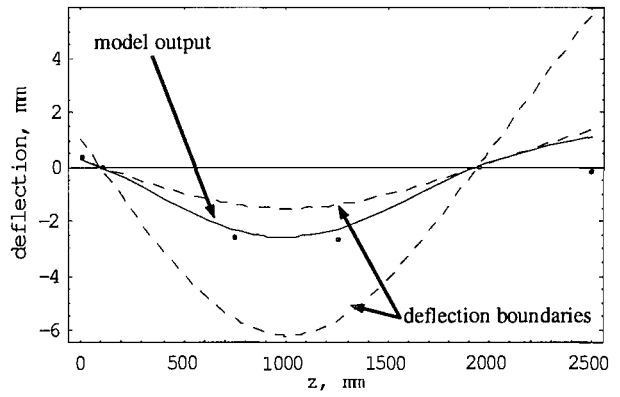

Fig. 7.13 Deflection calculated from moment-curvature relationship

7.2 Comparison between experimental and theoretical results

In order to establish the accuracy of the model the results of test series C (presented in Chapter 5) have been compared with the deflections and stresses predicted using the numerical model. Series C is arguably the most advanced of the loading arrangements considered and most closely matches the loading environment found in practical restrained steel sheet pile walls. It therefore provides a good test in which to establish the usefulness of the model in predicting pile behaviour in real SSP walls. The general layout of this test series is shown in Fig. 7.14 with the exact dimension shown in Fig. 7.15. This load setup provides an approximation to the triangular load distribution developed by active and passive pressures in retaining walls. For comparison purposes the test results reported in chapter 5 have been normalised to a total applied load of 1kN.

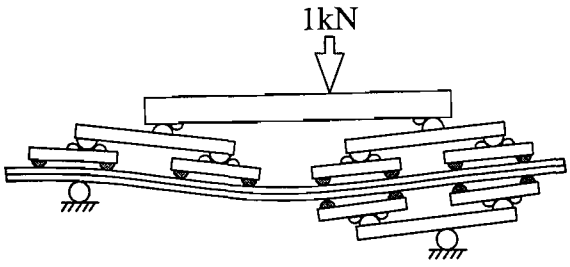

Fig. 7.14 General arrangement of test series C

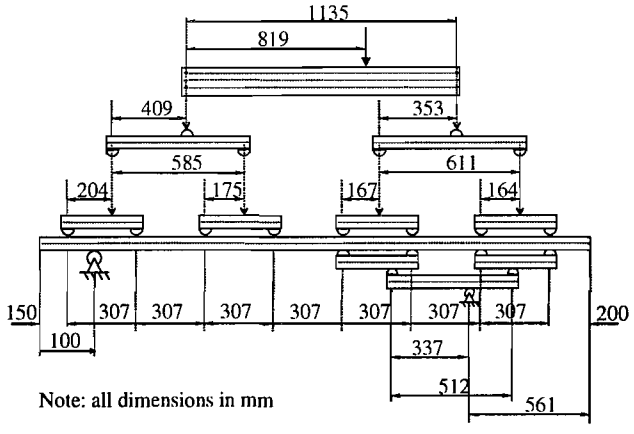

Fig. 7.15 Dimensions of test arrangement used in test series C

The loading arrangement inputted into the mathematical model is shown in Fig. 7.16, with associated bending moments shown in Fig. 7.17. Comparisons have been made with three sections with different tested conditions. These conditions are: plain interlocks, sand filled interlocks and sand filled interlocks with a simulated capping beam. These three conditions have identical bending moment distributions, but distributions of slip vary as one of the specimens had a simulated capping beam at the head of the pile.

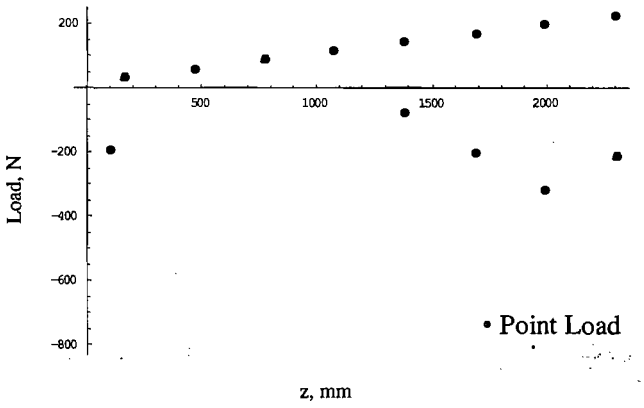

Fig. 7.16 Loading arrangement for test series C

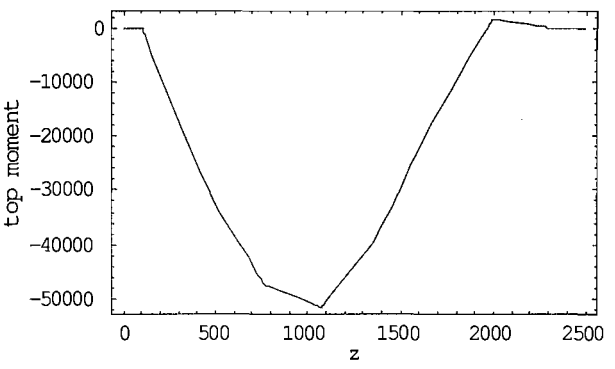

Fig. 7.17 Bending along the pile section for a 1kN applied load during test series C

The distribution of slip for any section tested without a capping beam has the form shown in Fig. 7.18i. A capping beam fixed at the head of the pile prevents movement at that point giving a form of slip shown in Fig. 7.18ii.

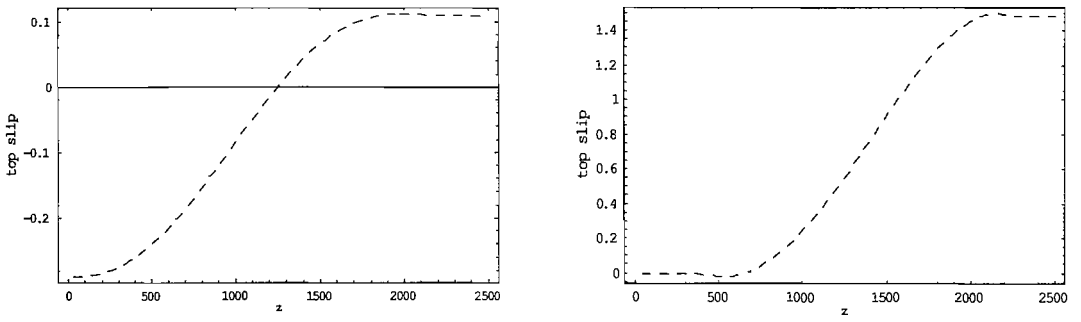

(i) (ii)

Fig. 7.18 Distribution of slip for non-capping beam (i) and capping beam (ii) pile section

The coefficients of friction and the adhesion factors used in the analysis are listed in Table 7.1, the background to which is detailed in Chapter 6. The results from the mathematical model are the distribution of stress at midpoint and deflection. Table 7.2 and Fig. 7.19 present the comparison between the relevant experimental and theoretical results.

Table 7.1 Coefficients used for theoretical analysis

Section tested	**Coefficient of friction, μ**	**Adhesion, f_{ad} (Nm^{-1})**
Plain interlocks	0.65	0
Sand filled interlocks	0.77	285

Generally, the correlation between observed and expected stress is generally good for the pile pans, although the model significantly overestimates interlock stresses. The dotted lines in the graphical representations (Fig. 7.19) of stress distributions present the stress envelope. This is the upper and lower bound limits of the stress distribution, full modulus action and fully reduced modulus action.

Table 7.2 Experimental and theoretical stress results for given test conditions

	Distribution of stress (Nmm^{-2})			
Gauge position 1250mm	**Pan**	**Interlock**	**Interlock**	**Pan**
Plain interlock test C4				
Experimental	-6.51	9.18	-11.15	6.71
Theoretical	-9.19	18.61	-18.61	9.19
Sand filled interlock test C3				
Experimental	-6.20	4.05	-4.64	6.73
Theoretical	-8.75	14.06	-14.06	8.75
Sand & capping test C2				
Experimental	-6.61	3.86	-2.18	7.40
Theoretical	-8.28	9.26	-9.26	8.28

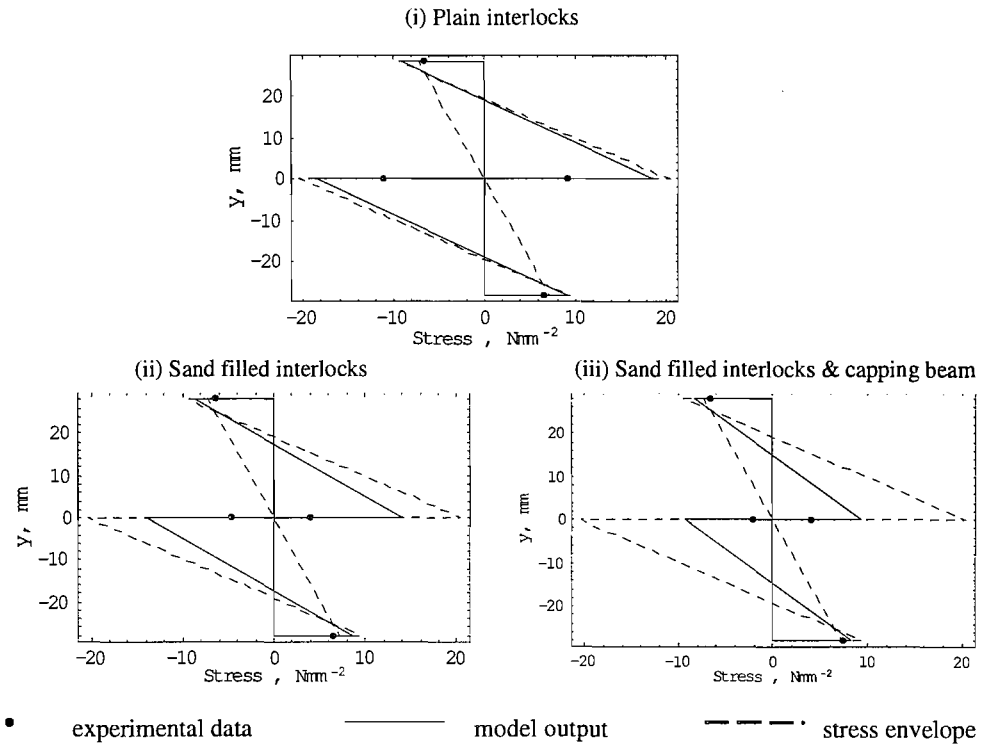

Fig. 7.19 Comparison of experimental and theoretical stress

Table 7.3 shows the data for the deflections along the length of the sections. The experimental data were taken at discrete points and the model produces a continuous function. For comparison the values of deflection at the related points have been calculated using the model.

Table 7.3 Experimental and theoretical deflection results for given test conditions

	Distribution of deflection (mm)					
Gauge position	**0mm**	**100mm**	**750mm**	**1250mm**	**1940mm**	**2500mm**
Plain interlock test C4						
Experimental	1.18	0	-3.92	-3.99	0	1.63
Theoretical	1.0	0	-5.23	-5.22	0	4.69
Sand filled interlock test C3						
Experimental	0.38	0	-2.53	-2.60	0	-0.16
Theoretical	0.86	0	-4.47	-4.31	0	3.31
Sand & capping test C2						
Experimental	0.16	0	-2.04	-2.21	0	0.32
Theoretical	0.28	0	-2.71	-2.90	0	2.21

Fig. 7.20 provides a graphical representation of the data in Table 7.3 and illustrates the accuracy of the model predictions. The section with a simulated capping beam shows the model at its best. The plain interlocks and the sand filled interlocks do not show such good correlations.

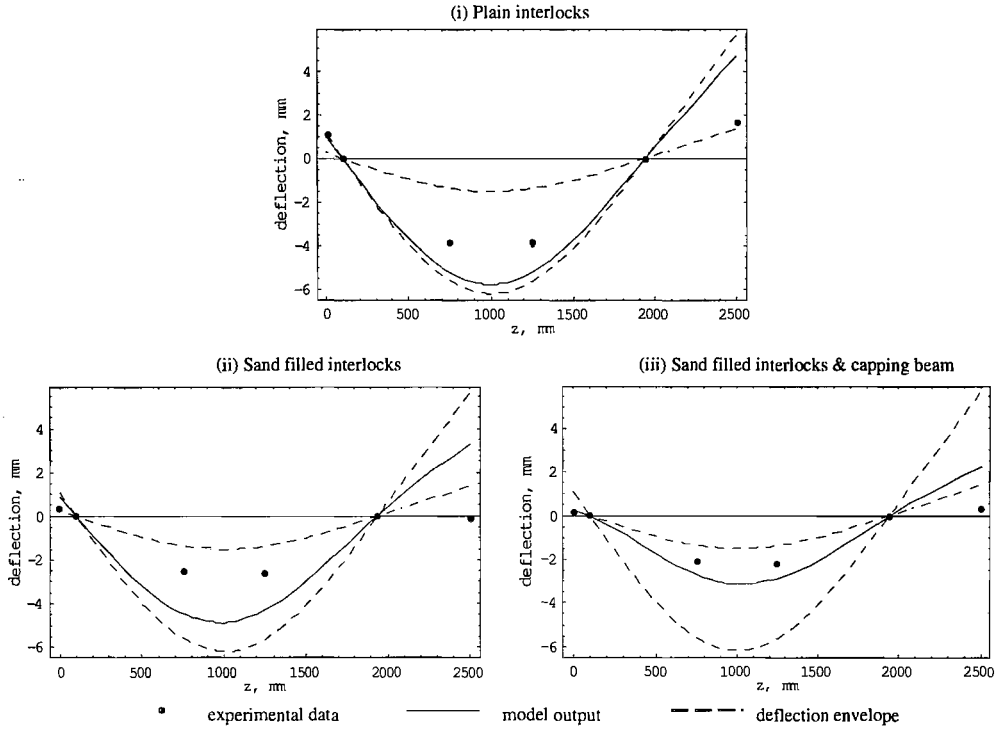

Fig. 7.20 Comparison of experimental and theoretical deflection

Using the data provided by the mathematical model a series of reduction factors have been calculated for both the theoretical data and the experimental data, see Table 7.4. The β_b-factors are given by the maximum bending stress assuming full composite action divided by the maximum bending stress predicted by the model. The table also lists the β_d-factors determined using the deflection data. All results have been compared to the stress or deflection expected for a fully composite section at the mid-span, 1250mm along the 2500mm specimen.

Table 7.4 Reductions factors using both methods of calculating interlock friction

		Reduction factors	
Section		β_b	β_d
Plain interlocks test C4			
	Experimental	0.65	0.34
	Theoretical	0.40	0.26
Sand filled interlocks test C3			
	Experimental	1.0	0.52
	Theoretical	0.52	0.32
Sand & capping test C2			
	Experimental	0.99	0.62
	Theoretical	0.78	0.47

7.3 Discussion

Table 7.4 summarises the results from the comparison between the experimental test results and the behaviour expected from the numerical model using the friction values determined experimentally. The model has produced conservative predictions of stress and deflection in all cases. It significantly over estimates the bending stresses and deflections in the plain sections and the sand filled specimens. More encouragingly it provided a more accurate estimate of behaviour for the final test (C2) in which a capping beam was simulated by preventing interlock movement at the head of the piles. In that case, the model predicted a β_b-factor of 0.78, which compared reasonably well with the experimentally derived factor of 0.99. A similar level of accuracy was achieved for the β_d-factor.

The moments generated in the sections based on the stress data compared well with the applied loading, see Chapter 5. Therefore the inconsistency between model prediction and experimental behaviour is unlikely to be as a result of poor quality bending tests. Rather, it is inaccuracies in the friction coefficients used that is more likely to account for the relatively poor correlation. The tests presented in Chapter 6 showed a wide variation. This variability may be due to the difficulty in providing a uniform level of sand in the interlocks. The result was that some of the tests produced μ-values in excess of 3, whereas others were less than 0.7. It is perhaps likely that the higher experimental strength and stiffness may be a result of sand jamming in the interlocks of the piles, thereby providing a higher value of friction than assumed in the modelling exercise.

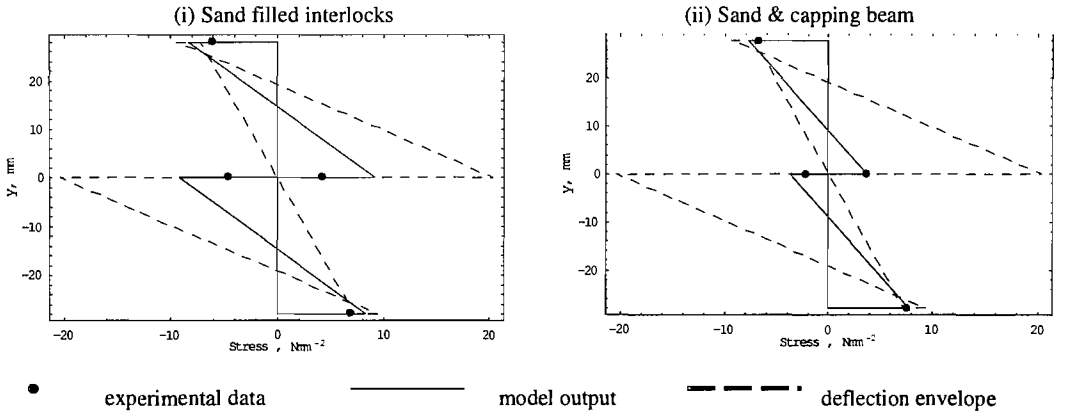

Fig. 7.21 Distribution of stress using μ=3.5 for sand and μ=1.85 for sand and capping beam

This conclusion seems justified by comparisons between the model predictions and experimental behaviour calculated using higher values of μ. A typical comparison is shown in Fig. 7.21 and Fig. 7.22. The friction in the interlocks of the sand filled specimens peaked at μ=3.5 (calculated assuming f_{ad}=0). Fig. 7.21 and Fig. 7.22 were calculated assuming that half of the peak value of μ was mobilised throughout the sections, i.e. μ=1.85 and f_{ad}=0. The comparison shows far greater agreement between experimental and theoretical results. Encouragingly, a consistency of agreement is shown between the comparisons of bending stress, as well as deflection. This provides evidence that the model can provide a reasonable lower-bound prediction of the effects of RMA, although the accuracy of the prediction is dependent on accurate measurements on interlock friction.

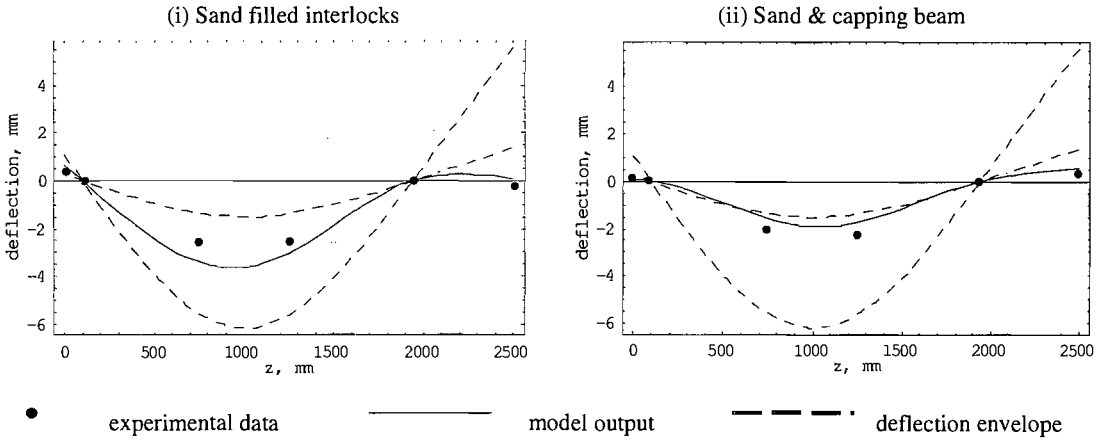

Fig. 7.22 Distribution of deflection using μ= 3.5 for sand μ= 1.85 for sand & capping beam

In particular, the jamming effect of sand in the interlocks may be due to the very small size of the scale piles. Jamming was not observed in the full scale test, in which case the model is likely to provide a more accurate prediction of the bending strength and flexibility of full scale piles.

7.4 Conclusions

In this chapter the mathematical model for predicting the behaviour of miniature sheet piles has been presented in detail. The model is based around the applied loading and the interaction between the sections due to friction. This provides a distribution of stress across the pile that consists of three components.

From the addition of the components the curvature can be determined allowing for the calculation of deflection.

The outputs from the model have been compared to experimental results carried out for this thesis and presented in earlier chapters. The only variant of the model was the level of friction generated in the pile interlocks, all other components of the model were based on known quantities and properties of the section tested. It is likely that the inaccuracies in the model outputs are a result of the variability of frictional force in the interlocks of the scale piles. The coefficient of friction was varied within the scope allowed from the tests presented in Chapter 6 and it was found to dramatically change the out come of the predicted results. Thus, it can be concluded that the model will provide a good lower bound estimate of strength and stiffness, although an accurate result is dependent on accurate measurements of interlock friction. The model is particularly accurate at modelling the behaviour of piles in which interlock movement is prevented at the pile head, such as is provided by a capping beam.

8 Application of mathematical model to full scale steel sheet piling

To understand the practical value of the research carried out in this thesis the model presented in chapter 7 has been applied to full scale steel pile sections. In producing these results a series of theoretical β-factors have been established for the full scale examples. These enable useful comparisons to be made with the current suggestions in Eurocode 3 Part 5.

Two wall types were analysed using the model. The first was a simulated cofferdam and the second a simulated propped cantilever wall. Both were analysed under different conditions in order to examine the influence interlock friction, capping beams and loading arrangement have on flexural behaviour. The conditions examined represent lower and upper bound limits of strength and stiffness. Firstly a simulation of a wall loaded by a pure hydrostatic loading was considered. The absence of soil structure interaction should facilitate the development of RMA and this should therefore correspond to a lower bound case on strength. This was followed by loading under sandy-soil conditions where granular material is expected to enter the interlocks. In addition to these conditions each wall was investigated with and without a simulated capping beam.

Table 8.1 Properties of LX 25 U-section steel sheet piles

Properties	**Single**	**Combine** (per pair)
Section length, (mm)	17500	17500
Area of cross section, (mm^2)	12100	24200
Second moment of area, (mm^4)	$10485x10^4$	$69187.2x10^4$
Elastic section modulus, (mm^3)	635000	3008400
Young's modulus, (Nmm^{-2})	205000	205000

The simulation was carried out using the mid-sized pile known as the LX25 U-section pile. All the simulations were carried out using 17.5m long piles. This length and section type represents typical geometric configurations for practical SSPs and therefore provides results that relate to practical retaining walls. The properties of the LX25 section are detailed in the Piling Handbook (British Steel, 1997) and are summarised in Table 8.1. These geometric properties are used in all the simulations

presented in this chapter. All the calculations reported are based on the on the full-scale interlock friction tests reported in Chapter 6. Under hydrostatic loads it is considered that no soil material is present in the interlocks. Therefore, when water is present the coefficient the friction of plain interlocks was used. However, when soil material is present, such as under soil loading, a higher level of interlock friction is required. For these tests the friction data reported in Chapter 6 for sand filled interlock tests in full scale piles were used, as summarised in Table 8.2. All of the analysis reported is elastic, therefore the exact magnitudes of load and corresponding bending stress is of less relevance than the comparison between the bending stress produced by full composite action and the stress predicted by the model for partial shear transfer in the interlocks. The hydrostatic load represents a situation where no material is present in the pile interlocks. This may be as a result of high water content or if the pile is driven into a peaty or soft clay material in which lower friction is likely.

Table 8.2 Interlock coefficients of friction

Interlock condition	**Coefficient of friction, μ**
Hydrostatic load (plain interlock)	0.78
Soil loading (sand filled interlock)	1.65

8.1.1 Cofferdam

The loading arrangement used for this analysis can be seen in Fig. 8.1 with the exact dimensions shown in Fig. 8.2. The triangular distributed load is provided by a series of increasing point loads.

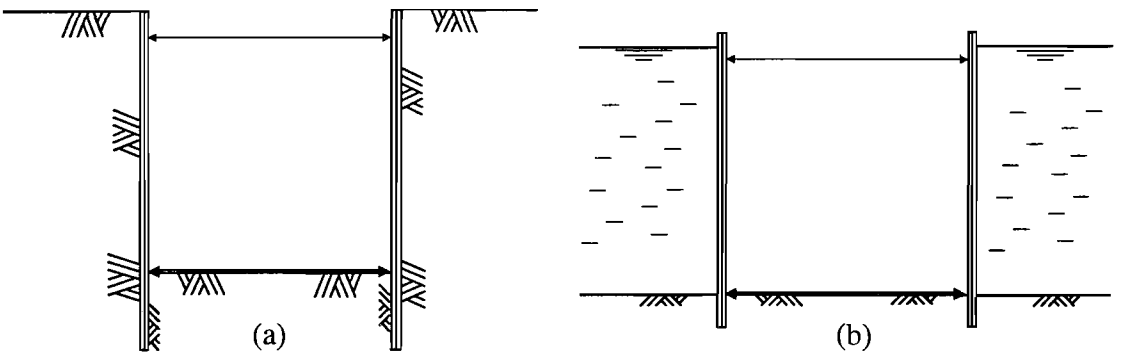

Fig. 8.1 Cofferdam style retaining wall under soil (a) and hydrostatic (b)

As with test series B the propping force at the toe of the pile wall is modelled as a point load. The reaction at the head of the pile simulates a high level prop load similar to that found in practical steel sheet pile walls.

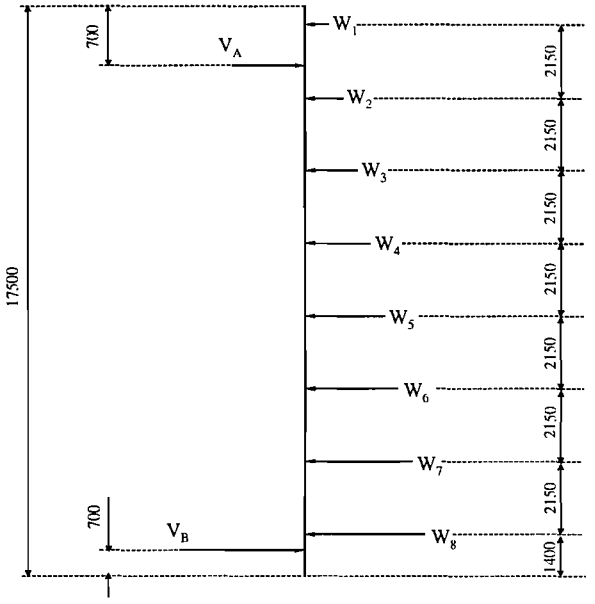

Fig. 8.2 Dimensions of the full scale LX 25 mathematical test for a cofferdam

The applied load was distributed along the section through 8 point loads of increasing magnitude, given in Table 8.3. These discrete loads approximate to a triangular distributed load similar to that found in practical situations. Knowing the distribution of load and the properties of the sections the system can be analysed.

Table 8.3 Points load applied to cofferdam test arrangement

Active point loads	**Magnitude, N**
W_1	5507.6
W_2	10917.2
W_3	16405.2
W_4	21756.0
W_5	27224.4
W_6	32477.2
W_7	38063.2
W_8	43649.2
Total	**196,000**

8.1.1.1 Results

Table 8.4 shows the outputs for the distribution of stress across two piles at their mid span. The model suggests that even with soil present in the interlocks the sections will only generate 65% of there full composite strength and 52% under pure hydrostatic conditions.

Table 8.4 Distributions of stress across a pair of LX 25 U-section piles in a cofferdam

Wall loading & type	Stress, Nmm^{-2}				β_b
	Pan	Interlock	Interlock	Pan	
A1 Hydro static load - no capping beam	-157.01	238.86	-238.86	157.01	0.52
A2 Hydro static load - capping beam	-154.95	223.61	-223.61	154.95	0.56
A3 Soil load - no capping beam	-155.02	224.13	-224.13	155.02	0.55
A4 Soil load - capping beam	-150.64	191.89	-191.89	150.64	0.65

The reduction for a hydrostatic load is close to the value achieved from the tests carried out in support of Eurocode 3 part 5. The comparatively small increase in strength due to material in the interlocks correlates with previous 3 point bending tests pile interlocks (Schillings & Boeraeve, 1996, Hartmann-Linden *et al.*, 1997) were only a 2-12% increase in strength was found due to interlock friction.

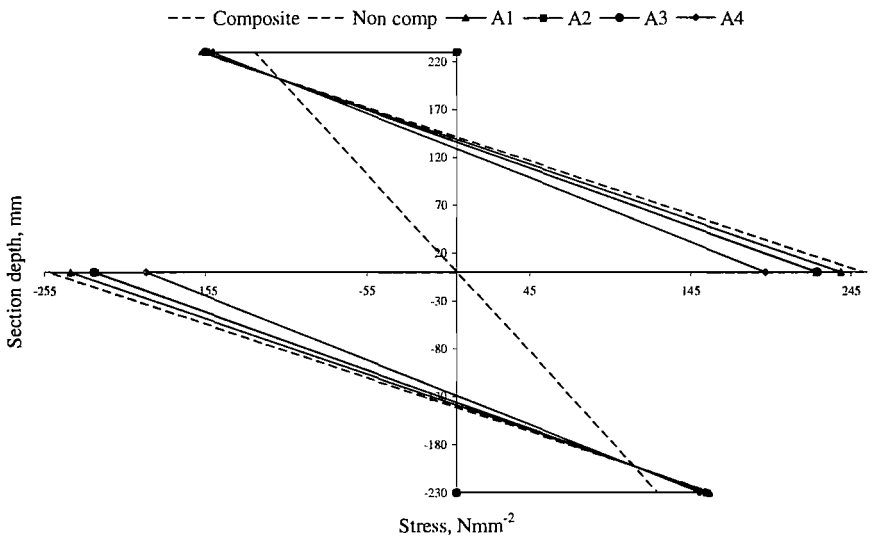

Fig. 8.3 Distributions of stress at the mid span for a cofferdam

Fig. 8.3 gives a graphical representation of the distributions of stress calculated across two piles at the mid-span. It can be seen from the illustration that a significant amount of stress is being developed in the interlocks. This demonstrates the

occurrence of a significant amount of RMA. The influence of sand reduces the magnitude of interlock stress by 14% for a cofferdam with a capping beam. However the overall effect of this reduction only provides an increased in the strength from 3-13% across the range of the tests.

Table 8.5 Distributions of deflection across a pair of LX 25 U-section piles in a cofferdam

Wall loading & type	Deflection, mm					β_d
	0	5250	8750	16800	17500	
A1 Hydro static load - no capping beam	29.58	-170.83	-225.90	0	32.83	0.31
A2 Hydro static load - capping beam	26.76	-160.44	-214.99	0	31.62	0.33
A3 Soil load – no capping beam	27.89	-162.07	-214.10	0	30.62	0.33
A4 Soil load - capping beam	21.92	-140.07	191.63	0	28.06	0.38

The deflection results for considerable reductions in stiffness. Table 8.5 shows the results from the simulations. The result for sections installed without a capping under hydrostatic loading exhibit a 69% reduction in stiffness. This level of stiffness could present serviceability problems, such as the settlement of structures adjacent to a cofferdam. Installing a capping beam provides only a 2% increase in the overall stiffness. When considering the same wall with increased interlock friction the flexural stiffness is 62% below the fully composite value.

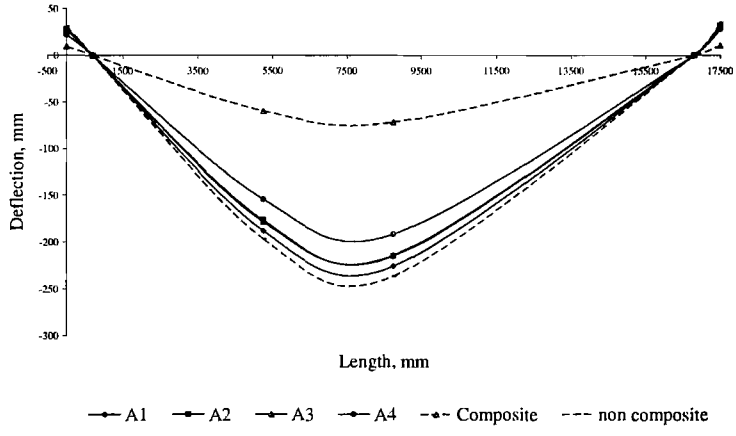

Fig. 8.4 Distributions of deflection along a cofferdam

The graphical representation of the results, Fig. 8.4 illustrates the significant reductions in stiffness. Although strength is mildly increased with sand in the interlocks the stiffness is still considerably lower than the composite value and would present a danger if not considered in design.

8.1.2 Propped cantilever wall

The loading arrangement used for analysing a propped cantilever steel sheet pile wall (Fig. 8.5) is shown in Fig. 8.6. As with the cofferdam arrangement the distribution synonymous with retaining wall loads is provided by a series of increasing point loads.

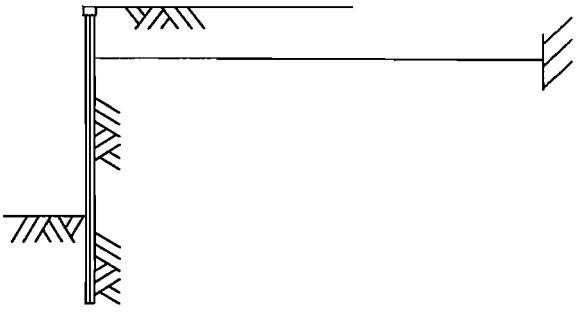

Fig. 8.5 Propped cantilever style retaining wall with high level anchor

This loading arrangement varies from the previous because of the much greater depth of embedment. This simulates the larger embedded depths that cantilever walls have. The reaction load at the head of the pile simulates the anchor or prop load. This arrangement presents a typical loading arrangement for a propped cantilever wall.

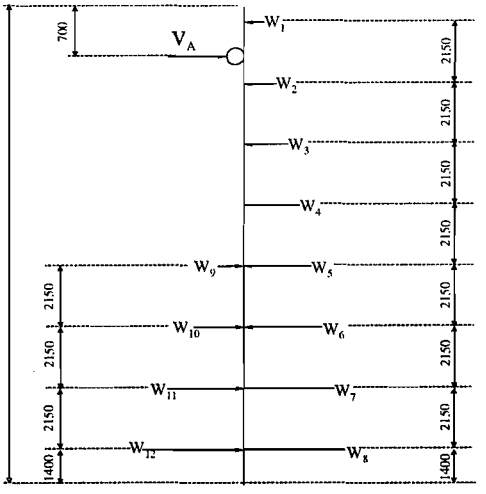

Fig. 8.6 Dimensions of the full scale LX 25 mathematical test for a propped cantilever wall

Table 8.6 presents the magnitudes of the forces applied directly to the test specimen, these are the active loads. The passive loads are derived from the reaction of the applied loads. The remaining difference between the active and passive loads is the reaction through the prop at the head of the pile.

Table 8.6 Points load applied to propped cantilever test arrangement

Active point loads	Magnitude, N
W_1	15145.9
W_2	30022.3
W_3	45114.3
W_4	59829.0
W_5	74867.1
W_6	89312.3
W_7	104673.8
W_8	120035.3
Total	**539,000**
Passive point loads	
W_9	40010.3
W_{10}	108175.1
W_{11}	171582.4
W_{12}	114389.0
Total	**434,156.8**

8.1.2.1 Results

The results presented below show that the influence of sand in the interlocks is more effective at increasing the strength and stiffness of LX 25 sections than in a cofferdam propped at the head and toe of the piles. The increased active-passive pressures acting on the wall increase the reactions at the point loads, approximately 3 times greater than that of the cofferdam loads to produce similar stress levels. This provides a greater friction force generated in the interlocks.

Table 8.7 Distributions of stress across a pair of LX 25 U-section piles in a cantilever wall

Wall loading & type	Stress, Nmm^{-2}				β_b
	Pan	Interlock	Interlock	Pan	
B1 Hydrostatic load - no capping beam	-137.25	196.58	-196.58	137.25	0.56
B2 Hydro static load - capping beam	-129.06	136.20	-136.20	129.06	0.81
B3 Soil load - no capping beam	-133.15	166.36	-166.36	133.15	0.66
B4 Soil load - capping beam	-115.81	38.63	-38.63	115.81	0.95

These results suggested by the model show that under soil loaded conditions and with a capping beam in place U-section piles achieve 95% of their full modulus. This prediction correlates with the aluminium small scale tests carried out in Chapter

5. When material is not present in the interlocks the addition of a capping beam could have the effect of increasing strength by 25%. In all sections a considerable amount of stress is generated in the interlocks but for section B4 this stress is lower than that in the pile pans, thus only allowing for the small reduction in strength due to RMA.

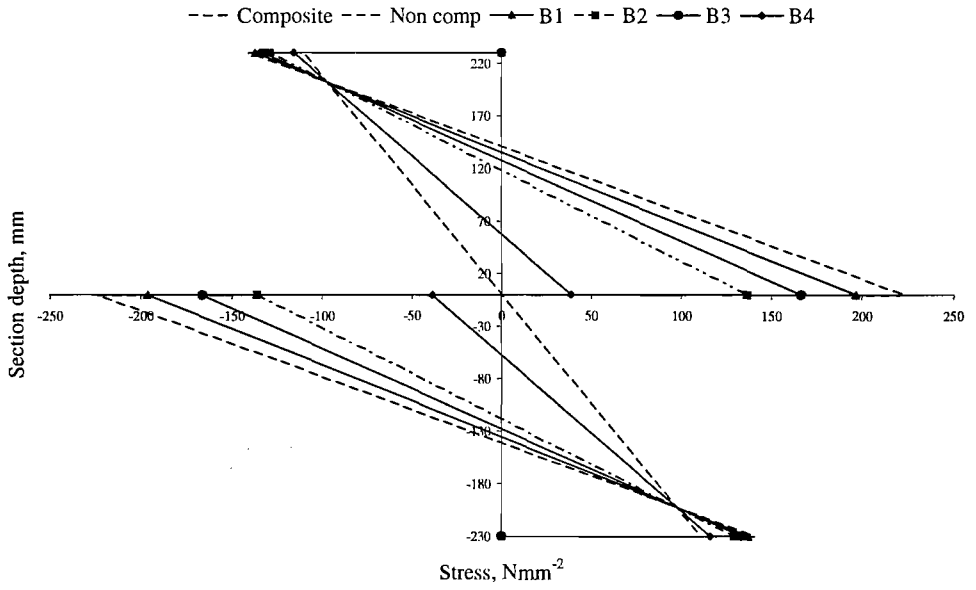

Fig. 8.7 Distribution of stress for a propped cantilever wall

The distributions of deflection are shown in Table 8.8 with the corresponding reduction factors. Only the soil loaded capping beam test, B4 provided a high level of stiffness. The model suggests large reductions in stiffness with the lowest reduction factor for a hydrostatic load with no capping beam giving a reduction factor of 0.34.

Table 8.8 Distributions of deflection across a pair of LX 25 U-section piles in a propped cantilever wall

Wall loading & type	**Deflection, mm**					β_d
	0	5250	8750	13580	17500	
B1 Hydro static load - no capping beam	23.15	-120.80	-120.07	0	104.12	0.34
B2 Hydro static load - capping beam	14.29	-89.96	-91.86	0	79.75	0.44
B3 Soil load - no capping beam	20.76	-108.99	-105.87	0	72.74	0.38
B4 Soil load - capping beam	2.05	-43.17	-46.21	0	21.21	0.87

These high levels of deflection conform to Schillings and Boeraeve's (1996) investigations of reduced length tests of U-sections in laboratory conditions. If RMA was not considered in design this wall would not satisfy serviceability limits and may be considered unsafe depending on the interlock conditions. However, under new Eurocode advice this extra flexibility would be compensated for using the suggested reduction factors.

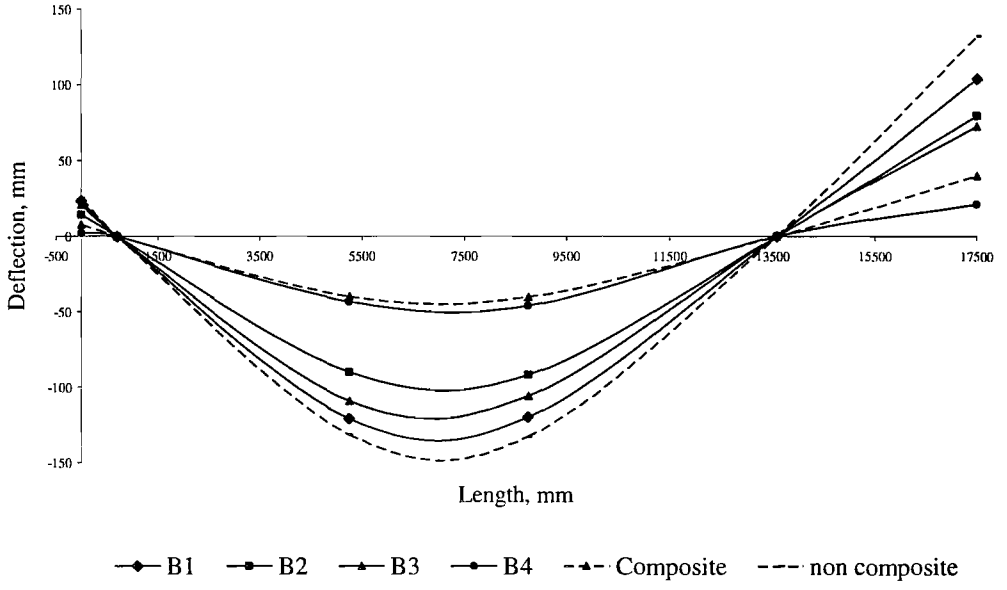

Fig. 8.8 Distribution of deflection for a propped cantilever wall

8.2 Effect of varying interlock friction in full scale SSPs

The comparison between the experimental and theoretical data in Chapter 7 showed that high levels of friction were required for the model to accurately predict behaviour. This may have shown the unpredictability of friction using simple pull-apart tests and that friction within a complex long sheet pile is unique to that situation. Due to this a progressive series of friction values have been examined where the coefficient of friction is raised in equal increments. The following analysis varied the level of friction generated in the interlocks from μ=0 to μ=2.0 in creasing in 0.5 increments.

8.2.1 Results

The upper section of Table 8.9 presents the range of β-factors for a cofferdam with and without a capping beam. The results suggest that β_b varies between 0.49 and 0.59 as μ increases from 0 to 2.0. However, with a capping beam β_b increase to 0.72. Therefore, for the case of a cofferdam, RMA can be expected to have a significant effect on strength, even where interlock friction is high.

Table 8.9 Reduction factors for a steel sheet pile wall

Coefficient of friction	No capping beam		Capping beam	
	β_b	β_d	β_b	β_d
	Cofferdam			
0.00	0.49	0.30	0.49	0.30
0.50	0.51	0.31	0.53	0.32
0.78	0.52	0.31	0.55	0.33
1.00	0.53	0.32	0.58	0.34
1.50	0.55	0.33	0.63	0.37
1.65	0.56	0.33	0.65	0.38
2.00	0.57	0.34	0.70	0.40
	Propped Cantilever wall			
0.00	0.49	0.30	0.49	0.30
0.50	0.53	0.32	0.67	0.38
0.78	0.56	0.34	0.81	0.44
1.00	0.58	0.35	0.88	0.50
1.50	0.64	0.37	0.94	0.74
1.65	0.66	0.38	0.95	0.87
2.00	0.72	0.40	1.0	1.0

The information in Table 8.9 is presented in two graphs. Fig. 8.9 shows the reduction factors relating to the section stiffness and Fig. 8.10 shows the reduction factors relating to the bending strength.

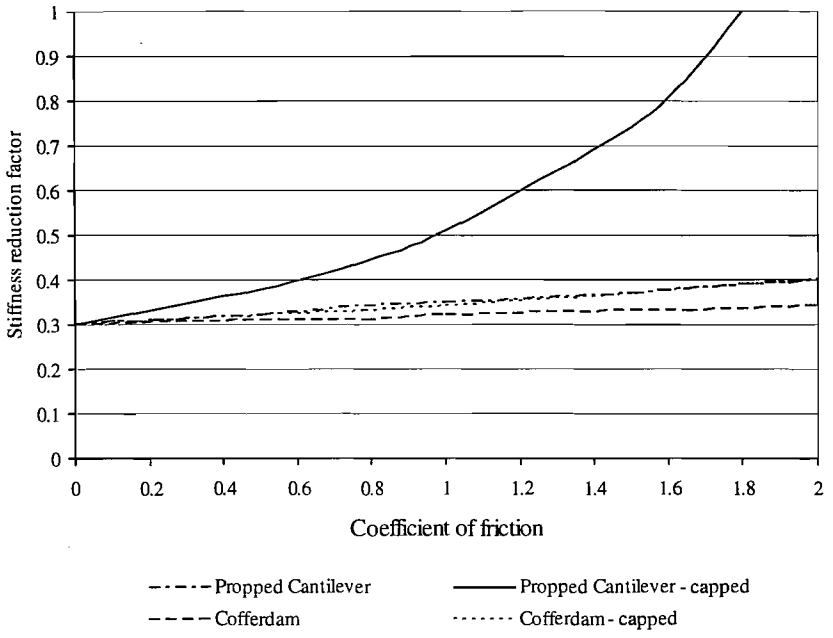

Fig. 8.9 Reduction factor β_d to be applied to the second moment of area

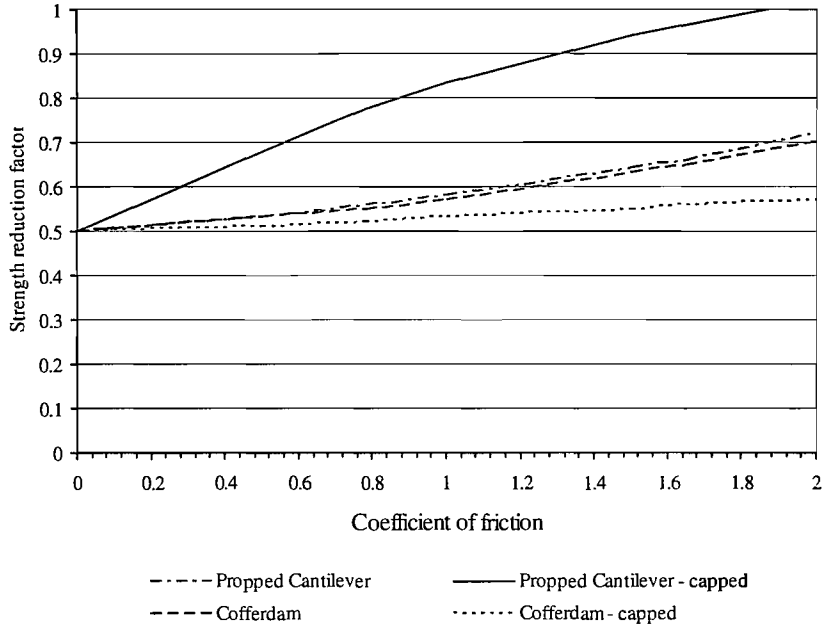

Fig. 8.10 Reduction factor β_b to be applied to the section modulus

The reduction factors for a propped cantilever wall with and without a capping beam under various different levels of interlock friction are shown in lower half of Table 8.9. The results suggest the inclusion of a capping beam in the design of the

wall would provide significant advantages for both stiffness and strength under high levels of interlock friction.

When a capping beam is not in place the increase in strength with friction is more pronounced than in the cofferdam situation improving by 23% overall. Unlike the cofferdam the increases in strength are not linear for the propped cantilever wall. However, the increase in stiffness is more uniform increasing by 2-3% for each 0.5 increase in the coefficient of friction. The increase in friction had the greatest influence in the propped cantilever wall with a capping beam. Overall the increase in strength and stiffness were 51% and 70% respectively. This suggests that at μ=2.0 full modulus action is achieved and there is no reduction in strength or stiffness. This level of friction is not unreasonable as full scale tests carried out in Chapter 6 showed sections with sand in the interlocks achieving coefficients of friction of μ = 1.65, and ignored skin friction. The results suggest that under given circumstances close to the full bending strength is achieved, albeit with a reduction in stiffness of the sections.

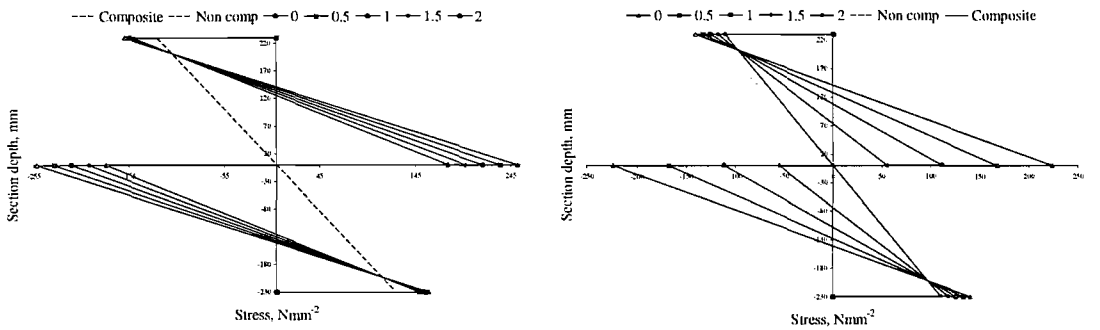

(Cofferdam with capping beam) (Propped cantilever with capping beam)

Fig. 8.11 Distributions of stress across sections with varying levels of interlock friction for a cofferdam and propped cantilever walls with capping beams

Fig. 8.11 shows the progressions of the distributions of stress with increasing interlock friction for the two example walls with capping beams. It clearly illustrated that the cofferdam even with high levels of friction shows significant amounts of stress in the interlock. These large stress values cause the low reduction factors presented. Conversely, the propped cantilever wall shows the increased friction slowly develops lower interlock stresses for the same levels of increasing friction. This results in the interlock stress becoming lower than the pan stress resulting in only a minor reduction in elastic bending strength due to RMA.

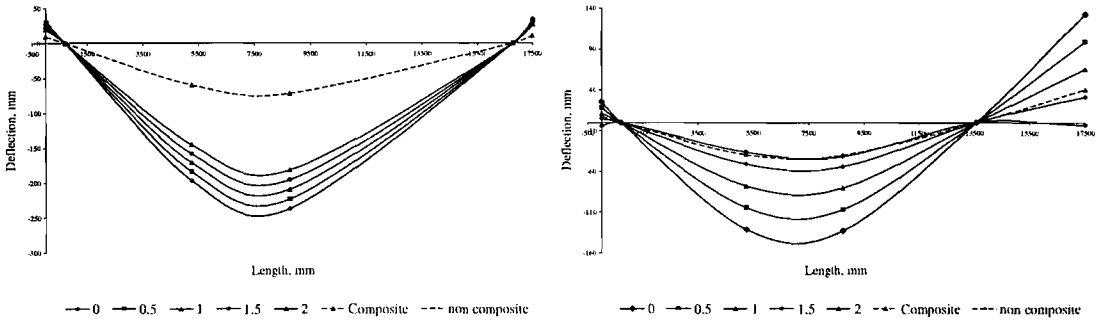

(Cofferdam with capping beam)

(Propped cantilever with capping beam)

Fig. 8.12 Distributions of deflection along specimen with varying levels of interlock friction for a cofferdam and propped cantilever walls with capping beams

The example walls shown in Fig. 8.12 illustrate a similar effect with the deflection. The increase in friction does not significantly affect the stiffness of cofferdam, although it is found to have a substantial stiffening effect for propped cantilever walls. It can be seen that the cofferdam only achieves half the stiffness of a composite section, for the same coefficient of friction, as for the propped cantilever. The increased reactions between the sections in the propped cantilever wall are arguably the reason for these results suggested by the mathematical model.

8.3 Conclusions

The analysis reported herein provides an insight into the behaviour of U-section steel sheet piles in practical situations. The tests have suggested that RMA has a significant effect on cofferdams (propped top and bottom) and comparatively less effect on propped cantilevered walls.

Overall the two situations analysed behave quite differently under similar levels of interlock friction. A cofferdam propped top and bottom or with little embedment, akin to simple supports top and bottom, presents a situation conducive to RMA and confirms findings by Schmitt (1998). Both Schmitt's results and the findings in this thesis suggest that RMA can be a serious design issue in these situations. A method of prevention of slippage, such as a capping beam or welding of pile heads, can be expected to have only a minor influence on strength and stiffness. β-factors for this situation are presented in Table 8.9 and range from β_b= 0.52-0.65

and β_d= 0.31-0.38. These suggestions conform to recommendations in BS8002 (BSI, 1994) which states that piles should be crimped when in soft clays, with long cantilevers or not driven to their full embedded depth. Situations presenting low β_d could be expected to result in excessive deflections.

The second situation representing a propped cantilever steel sheet pile wall, in which passive resistance at the front of the pile is expected to provide the lower support. This thesis presents the first laboratory based experimental tests of this loading arrangement. BS8002 states RMA should not be a problem:

> *'...trough type steel sheet piling... develops the strength of the combined section only when the piling is fully driven into the ground... The shear forces in the interlocks may be considered as resisted by friction due to the pressure at the walings and the restraint exercised by the ground'.*

These investigations confirm the approach. If soil is present in the interlocks then suggested reduction factors for a propped cantilever wall range from β_b= 0.56-0.66 and β_d= 0.34-0.38. However, with a capping beam placed at the head of the pile higher values of β_b= 0.81-0.95 and β_d= 0.44-0.87 can be recommended. The more complex bending moment and deflected shape combined with multiply points of contraflexure could account for this amplified effect as well as the increased reactions due to the active-passive loading arrangement.

The recommendations for the reductions factors are conservative estimates or lower bound limits. They have not taken into consideration other possible external elements that aid the strength and stiffness of a retaining wall, such as the effect of skin friction.

9 Discussion of results and design considerations

Piling has been used for centuries, but it was Larssen in 1897 that provided the world with the first U-section profile. Since that time U-sections have been used widely around the world. In the UK and Japan guidelines such as BS8002 have generally proved successful in providing useful information on which to base SSP design. The effect RMA has on the strength and stiffness of U-section piles has been a topic of debate for generations with the earliest known reference in 1934 (Lohmeyer, 1934). In the absence of clear guidance RMA has rarely been considered in design, with the exception of the well defined set of situations itemised in BS8002, such as large cantilever walls. Until recently this was acceptable in most situations but with the impending introduction of Eurocode 3 Part 5 and the research in its support, RMA has become an issue that significantly affects the economics of this form of construction. In particular, the β_b reduction factor applied to flexural strength calculations ranges from 1.0 to 0.55, thus it could almost half the efficiency of this pile type. However, anecdotal evidence tends to suggest that RMA has not been a problem in permanent works, although it has been known to occur under hydrostatic conditions, such as temporary cofferdams in marine works. The difference between the laboratory and practical views of the behaviour of U-section steel sheet piles has remained constant through the development of retaining wall design. Practicing engineers tend to disagree with the laboratory findings and suggest that RMA rarely occurs in propped cantilever retaining walls, (Thompson, 2003).

The largest market for U-section piles is Japan, yet their engineers do not take RMA into consideration during the design process. Conversely, the Netherlands take a more conservative attitude towards the ability of the U-section piles to generate sufficient shear transfer in the interlocks to provide a composite structure. The major differences between these nations is the ground in which they install the piling. The Netherlands predominantly consists of soft weak peaty soils. This provides excellent conditions in which to drive piles, but it may provide the freedom for piles to slip freely and thereby facilitate the development of RMA. This may explain Dutch concern over its effect. In the UK, where RMA has typically been ignored during the design of most permanent retaining walls, it generally is not a design consideration

and the predominant ground conditions are granular soils and over consolidated boulder clays. These conditions often present problems with instillation although problems with RMA have been rarely observed, outside the use of cofferdams retaining hydrostatic loads. These differences in ground conditions may explain the difference in design approach.

Research concerning the effects of RMA in U-section SSPs is relatively sparse, (Williams & Little, 1996). The research into retaining wall design has predominantly been focused upon the geotechnical aspects of retaining walls, rather than the structural response to load. More recently research has begun to look at the structural elements of the retaining walls examining the effects of flexibility and ultimate strength depending on the type of wall and construction materials (Potts & Fourie, 1984, 1985).

Due to effects of RMA, a solution in overcoming the short falls of a U-section in soft soils, known as crimping, has been the focus of recent research. It has been suggested in several design codes that RMA can be overcome by simply welding or crimping pairs of U-sections together in order to create a quasi composite section (BSI, 1994 and CEN, 1996). However, this causes problems with handling and driving and is therefore often an unsatisfactory option (Rowbottom *et al.*, 1996). There is also the effect of oblique bending that has to be addressed. If piles are crimped together arguably they still do not achieve full modulus making crimping an unnecessary expense.

It has been the task of this thesis to deal solely with individual sections. Thus taking on the question of how individual steel pile sections behave with varying interlock conditions under realistic loading conditions. For the first time U-section sheet piles have been tested under realistic loading arrangements in laboratory conditions. The interaction between the interlocks and the effects of varying levels of friction has been investigated. As discussed in this thesis, full-scale testing is problematic due to size constraints. The present work overcomes this problem using an innovative approach to testing whereby miniature piles have been extruded from aluminium. These pile sections were U-shaped in profile but unlike a typical pile both interlocks connected together to form a tubular section. The tubular arrangement provides a symmetrical section and eliminates the free interlocks that could cause early failure through local buckling. To aid the adaptation of the analyses and to enable comparisons to be made with steel sections an additional

series of reduced size steel interlock pull-apart test were conceived to investigate levels of friction developed in steel on steel situations.

The majority of research carried out on steel sheet piling has been from a geotechnical perspective. These investigations tend to look at the activity behind the wall rather than how the structure itself is behaving. The limited laboratory experiments into the behaviour of U-section steel sheet piles have arguable provided a partial model of reduced modulus action. It is recognised that the scale test carried out to analyse the behaviour of sheet piles presents different problems, such as differences in material properties and scaling factors. However, the experiments presented provide a qualitative indication of the behaviour of U-section steel sheet piles. They also provide an opportunity to test a numerical model reported in Chapter 6, where parameters can be changed to investigate the behaviour of full scale piles.

The initial tests presented in Chapter 3 are simple 3-point bending tests using short span sections, carried out in support of the development of Eurocode 3 Part 5 by Hartmann-Linden *et al.* (1997) and Schillings and Boeraeve (1996). An increase in strength of between 2-12% was attributed to the influence of sand in the interlocks. The results of the 3-point bending short span tests using the U-section extruded aluminium showed large variations in the data. The tests suggested that with the influence of sand in the interlocks the overall bending strength increased by 12%. This is in close agreement with Hartmann-Linden's investigations. This could provide evidence to suggest that short span tests suffer from RMA. However, as they do not represent the loading arrangement experienced by real SSP walls it may be considered as unrepresentative of practical steel sheet pile walls.

Continuing on from the short span experiments a more elaborate test was carried out in series B. These series of tests set out to closely simulate the loading configuration applied to real SSP walls. In particular the span to depth ratio closely matched those found in typical pile walls. In addition, a triangular load distribution was provided to simulate active pressure from a soil or hydrostatic load. Comparisons between moments generated from strain gauge data with the moments predicted from the applied load and frame geometry initially showed poor agreement. It was necessary to incorporate low friction PTFE bearings covered with silicone grease in order to provide a close agreement between expected bending stresses and those observed with the strain gauges. The series of experiments reported in Chapter 4 and 5 presents for the first time laboratory based experiments

using loading arrangements akin to those found in practical pile walls. The two experimental situations present the upper and lower bound limits for the development of reduced modulus action. Firstly the cofferdam arrangement, highlighted in BS8002 (BSI, 1994), presents the situation most likely to suffer the consequences of RMA.

During testing many factors proved difficult to overcome to produce accurate results. The most predominant factor was friction generated between the load applicators and the specimen. However, as discussed this friction was largely eliminated using PTFE and silicone grease. Test series B1-5 investigated the behaviour of piles with a large cantilevered section above the top anchor level. Observed and expected bending stress correlated very closely for all tests performed. Lubricated interlocks provided the worst case for strength and stiffness showing reductions of β_b=0.45 and β_d=0.32. This provided the lower boundary condition simulating almost zero interlock friction or total reduced modulus action. The plain sections behaved similarly showing reduction factors of β_b=0.47 and β_d=0.32 improving slightly but only in bending strength but still performing similarly to the fully reduced modulus specimen. Strength and stiffness was improved with sand introduced into the interlocks showing reduction factors of β_b=0.99 and β_d=0.81. This increase in both strength and stiffness was in excess of Schillings & Boeraeve (1996) findings. However, in this particular series a capping beam was simulated by locking the interlocks at the head of the pile. This resulted in reduction factors of β_b=0.95 and β_d=0.62.

Using a similar loading arrangement test series B6-11 are presented but with a smaller cantilever above the height of the prop load. Under the same load the influence of sand in the interlocks causes a reduction in the peak stress from 56.7Nmm^{-2} to 25.2Nmm^{-2} for a 1kN applied load. The test containing sand in the interlocks behaved similar to the composite section for bending strength giving β_b=1.0. The deflection data presented slight reductions in stiffness with β_d=0.90 with a capping beam and β_d=0.84 without a capping beam. The results of this series of tests suggest that under these specific loading conditions that the influence of sand in the interlocks produces significantly larger increases in strength and stiffness than previously suspected (Schillings & Boeraeve, 1996). These increases in performance could be due to the modelling of the loading commonly found in practice, in which

the earth pressure distributions in effect help to clamp the base of the piles producing larger reactions between the interlocks. The tests suggest the effect of increasing the cantilever at the head of the pile above the top prop increases the effect of RMA, as outlined in BS8002 (BSI, 1994).

Fully restrained walls consist of a comparatively large depth of embedment and are anchored near the head of the pile. This situation presents a loading arrangement comprising of an active-passive pressure distribution. Test series C sets out to accurately model the active-passive loading arrangement by using the same active loading arrangement from test series B, in addition to a support system that aims to replicate the triangular load distribution created by passive resistance.

Two prop or tie rod positions were modelled during this series of experiments to establish if the height of the top support affected the development of RMA. The first series (C1-C5) were tested with the prop positioned 100mm from the head of the pile. The results were similar to test series B. When sand was introduced into the interlocks the performance of the sections increased considerably in both strength and stiffness over the plain interlock sections. This presented reduction factors of β_b=0.97 and β_d=0.63. The small amount of stress in the interlocks shows that the sections did not act fully compositely. This is echoed in the deflection data where the reduction in stiffness is still significant and may present problems with serviceability limits.

Tests C6-C10 simulated a propped cantilever wall with a tie-rod or prop positioned at a lower position. This is a situation regarded in BS8002 as having considerable risk of RMA as it had a large cantilever above the highest prop. Generally, the results showed an increase in strength and stiffness with the increase of friction in the interlocks. The increases in both strength and stiffness were not as pronounced as with the propped cantilever wall with a higher positioned prop.

The tests containing sand within their interlocks suggest that soil-structure interaction can largely mitigate the effects of RMA. However, RMA is not totally eliminated and inter-pile movement was still observed. The friction generated in the interlocks was enough to produce levels of interlock stress less than the pan stresses. This indicates a significant step towards the generation of composite action, with β_b=0.77 and β_d=0.61.The addition of a capping beam produced mixed results reducing the strength of the sections but increasing the stiffness thus providing

reductions factors of β_b=0.71 and β_d=0.68. From the data provided from the propped cantilever wall tests it is not possible to draw definitive conclusions regarding the effect of a capping beam on RMA. However, generally it seems to increase stiffness but not strength.

The propped cantilever wall test series have provided the upper bound limit of strength and stiffness for sheet pile wall situations for this these test series. As previously mentioned, friction between the test specimens and the load applicators caused a considerable reduction in the bending moment in the section. This effect of skin friction was reduced to a minimum in all experiments to provide accurate bending moment comparisons between measured and theoretical data. Thus soil-structure interaction causing increased skin friction can be expected to have a considerable effect on RMA and the test series reported should be regarded as a worst case scenario within the prescribed conditions. The objective of these tests was to provide a suggestion to the reduction in both strength and stiffness to facilitate the safe design of retaining walls and to aid the estimation of the serviceability limits of the walls. If these tests are representative of full scale sections in practical applications these results could justify a recommendation for reduction factors of β_b=0.90 and β_d=0.70 for soil loads and β_b=0.55 and β_d=0.50 in hydrostatic conditions. In addition to these reduction factors results suggest that the top prop be placed as high as possible on the face of the retaining wall.

In order to further understand the level of friction generated in the interlocks of U-section sheet piles a series of pull apart tests were devised. Similar tests have been reported by Vanden Bergh (2001), in which interlock friction was measured in short lengths of pile interlocks extracted from containers of sand. The tests reported in this thesis differ as they were carried out horizontally with one interlock fixed in position and the adjacent pile pulled away while under a known vertical load. This system enables the calculation of the coefficient of friction under different interlock conditions. Vanden Bergh tests did not provide this information as the normal force was unknown. Two series of tests were carried out using this system of loading. Firstly the aluminium sections were tested with plain interlocks and sand filled interlocks and secondly LX 25 steel pile interlocks were tested to provide comparison between materials.

The tests provided a range of coefficients of friction that could be later used in the development of a mathematical model to predict the behaviour of U-section piling. It was apparently that with no load applied and with sand in the interlocks a force was still require in pulling apart the miniature piles. This effect was not present with the full-scale pile interlocks and it may be because the sand grains became jammed in the miniature pile interlocks, thus producing friction forces in the absence of a normally applied load. This jamming effect may have been responsible for the wide variation in friction values determined for the sand filled miniature pile interlocks. The coefficients of friction found in these experiments ranged from μ=0.63 for plain aluminium interlocks and μ=0.78 for plain steel, but with sand the average value was μ=1.2 for aluminium interlocks and μ=1.65 for steel.

A mathematical model of the behaviour of U-section piles was developed that was validated using the results from the experimental investigation. The components of stress are generated from the externally applied bending moment, the secondary bending stress cause by the eccentricity of the axial frictional force and the direct axial stress from the frictional force. The resulting stress distributions were used to calculate the curvature distributions which were integrated twice thereafter to calculate deflection.

The accuracy of the model was compared against the results from Series C tests, which is arguable the most realistic series of tests. The comparison showed that the mathematical model provides good but conservative estimating of strength and stiffness. The reduction factors suggested by the model for hydrostatic conditions are β_b=0.40 and β_d=0.26 and with soil material in the interlocks and a capping beam β_b=0.78 and β_d=0.47. The μ-values measured during the experiments reported in Chapter 6 were varied when considering sand in the interlocks. The mathematical model analysed the same propped cantilever wall using the peak μ-values, μ=3.5. The theoretical and the experimental results for the capping beam example correlated very closely using this higher value of friction, which may be as a result of sand jamming the interlocks of the miniature piles.

Having validated that the model produces a good, albeit conservative assessment of the strength and stiffness of the miniature piles, it was used to assess the behaviour of full-scale piles. This was achieved by modifying the material and

geometric properties within the model, as well as coefficients of friction for full-scale interlocks.

Looking firstly at the cofferdam situation the model suggested large reductions in the flexural rigidity. The model simulated both hydrostatic and soil loaded piles with and without capping beams. The model suggested that capping beams provide increases in both strength and stiffness by a considerable amount. Reduction factors suggested by the model for the cofferdam were β_b=0.52 and β_d=0.31 under hydrostatic conditions and with soil material in the interlocks β_b=0.65 and β_d=0.38. These reduction factors show that cofferdams propped top and bottom are likely to experience substantial problems from RMA. The model suggests that serviceability limits are the major concern for this type of construction, even under soil loaded conditions where interlock friction is comparatively high. Excessive deflections could be avoided with the addition of multiple props along the length of the face of the wall with the top prop positioned as high has possible, leaving only a small cantilever.

Having considered the cofferdam the model was reset for the analysis of a propped cantilever wall. This is arguable the most common type application of U-section SSPs. From the model the interlocks stresses predicted for a hydrostatically loaded piles were 197Nmm^{-2}. With the introduction of sand this was reduced to 166Nmm^{-2}. The interlock stress was lowered even more when a capping beam was simulated reducing the stress to 129Nmm^{-2} under hydrostatic loads and 39Nmm^{-2} under soil loaded conditions. The steel piles in a propped cantilever wall with a capping beam showed a reduction factor of β_b=0.81 under hydrostatic loads and β_b=0.95 under soil loads. These values are considerably more optimistic than Eurocode 3 Part 5's suggestion for strength.

The deflection data presented suggests that an increase in deflection can be expected under all conditions tested. The influence of the capping beam on the serviceability limits of U-section steel piles has a small effect and the influence of sand in the interlocks only slightly increases stiffness. The reduction factors for the propped cantilever wall ranged from β_d=0.34 for a hydrostatic load and β_d=0.87 for a soil loaded example with a simulated capping beam.

A series of results were obtained using the model over a range of coefficients of friction. These results were presented in table form with the relevant reduction

factors that could be applied for each situation. Knowing the loading situation and the level of interlock friction expected the engineer would be able to pick a suitable reduction factor to be used in the design of the U-section steel sheet pile wall. Although in this analysis high values of friction were needed to produce full composite action the model only considers interlock friction as a means of transferring longitudinal shear stress. Therefore the reduction factors recommended in both the theoretical and experimental analyses of reduced modulus action should be regarded as lower bound limits or worst case scenarios. These recommendations provide a conservative approach to design.

These tests also suggest that RMA does not occur to the extent to which Eurocode presents when material is in the interlocks of the sections. However, where material is not present in the interlocks, such as a hydrostatic loading, then RMA has a significant influence on the performance of the sections. The reduction in strength and stiffness is outside that allowable by the factors of safety applied during design. Therefore an additional reduction in strength and stiffness of the section would be required to achieve safe design and to conform to serviceability limits imposed when in built-up areas.

Finally, the implication of this thesis is that it confirms the accuracy of the British Standards Institute's BS8002 for the design of steel sheet piles. Its suggestions and guidance offer the engineer a good basis for design. It also suggests that that RMA is not black and white. The generation of interlock friction aids the strength and stiffness but to varying affect and that it may well lay in the engineers hands to decide a reasonable reduction in strength or stiffness that can be expected for different soil types. This returns us back to one of the opening statements made in this thesis, a quotation from Tomlinson (1977) that 'piling is both an art and a science'.

10 Conclusions

This thesis has discussed the effect of friction generated in the interlocks of U-section steel sheet piles. This has been done by eliminating the effects of other parameters such as skin friction and the effects of corrosion. This has provided results that accurately assess the benefits of material entering the interlocks and its effect on the performance of U-section steel sheet piles.

This thesis aims to provide what influences reduced modulus action, whether it can be quantified and what are the effects of soil-structure interaction using laboratory based tests. To increase the accuracy of tests previously carried out, in support of Eurocode, a new system was developed and used to validate a mathematical model that predicts the behaviour of U-section sheet piles in varying conditions. The system used has various advantages over previous work carried out in similar areas of research. These aspects of originality are:

- Accurate scale modelling of U-section interlocks similar to interlocks of U-section steel sheet piles.
- Span to depth ratios similar to full scale sections in practical pile walls providing similar deflection characteristics enabling the mobilisation of material in the pile interlocks to generate high friction values.
- Realistic loading arrangement producing a similar distribution of bending moment to practical retaining walls.
- Fully monitored specimens enabling the distribution of stress at the interlock to be accurately measured.

From the experimental and analytical work the following summarise the findings of this research:

- Experimental test provide a qualitative assessment of reduced modulus action in U-section sheet piling
- Experimental test suggest that full composite action is almost achieved with soil material placed in the interlocks to provide a greater level of friction. Thus providing a increase in shear transfer between adjacent sections.

- The reduction in stiffness and strength due to reduced modulus action could be a problem when soil material is absent from within interlocks. Such situations where this may occur are when piles are hydrostatically loaded.
- The results and subsequent analysis in conjunction with the results of the mathematical model are consistent to recommendations in BS8002 and practice. Thus providing scientific evidence to support anecdotal evidence of practical sheet pile walls and the guidance given BS8002.
- Soil-structure interaction curves have been generated from the mathematical model. These provide a lower bound estimation of the reduction of strength and stiffness with regards to the level of friction in the pile interlocks depending on the wall type.

Table 10.1 present a summary of the reduction factors for the bending strength and stiffness of a cofferdam retaining structure using U-section piling. Table 10.2 summarises the reduction factors for a propped cantilever wall.

Table 10.1 Reduction factors for a cofferdam

	Experimental		Theoretic	
Cofferdam	β_b	β_d	β_b	β_d
Sand & capping	0.95	0.80	0.65	0.38
Sand	0.95	0.80	0.56	0.33
Plain	0.50	0.40	0.50	0.30

The effect of varying friction caused by soil-structure interaction within the interlocks suggests that friction is low then pile stiffness and strength and considerable affected. These low friction examples are in line with the reduction factors expressed in Eurocode 3 part 5. However, Eurocode does not offer situations in which these reduction factors should be used and to what extent.

Table 10.2 Reduction factors for a propped cantilever wall

	Experimental		Theoretic	
Propped Cantilever	β_b	β_d	β_b	β_d
Sand & capping	0.90	0.70	0.95	0.87
Sand	0.90	0.70	0.66	0.40
Plain	0.55	0.50	0.50	0.30

These tables can be used together with the research undertaken in this thesis to predict a level of friction and a respective reduction factor. Therefore, this provides a

more accurate prediction of the behaviour of U-section piling leading to both safe and economical design.

The answer to why reduced modulus action is more pronounced in previous laboratory experiments than in practical walls has been addressed. Practical walls are long and slender and there deflection is relatively greater than those shown in previous work. However, the series of experiments reported in this thesis have addressed the issue of larger deflections and span to depth ratios. These tests have shown that any amount of material contained in the interlocks dramatically increases strength and stiffness beyond the findings of any previous laboratory based research. It can therefore be arguably assumed that any pile wall driven through soil will retain material within the interlocks. Thus, it could also be assumed the tests containing soil in their interlocks are representative of the performance of U-section piles in practical situations.

11 Further work

During the period of producing this thesis several areas of research concerning steel sheet pile walls were found where more information would be advantageous to the increased understanding of their behaviour. It is shown in the literature review that geotechnical studies into the behaviour of the soil behind a wall are numerous and well researched for both stiff and flexible walls. However, there is less material on what governs the behaviour of the wall itself. Obviously, the material and construction of the wall dictate the majority of varying stiffnesses in retaining walls. Concrete walls will, by nature of the material provide a stiff section, but steel can provide both stiff and flexible systems depending on the limits of design.

It is the limits of design that have caused the concern with U-section steel sheet piles. As this thesis has confirmed, unlike their Z-section stable mate, the effective section modulus can vary with the amount of friction generated in the interlocks. Although this investigation has shown that the reduction in performance due to RMA may not be as dramatic as initially believed, in the majority of practical applications it should still be a design consideration. Prior to these tests and literature searches, areas in which information was limited in regards to the behaviour of interlock friction have been addressed, however there are still a few issues that have arisen from this research that have not been addressed within the scope of this thesis. In order to develop a model based on the interlock friction alone, other factors suspected to govern the behaviour of U-section steel sheet pile have been deliberately omitted. It is these factors which would need to be address to continue the advance in this subject area.

11.1 Skin friction

The effect of skin friction on the development of RMA has remained unresearched. It is believed that the soil around the pile sections aids the development of full modulus action. In the development to produce an accurate testing system if was found that even with small levels of friction between the load applicators and the specimen the moment in the section was reduced by a considerable amount. Once the friction was removed then the moment transferred to

the section from the same applied load increased. A 10m deep mass of soil produces a distribution of load. The surface of the pile in contact with this load will have a certain level of friction. The friction generated between the soil and the structure, skin friction, may prevent the moment being transferred to the structure. Therefore, in practice the moment in the pile wall is not equivalent to that presumed to be applied. This would explain why steel sheet pile walls do not deflection as much in practical situations. This phenomenon in itself presents an area in which further research is required before the full understanding of the behaviour of U-section piles is achieved.

It is possible that the skin friction may cause the pile sections to transfer load into the surrounding soil forming a quasi-composite section: The interaction between soil and structure produces an effective composite section with the soil acting as part of the structure. The strength of this composite section depends on the shear strength of the retailed soil and the level of friction generated between pile and soil. This system effectively acts like a profiled metal deck only relying on friction and not shear studs. Strain gauge monitoring of full-scale piles and the shearing capacity of disturbed soils could be used to establish the effectiveness of skin friction in mitigating the effects of RMA.

11.2 Permanency

Permanency relates to the length of time the retaining wall is going to be in place. Is the structure a temporary or permanent structure? Does this have an effect on the development of RMA? The question of permanency is really a question about corrosion. It is well know that oxidation between to separate objects can make them very difficult to separate. It may be obvious to consider that corroded steel sheet piles will act as a composite section if the level of corrosion has caused them to fuse. However, what is the amount of time required for this to occur? Could corrosion be the answer to why old steel sheet pile walls do not fall down. It would be a worth while investigation the look into the effects of rust between adjacent piles and the time needed for enough rust to develop to form a bound. It is also well know that corrosion cause expansion, thus effectively reducing the internal size of the interlocks making them tighter. Tighter interlocks would make separation more

difficult and thus leading to the suggestion that the effects of RMA would be reduced.

Permanency could also have and effect on the load distribution. A flexible pile wall may initially settle causing the earth behind to relax and reducing its applied load (Rowe, 1955). This initial relaxing may also allow for a slight movement in the interlocks of the sheet pile mobilising material in the interlocks and getting jammed. Therefore, after the initially settlement the piles act as a composite pair. This would be relevant for a permanent structure, but for a temporary wall the initially settlement may not occur during the design life of the wall. This would provide reason to design a wall with reduction factors. The investigation f permanency requires time a patients in order to fully investigate the effects and may also require full scale testing. However, it would be advantages in developing a accurate model of the behaviour of sheet pile walls with varying design lives.

11.3 Modelling of steel sheet pile walls

The model provided in this thesis is based on small scale tests and adapted to predict the behaviour of full size steel sheet piling. Comparing the model results with those of full scale test would provide an answer to the exact validity of the model presented. Beyond tests already carried out on full scale piling, new test could be developed using full scale sections along the same lines as the experiments reported within this thesis. This would allow for easily comparable results and an idea of the level of interlock friction that can be expected in steel U-sections under varying conditions. Further the knowledge in this area would provide the greatest benefit as the model already created could be validated or corrected with ease.

11.4 Summary

To truly understand the behaviour of U-section steel sheet piles beyond the research contained in this thesis, full scale steel sheet pile test would provide the greatest number of answers. However, has it has been previously discussed testing sections of their size is an extremely difficult and expensive process. Investigations into skin friction and soil-structure interaction could be done on a small scale in controlled laboratory conditions and would provide another piece of the jigsaw into

determining the differences between the practical and theoretical behaviour of U-section steel sheet piling.

12 References

Baumann, P. 1934. Analysis of sheet pile bulkheads. *Proc. Am. Soc. Civ. Engrs,* **Vol. 60** (3): 289-322.

Blum, Dr. Ing. 1931. 'Einspannungsverhaeltnisse bei Bohlwerken', Berlin, Wilhelm Ernst & sohn.

Bransby, P. L. & **Milligan**, G. W. E. 1975. Soil deformation near cantilever sheet pile walls. *Geotechnique*, No 2: 175-195.

BSI, 1951. *CP 2: Code of Practice for foundations*. London, UK: British Standards Institute

BSI. 1972. *CP 2004: Code of Practice for Foundations*. London, UK: British Standards Institute

BSI, 1994. *BS 8002: Earth retaining structures*. London, UK: British Standards Institute

British Steel, 1997. *Piling Handbook*. British steel Plc.

Burland, J. B., **Potts**, D. M. & **Walsh**, N. M. 1981. The overall stability of free and propped embedded cantilever retaining walls. *Ground Engineering*. **Vol. 14** (5): 28-38.

Byfield, M. P. & **Crawford**, R. J. 2002. Oblique Bending in U-section steel sheet piles. Awaiting publication.

Byfield, M. P. & **Mawer**, R. W. 2002. Analysis of reduced modulus action in U-section steel sheet piles. *Proc. Conf. Steel Structures*. Eurosteel Coimbra: **Vol. 1**, 281-289.

Byfield, M. P. & **Mawer**, R. W. 2004. Analysis of reduced modulus action in U-section steel sheet piles. *Journal of Constructional Steel Research (JCSR).* **Vol. 60** (3-5): 401-410.

CEN. 1996. *Eurocode 3: Design of steel structures, Part 5: Piling*. London, UK: BSI.

Cobb, F. 2004. Structural Engineer's Pocket Book. Elsevier Butterworth Heinemann. ISBN: 0-7506-5638-7.

Craig, R. F. 1997. Soil mechanics, 6th Edition. E & FN Spoon. ISBN: 0 419 22450 5. Chapter 6, 179-247.

Crawford, R. J. 2003. PhD Thesis: *Analysis of oblique bending in crimped U-profile pile pairs*. Cranfield University, RMCS, Shrivenham, UK.

Crawford, R. J. & **Byfield**, M.P. 2001. A numerical model for predicting the bending strength of Larssen steel sheet piles. *Proc. Conf. on Structural Engineering, Mechanics and Computation (SEMC).* Cape town: 393- 400.

Crawford, R. J. & **Byfield**, M. P. 2002. "A numerical model for predicting the bending strength of Larssen steel sheet piles". Journal of Constructional Steel Research, No. 58, 1361-1374.

Day, R. A. & **Potts**. D. M. 1989. A comparison of design methods for propped sheet pile walls. *SCI publication 077.* The Steel Construction Institute.

Hartmann-Linden, R et al. 1997. Development of Rules for steel piles and introduction into Eurocode 3, Part 5. *ECSC-Project 7210-SA 127/523/840: Final Report.* Germany: RWTH Aarchen.

Herbet, P. *et al.*1978. Report on an experiment conducted during the construction of a sheet-piling wharf at the Port of Le Havre (roll on/roll off pier no. 3). In *7th Internationale Havenkongres. Antwerpen,* pages 1.12/1 – 1.12/8. KVIV, May 1978

Hibbeler, R. C. 1992. Engineering Mechanics Statics and Dynamics. 6th Edition. Macmillian, New York. ISBN: 0-02-354081-8.

Kerisel, J. 1987. Down to earth – Foundations past and present: The invisible art of the builder. A. A. Balkema/Rotterdam/Boston. ISBN: 90 6191 688 7.

Kort, D. A. 2001. Test results of the Rotterdam sheet pile walls. Technical Report 438, Delft University of Technology, Geotechnical Laboratory.

Kulhawy, F. H. 1984. Limiting tip and side resistence. Proc. Symposium Analysis and Design of Pile Foundations. Edited by Meyer, J. R. California. 80-98.

Larousse, 1995. Dictionary of Science and Technology, Edited by Prof. M. B. Walker. Printed by Clays Ltd. St. Ives plc. ISBN: 0-7523-0011-3.

Loctite, 2002a. Loctite UK Limited, Welwyn Garden City, AL7 1JB Telephone conversation with Technical Advisor: 20-5-2002. Tel. No. 01707 358800

Loctite, 200b. Loctite UK Limited, Welwyn Garden City, AL7 1JB Telephone conversation with Technical Advisor: 27-5-2002. Tel. No. 01707 358800.

Lohmeyer, E. 1934. Discussion to 'Analysis of steel pile bulkheads' by P. Baumann. *Proc. Am. Soc. Civ. Engs,* **Vol. 61** (3): 347-355.

Mackley, F. R. & **Buckley**, P. J. C. 1977. 'The history and development of steel piling'. *Proc. ICE* **Vol. 62**: 153-5.

Matich, M. A. J. *et al.* 1964. Performance measurements on two anchored bulkheads. *Canadian Geotech. J.,* **Vol. 1** (3): 167-178.

McNulty, T. A. & **Little**, J. A. 1987. The behaviour of a ground anchor supporting a sheet pile wall in granular soil. *Proc. 1st Int. Conf. On Foundations and Tunnels,* **Vol. 2,** 107-111. London.

Megson, T. H. G. 1987. 'Strength of Materials for civil engineers.' 2nd Edition, London, Arnold.

Padfield, C. J. & **Mair** R. J. 1984. CIRIA 104: Design of retaining walls embedded in stiff clay. *Construction Industry Research and Information Association Report.* London.

Potts, D. M. & **Burland**, J. B. 1983. A parametric study of the stability of embedded earth retaining structures. *Transport and Road Research Laboratory.* Supplementary Report 813.

Potts, D. M. & **Fourie**, A. B. 1984. The behaviour of a propped retaining wall: results of a numerical experiment. Geotechnique, **Vol. 34**, No. 3.

Potts, D. M. & **Fourie**, A. B. 1985. The effect of wall stiffness on the behaviour of propped retaining walls.. Geotechnique, **Vol. 35**, No. 3, 347-352.

Puller, M. & **Lee**, C. K. T. 1996. A comparison between the design methods for earth retaining structures recommended by BS8002: 1994 and previously used methods. *Proc. Instn. Civ. Engrs.* **Vol. 119** (1): 29-34

Puller, M. & **Lee**, C. K. T. 1996. Comparative studies by calculation between the design methods for embedded and braced retaining walls recommended by BS8002: 1994 and previously used methods. *Proc. Instn. Civ. Engrs.* **Vol. 119** (1): 35-48

Rowbottom, D., **Thompson**, D. & **Johnson**, K. 1996. Permanent steel piling for structures on land: 1994 Dennis Wait Lecture. *Proc. Instn. Civ. Engrs.* **Vol. 119** (3): 182-185

Rowe, P. W. 1951. Cantilever sheet pilling in cohesionless soil. *Engineering,* Sept., 316-319.

Rowe, P. W. 1952. Anchored sheet-pile walls. Proc. *Instn. Civ. Engrs,* **Vol. 1** (1): 27-70.

Rowe, P. W. 1955. A theoretical and experimental analysis of sheet-pile walls. Proc. *Instn. Civ. Engrs,* **Vol. 4** (1): 32-69.

Rowe, P. W. 1955a. Sheet-pile walls Encastré at the anchorage. Proc. *Instn. Civ. Engrs,* **Vol. 4** (1): 70-87.

Rowe, P. W. 1956. Sheet pile walls at failure. Proc. *Instn. Civ Engrs.* **Vol. 5** (1): 276-315

Schillings, R & **Boeraeve**, P. 1996. Design Rules for Steel Sheet Piles. *ECSC-Project 7210-SA 127/523/840.* Liège, Belgium: CIRF Dep. of Steel Con.

Schmitt, A. 1998. Bending behaviour of double U sheet piles, the causes and effects of oblique/biaxial bending in U sheet pile walls. International Sheet Piling Company (ISPC). Profil ARBED. Luxembourg.

SCI, 1994. Steel Designers' Manual. 5th Edition, The Steel Construction Institute. Blackwell Science, UK.

Scott, C. R. 1980. Soil mechanics and foundation, 3rd Edition. Applied Science Publishers Ltd, Barking.

Smith, G. N. & **Smith**, I. G. N. 1998. *Elements of soil mechanics*, 7th edition, Blackwell Scientific, Oxford, Uk.

Stroyer, J. 1935. 'Earth-pressure on flexible walls', *Journal of the ICE,* **Vol. 1** (1):. 94-139. London, UK.

Symons, I. F. 1983. Assessing stability of a propped insitu retaining wall in over consolidated clay. *Proc. ICE* **Vol. 75** (2): 617-633

Symons, I. F. *et al.* 1987. Behaviour of a temporary anchored sheet pile wall on A1(M) at Hatfield. *Department of Environment, Transport and Road Research Laboratory,* Crowthorne, Research Report 99.

Symons, I. F. & **Kotera**, H. 1987. A parametric study of the stability of embedded cantilever retaining walls. *Transport and Road Research Laboratory.* Research Report RR116.

Thompson, D. 2003. Private conversation with experienced piling engineer.

Thompson, P. J. & **Matich**, M. A. J. 1961. The performance of some steel sheet pile bulkheads. *Proc. 15th Canadian Soil Mechanics Conference.* National Research Council Technical Memorandum, No. 73, Section 4, 80-114.

Tomlinson, M. J. 1977. *Pile Design and Construction Practice.* Viewpoint Publications.

Tomlinson, M. J. 1998. Foundation design and construction. 6th edition. Longman,.

Tschebotarioff, G. P. 1949. Large scale earth pressure tests with model flexible walls. Final report, Princeton University.

Vanden Berghe, J-F. *et al.* 2001. Interlock friction in a steel pile wall: laboratory tests. Proc. 15th Internation conf. Soil Mechanics and Geotechnical Engineering. Istanbul, 1273-1279. A. A. Balkema.

Vishay, 1999. *Strain gauge application guides*, Micro-measurement division. North Carolina, USA.

Williams, S. G. O. 1989. PhD Thesis: *The behaviour of an anchored sheet pile wall in a granular soil*, Heriot-Watt University, Edinburgh, UK.

Williams, S.G.O. & **Little**, J.A. 1992. Structural behaviour of steel piles interlocked at the center of gravity of the combined section. *Proc. Instn. Civ. Engr. Structures & buildings.* Vol. 94, No. 2: 229-238

Wolffersdorf, P.A. von. 1997. Verformungsprongnosen fur Stutzkonstruktionen. Germany: Universität Fridericiana in Kalrsruhe.